

DEPARTMENT OF THE INTERIOR

U.S. GEOLOGICAL SURVEY

Chemical traits and trends of the granitic rocks of the
southern Sierra Nevada, California

by

Donald C. Ross ¹

Open-File Report 88-374

This report is preliminary and has not been reviewed for conformity with U.S. Geological Survey editorial standards and stratigraphic nomenclature. Any use of trade names is for descriptive purposes only and does not imply endorsement by the USGS.

¹ Menlo Park, California

CONTENTS

Abstract	1
Introduction	2
Discussion	4
Major elements	
Silica variation ("Harker") diagrams.....	4
Peacock index	5
Iron, magnesia, and lime relations	6
Iron, magnesia, and alkali relations	6
Normative quartz and feldspar relations	7
Relation of southern Sierra Nevada granitic rocks to trondhjemite based on a lime-soda-potash triangular plot	8
Chemical data on the Kernville pluton of Fox (1981)	10
Trace elements	
Trace element abundances	11
Rare earth element (REE) abundance diagrams.....	13
Ratio of lanthanum to ytterbium	14
Europium anomaly	15
Barium-rubidium relations.....	17
Potassium-rubidium relations	18
Cobalt-magnesium relations	19
Modal data for chemically analyzed rocks	
How valid a sample of the granitic rocks of the southern Sierra Nevada are the rocks selected for chemical analysis?.....	20
Modal mineral content as a key to silica abundance.....	21
References cited	22

ILLUSTRATIONS

Plate

1. Generalized geologic map of basement rocks showing location of chemically analyzed granitic samples, southern Sierra Nevada, California

Figures

1. Silica variation ("Harker") diagrams showing Al_2O_3 , Fe_2O_3 , FeO , MgO , Na_2O , CaO , K_2O , TiO_2 , and normative anorthite plotted against SiO_2 .
2. Plot of CaO and Na_2O plus K_2O against SiO_2 . Intersection of the two trends is the Peacock Index.
3. Peacock Index, by rock type (granite, granodiorite, tonalite, and quartz diorite).
4. Total Fe as FeO ($0.9 \text{Fe}_2\text{O}_3$ plus FeO) plotted against MgO .
5. Total Fe as FeO plus MgO plotted against CaO .
6. Triangular Alk-F-M plot.
7. Triangular plot of normative quartz (Q), orthoclase (or), and albite plus anorthite (ab+an).
- 7a. Diagrams showing CIPW normative approximation to modal classification of chemically analyzed granitic rocks from the southern Sierra Nevada by the method of Streckeisen and Le Maitre (1979)
 - I.) Classification scheme of Streckeisen and Le Maitre
 - II.) Granite
 - III.) Granodiorite
 - IV.) Tonalite
 - V.) Quartz diorite and quartz monzodiorite
8. Triangular plot of normative orthoclase (or), albite (ab), and anorthite (an).

9. CaO-Na₂O-K₂O plot comparing samples from the southern Sierra Nevada and Klamath Mountains.
- 9a. CaO-Na₂O-K₂O plot comparing samples from the southern Sierra Nevada with selected trondhjemites.
- 9b. Trondhjemite field of Barker (1979) superposed on or-ab-an triangular diagram.
10. Index map showing trondhjemite localities in the Sierra Nevada and Klamath Mountains.
11. CaO-Na₂O-K₂O plot showing relation of some Cedar Creek tonalitic samples to trondhjemite and other southern Sierra Nevada samples.
12. Kernville pluton of Fox (1981)
 - A. Index map showing location of chemically analyzed samples and outline of units "A" and "B".
 - B. Triangular plot of normative quartz (Q), orthoclase (or), and plagioclase (ab+an).
 - C. Triangular plot of normative orthoclase (o), albite (ab), and anorthite (an).
13. Histograms of trace element abundances.
 - A. Ba, Co, Cr, Cs, Hf, Rb, and Tl.
 - B. Th, U, Zn, and Zr.
 - C. Sc, La, Ce, Nd, and Sm.
 - D. Eu, Gd, Tb, Tm, Yb, and Lu.
14. Rare earth element (REE) chondrite normalized abundance diagrams for granite bodies.
 - A. Arrastre Creek
 - B. Bodfish Canyon
 - C. Brush Mountain
 - D. Five Fingers
 - E. Kern River

- F. Portuguese Pass
 - G. Sherman Pass
 - H. Tehachapi Airport
 - I. Tejon Lookout
- 15. Rare earth element (REE) chondrite normalized abundance diagrams for granodiorite bodies.
 - A. Alder Creek
 - B. Alta Sierra
 - C. Brush Creek
 - D. Castle Rock
 - E. Deer Creek
 - F. Gato-Montes
 - G. Hatchet Peak
 - H. Keene
 - I. Lebec
 - J. Peppermint Meadow
 - K. Pine Flat
 - L. Poso Flat
 - M. Rabbit Island
 - N. Sacatar
 - O. Sorrell Peak
 - P. Wagy Flat
 - Q. Whiterock
- 16. Rare earth element (REE) chondrite normalized abundance diagrams for tonalite bodies.
 - A. Antimony Peak
 - B. Bear Valley Springs
 - C. Carver-Bowen Ranch

- D. Dunlap Meadow
 - E. Fountain Springs
 - F. Hoffman Canyon
 - G. Mount Adelaide
 - H. Walt Klein Ranch
 - I. Zumwalt Ranch
17. Rare earth element (REE) chondrite normalized abundance diagrams for quartz diorite bodies.
- A. Caliente
 - B. Freeman Junction
 - C. Long Valley
 - D. Tehachapi Mountains
 - E. Walker Pass
18. Composite REE abundance diagrams.
- A. Granite
 - B. Granodiorite
 - C. Tonalite
 - D. Quartz diorite
19. Lanthanum/Ytterbium ratio plotted against SiO_2 .
- A. Individual samples
 - B. Average of each granitic unit
20. Ratio of chondrite normalized lanthanum to ytterbium plotted against SiO_2 .
21. REE abundance diagram showing belt of individual sample concentration for bodies whose average La/Yb is in the upper field of figures 19 and 20.
22. REE abundance diagrams showing belt of individual sample concentration for bodies whose average La/Yb is in the lower field of figures 19 and 20.
23. Superimposed upper and lower fields from figures 21 and 22.

24. Examples of how Eu* is determined.
25. Examples of gadolinium (Gd) "hump" and its effect on Eu*.
26. Europium anomalies (Eu/Eu*) plotted against silica content.
27. Histograms showing range of Eu anomalies (Eu/Eu*).
28. Barium plotted against rubidium for each rock type and a composite plot for all granitic samples.
29. Barium and rubidium plotted against silica content.
30. Potassium plotted against rubidium for each chemically analyzed sample.
31. Potassium plotted against rubidium for average of each granitic unit.
32. Histogram plotting average potassium-rubidium ratio for each granitic unit and patterned by rock type.
33. Cobalt plotted against magnesium.
34. Modal plot of chemically analyzed samples.
35. Modal plots showing comparison between modal distribution of chemically analyzed samples and all modal samples.
 - A. Comparison of individual chemically analyzed samples and average of modes for each granitic unit.
 - B. Comparison of outlines of fields of largest concentration of modes of chemically analyzed samples and of all samples.
36. Modal plots of averages by rock type; chemically analyzed samples compared with all modes.
37. Modal mineral and color index plotted against silica content for chemically analyzed samples.

Tables

1. Chemical data on samples of granite.
2. Chemical data on samples of granodiorite.
3. Chemical data on samples of tonalite.
4. Chemical data on samples of quartz diorite.
5. Chemical data on sample of quartz monzodiorite.
6. Analysts (all USGS) for chemical data on tables 1, 2, 3, 4, and 5.
7. Ca₂O, Na₂O, and K₂O values for trondhjemite samples plotted on figure 10.
8. Ca₂O, Na₂O, and K₂O estimated from modes and modes for selected samples of tonalite of Cedar Creek.
9. Average of chemical analyses of units "A" and "B" of Kernville pluton of Fox (1981).
10. Comparison of crustal abundance estimates for the lanthanide series between Turekian and Wedepohl (1961) and Taylor (1965).
11. Averages of potassium and rubidium values and K/Rb ratios of chemically analyzed samples for each plutonic unit.
12. Average modes by rock type for chemically analyzed samples and for all modes.

ABSTRACT

Chemical analyses have been determined for 134 samples of granitic rocks, ranging in composition from granite to quartz diorite, from the southern Sierra Nevada, California. On 115 of these samples, instrumental neutron activation analyses have also determined certain trace elements, including various rare earth elements. Comparison of the chemically analyzed samples with a vast number of modal analyses show that the suite of chemically analyzed samples adequately represents the compositional range of granitic rocks of the study area. The Peacock index shows that these rocks on average are calcic, but are near the calc-alkalic field. No definitive characteristics emerge from the numerous graphs and plots presented to characterize these rocks--they are grossly comparable to other granitic suites of southern and central California.

INTRODUCTION

In the course of a regional geologic study of the basement rocks of the southern Sierra Nevada, chemical analyses were obtained from 134 samples of granitic rock ranging compositionally from granite to quartz monzodiorite. In addition, instrumental neutron activation analyses were made for 115 of these samples to determine selected trace elements, including various rare earth elements. Those chemically analyzed rocks for which there are no trace element data are generally samples analyzed during earlier rubidium-strontium isotopic studies (Kistler and Peterman, 1973, 1978). All analyses, except three from the Rabbit Island mass (IS-638, 655, and 727 from Fox, 1981), are by analysts from the laboratories of the U.S. Geological Survey.

Samples selected for analysis are relatively unaltered and representative of the various rock bodies. However, typicalness of a group of 134 rocks from an area of several thousands of square kilometers that consists of several tens of different granitic bodies is uncertain. Comparisons of modes from many granitic samples with those of the chemically analyzed rocks suggests that the chemical sampling was indeed representative.

The main purpose of this report is to show the overall chemical character of the granitic rocks of the southern Sierra Nevada, by various graphs and plots. The chemical samples include Triassic, Jurassic, and dominantly Cretaceous bodies, so there is some possibility that an overall summary will suppress differences that undoubtedly exist. This is particularly true of the smaller Triassic and Jurassic bodies. However, there does seem to be an overall consistency for the whole granitic population in most graphs and plots in this report.

The basic data presented here can be grouped in a number of different ways. The general pattern of this report was to use variation by rock type. As an aid to other groupings of these rocks, the best estimates of the radiometric ages of about half of the granitic units are shown on the screened base of Plate 1, brief descriptions of the granitic units can be found in Ross (1987a), and modal data are reported in Ross (1987c).

In this summary report, some of the variations in the major oxides and relations between selected major oxides are discussed first; the trace elements are discussed with particular emphasis on the rare earth elements; and finally, the modal data on the chemically analyzed samples are used to evaluate whether the chemical sample is representative. Throughout the text various chemical relations are discussed briefly, but the major emphasis in characterizing the granitic rocks is made in the numerous graphic plots.

DISCUSSION

Major Elements

Silica variation ("Harker") diagrams

Silica variation ("Harker") diagrams that plot each major oxide against SiO_2 show rather strong linear trends for all oxides (fig. 1). The greatest variation, and overall the least scatter, is shown by CaO . Na_2O varies the least throughout the range of SiO_2 values. There is some spread in all plots, but there are few obviously anomalous points. Two samples from the Antimony Peak mass (784B and 3023) are very much higher in Al_2O_3 than any other of the chemical samples. These Antimony Peak samples are also low in K_2O and TiO_2 . Two samples from the Tehachapi Mountains unit are also very low in K_2O . Both of these two units are associated at least in part with the mafic gneiss terrane of the Sierran tail with "oceanic" crust affinities, where abnormally low K_2O is characteristic (Bailey and Blake, 1974). Another aberrant sample is of the quartz monzodiorite (RWK-11) of unknown affinity that is an inclusion(?) in the granite of Tejon Lookout south of the Garlock fault. It is low in CaO and high in Na_2O , thus has abnormally low normative anorthite for a rock of rather low SiO_2 . The quartz monzodiorite is also abnormally high in TiO_2 , having the highest value of all the samples. In addition, one sample from the Tejon Lookout mass (3752) is 2 percent higher in K_2O than any of the other samples.

With the exception of those few anomalous samples, all the samples show a rather consistent variation with SiO_2 for all oxides except Na_2O , which is essentially invariant. It is tempting to suggest that all these granitic rocks, except possibly those related to the mafic gneiss complex, are a comagmatic, related suite. However, this "suite" consists of Triassic, Jurassic, and Cretaceous bodies of a wide range of compositions, and possibly these plots indicate that

silica variation diagrams are not the best way to distinguish between types and various ages of granitic rocks.

Peacock index

Peacock (1931) determined the alkalic to calcic nature of igneous suites by plotting CaO and Na₂O+K₂O on standard silica variation diagrams; the Peacock index is where those trend-lines cross. Values lower than 51 are classified as calcic, values between 51 and 56 are alkalic-calcic, and values above 61 are calcic. The granitic rocks of the southern Sierra Nevada are calcic with a Peacock index of 62.5 (figure 2). The trend-lines of figure 2 are visually estimated. A computer-derived least-squares solution placed the intersection of these two trends at 62.73 (J.G. Moore, written communication, 1988), confirming the reliability of the visually estimated trends for these well-defined linear plots.

To determine what effect rock type had on the Peacock index samples were divided into those whose unit modal average was granite, granodiorite, tonalite, and quartz diorite and plotted separately. These four plots (fig. 3) show a decided tendency for the Peacock index to decrease in the more felsic, and generally younger, rocks of the suite. The granites and granodiorites are near or on the boundary between the calc-alkalic and calcic fields and the tonalites and quartz diorites are well within the calcic field. This trend of more alkalis and less lime in the more felsic rocks is hardly a startling relation. Plagioclase is more sodic, and K-feldspar is more abundant in these rocks, a long known and easily predicted reason for the Peacock index variation. Perhaps the best reason for using the Peacock index is that it quantifies this empirical relation and enables an easy index for comparing and contrasting various rock suites and parts of those suites.

Iron, magnesia, and lime relations

Plots using only iron, magnesia, and lime have been made to suppress the influence of SiO_2 of the standard variation diagrams. The plot of total Fe as FeO against MgO (fig. 4) shows a well confined linear field of points that shows the progressive increase in these oxides from granite to tonalite and quartz diorite (reflecting the modal increase in mafic minerals). The impressive thing in this plot is how confined and regular it is with only a few anomalous points, thus suggesting a consistent relation between iron and magnesium in these rocks. The few anomalous points are higher in MgO relative to their Fe content. Three of these samples (784B, 3023, and 3442) are associated with the mafic gneiss complex in the San Emigdio Mountains. The only anomalous sample in the "normal" granitic rocks is from the granodiorite of Poso Flat (6373).

The plot of total Fe as FeO plus MgO against CaO (fig. 5) is somewhat more diffuse, but still makes a well-defined linear belt that is rather tightly confined at the granite end and fans out toward the other rock types. The only samples outside this belt are also from the Antimony Peak body. Samples 784B and 3023 are relatively enriched in CaO and conversely sample 3158 is relatively depleted in CaO . This brings out the point of the usefulness of these data for correlation problems. Sample 3158 is from a poorly exposed sliver on the opposite side of a major fault from the main Antimony Peak body. Modally the sliver is somewhat different and correlation with the main mass is very tentative. The FeO , MgO , and CaO relations tend to confirm these suspicions about correlation and suggest the "sliver" may not be part of the Antimony Peak body.

Iron, magnesium, and alkali relations

A standard triangular plot for granitic rocks relates iron, magnesia, and the alkalis normalized to 100 percent (fig. 6). If molecular amounts are used instead, the field would move somewhat closer to the line joining the Alk corner and the mid-point joining the F and M corners.

The Alk-F-M plot (fig. 6) shows a relatively tightly constrained field elongate from the Alk corner to relatively near the F and M join. This is a rather standard looking field for a large group of granitic rocks and interestingly there are no aberrant points outside of the field in contrast to many other plots of southern Sierra Nevada rocks.

Normative quartz and feldspar relations

Normative quartz (Q) and the three feldspar components (orthoclase, or; albite, ab; and anorthite, an) make up the bulk of these rocks, generally about 85 to 95 percent. A triangular plot utilizing all four of these components (fig. 7) is essentially the normative counterpart of the quartz-K-feldspar-plagioclase modal plot. The normative field is much more tilted toward the ab+an (normative plagioclase) corner and is more compressed than the modal field (Ross, 1987c, fig. 10). Most points fall in the granodiorite field in the triangular plot of the normative quartz and feldspar, with far fewer in the tonalite and quartz diorite fields relative to the modal plot. Also normative points occupy only the calcic side of the granite field (with the exception of the anomalous 3752 of the granite of Tejon Lookout). The normative plot has numerous points in the quartz monzodiorite field, a field rarely occupied in modal plots of the southern Sierra Nevada. Part of this difference between modal and normative fields is because normative feldspar includes some oxides also present in mafic minerals.

A classification diagram (fig. 7A-I) has been devised by Streckeisen and Le Maitre (1979) that relates normative quartz and the feldspar components (or, ab, and an) to fields somewhat comparable to the IUGS modal classification (Streckeisen, 1967). The chemically analyzed samples of the southern Sierra Nevada are plotted on this diagram and divided, as in Tables 1 through 5, into rock types whose modal average is granite (fig. 7A-II), granodiorite (Fig. 7A-III), tonalite (fig. 7A-IV), and quartz diorite and the one sample of quartz monzodiorite (fig. 7A-V). The great bulk of the samples of granite, granodiorite, and tonalite plot in their respective "normative" fields. Some scatter into adjoining fields is a normal consequence of the

variation in these bodies. Similar spreads are seen in the modal plots by rock type (Ross, 1987c). The quartz diorite samples, however, plot dominantly in the "normative" tonalite field. The number of quartz diorites is relatively small, but there is some suggestion that modal and normative quartz diorite are not as comparable in the southern Sierra Nevada as the other major granitic rock types. Another way of saying this is that in the quartz diorites modal quartz is generally lower than normative Q'.

The normative feldspar components only are plotted in an or-ab-an triangular diagram (figure 8). The field is somewhat diffuse, but shows a good elongation from the mid-point of the ab-an join to the mid-point of the or-ab join. The only anomalous point from this trend is again sample 3752 of the granite of Tejon Lookout. It contains nearly 7 percent K₂O in contrast to 3 to 5 percent in other granitic samples. This Tejon Lookout sample may be altered or enriched with late K-feldspar.

Relation of southern Sierra Nevada granitic rocks to trondhjemite based on lime-soda-potash triangular plot

Chemically analyzed samples from the southern Sierra Nevada form a fairly compact elongate field on a CaO-Na₂O-K₂O triangular plot (fig. 9A). For comparison purposes, selected trondhjemites from the nearby central and northern Sierra Nevada and the Klamath Mountains (fig. 10), and from Idaho and the type area in Norway (Table 7) are plotted on the same triangle (fig. 9A). It is apparent that the southern Sierra Nevada rocks plot separately from the selected trondhjemites on figure 9A. For comparison, the field enclosing these same selected trondhjemites is shown on an or-ab-an triangular plot (fig. 9B) on which is also shown the trondhjemite field of Barker (1979). This plot virtually duplicates the CaO-Na₂O-K₂O plot and shows that the central Sierra Nevada Ward Mountain samples are only marginally trondhjemites and that the chemically analyzed samples from the southern Sierra Nevada are all outside Barker's trondhjemite field. Additionally, figure 9B shows that the comparative trondhjemites I

selected fall in part outside of Barker's (1979) trondhjemite field in a field he designates as "granite."

Only three southern Sierra samples plot close to trondhjemites (fig. 9A), which typically average 3 percent CaO, 5 percent Na₂O, and 1.5 percent K₂O (Table 7). The Alta Sierra sample (5423) has Na₂O in excess of CaO, but more K₂O than a true trondhjemite. The Walt Klein sample (RWK-2) as well as the Alta Sierra sample are also lower in Na₂O than typical trondhjemites. The Mount Adelaide sample (3631) is rather high in CaO but does come from a body that modally somewhat resembles a trondhjemite. Much of the southern Mount Adelaide body contains no K-feldspar or hornblende, but if it is to be called trondhjemite it would be calcic trondhjemite (Davis, 1963) as it contains intermediate andesine throughout.

Small bodies and dikes of relatively fine-grained rocks are exposed in the Cedar Creek area near Glennville (fig. 10). Some samples of tonalite are trondhjemitic based on their modes, which are chiefly plagioclase, quartz, and biotite with at most minor amounts of K-feldspar and hornblende (Table 8). Chemical data are not available for these samples, but gross amounts of CaO, Na₂O, and K₂O calculated from the modes indicate they fall in a field transitional between the main southern Sierra Nevada trend and the trondhjemite field (fig. 11). These samples were selected to most likely show trondhjemitic character from a larger number of modes. Even if some are trondhjemite, they are "calcic trondhjemite" as they contain sodic to intermediate andesine.

Trondhjemites are rare in the main mass of the Sierra Nevada batholith, and uncommon in the nearby northern Sierra Nevada and Klamath Mountains (fig. 10). For example, in the area of the Mariposa 1° x 2° AMS sheet, Bateman and others (1984) report 499 chemically analyzed granitic rocks. Only four from the Ward Mountain body are reported as trondhjemite; three of the samples plot in the trondhjemite field (fig. 9) although two are marginal and the fourth sample plots well out of the trondhjemite field with normal granitic rocks. Elsewhere in the

Sierra Nevada trondhjemites appear to be limited to occurrences within isolated plutons that intrude wallrock north and west of the main batholith -- most noteworthy is the Bald Rock pluton (fig. 10).

In summary, no granitic bodies in the southern Sierra Nevada are trondhjemites in the strict sense. At best some bodies of tonalite locally contain limited areas of biotite tonalite with very sparse to absent K-feldspar and hornblende and these contain plagioclase that is invariably sodic to intermediate andesine, and thus are not trondhjemite in the classic sense.

Chemical data on the Kernville pluton of Fox (1981)

Abundant chemical data have been reported by Fox (1981) on the Kernville pluton, which is the same body that I have referred to as the quartz diorite of Cyrus Flat (Ross, 1987a). The analyses that Fox reported are not strictly comparable with the other analyses from the southern Sierra Nevada. For example, the ferrous and ferric iron were not separated and the analyses generally total only 97 to 98 percent. However, as there are no other chemical data on this mass, the data of Fox (1981) are summarized here.

Fox divided the Kernville pluton into two units (fig. 12A), a small unit "A" that ranges in composition from pyroxene-hornblende gabbronorite to leucogabbro, and a unit "B" that forms the bulk of the Kernville pluton and is grossly equivalent to my quartz diorite of Cyrus Flat. An average of seven chemical analyses from unit "A" and 14 from unit "B" are shown on Table 9. Normative plots of Q, or, ab, and an show the strong distinction between units "A" and "B" (fig. 12B). Unit "A" may have some relation to the gabbronorite of Quedow Mountain (Ross, 1987b) or to gabbroic rocks associated with the mafic gneissic complex (Sams, 1986), or both.

The or-ab-an plot (fig. 12C) of unit "B" shows a field that overlaps the or-poor part of the same field for the other southern Sierra Nevada rocks and seems normal for a quartz diorite.

The Q-or-(ab+an) plot shows a strong linear trend for unit "B" wholly in the quartz monzodiorite field (fig. 12B). The Kernville (Cyrus Flat) is chemically somewhat different from the other analyzed southern Sierra Nevada rocks (fig. 7).

Trace elements

Trace element abundances

Histograms (fig. 13A-D) summarize the abundance data for each trace element. For most elements the histogram is a composite of all rock types. However, some trace elements seem to vary by rock type and these have separate histograms for each rock type (granite, granodiorite, tonalite, and quartz diorite).

The abundances of these trace elements from the southern Sierra Nevada are generally compatible with crustal abundances data reported for granodiorite and granite by Taylor (1965). He acknowledges the well-known objections to compiling such crustal abundance averages, notably problems in sampling, nomenclature, and in varying quality of analytic data. Though the selection of data is necessarily subjective, he reasons that the averages are nevertheless useful for general abundances. Turekian and Wedepohl (1961) also compiled a table of crustal abundances of most of the elements in which their categories for "high calcium" and "low calcium" granitic rocks equated grossly to granodiorite and granite, respectively. Their values differ somewhat from Taylor's compilation, particularly for the lanthanide series. Values for scandium are roughly comparable in the two compilations but for the lanthanides, Turekian and Wedepohl's compilation shows significantly greater concentrations (Table 10). Taylor (1965) in his compendium did not report average values for several of the lanthanides as he felt that data were lacking to support even an order of a magnitude estimate. However, most of Turekian and Wedepohl's average values for lanthanides compare quite closely with average values from the southern Sierra Nevada. Only values for Sm, Gd, Tb, and Lu are somewhat lower than Turekian and Wedepohl's estimates. Taylor's estimates, particularly for Tb, Yb, and Lu, seem much too low.

The trace elements that vary by rock type reflect selective enrichment in certain modal minerals. Those trace elements that vary by rock type (some rather subtly) are cobalt, rubidium, tantalum, thorium, uranium, zinc, zirconium, and scandium. Following are some thoughts on possible reasons for the varying concentrations of these trace elements.

Cobalt (fig. 13A) shows a strong progressive increase from granite to quartz diorite that is almost surely based on cobalt's affinity with the mafic minerals. This will be emphasized later in the report by a discussion of the strong positive correlation between cobalt and magnesium.

Rubidium shows a progressive enrichment toward the more felsic rocks (fig. 13A) which is probably mostly the result of the common association of rubidium with K-feldspar. This relation is emphasized further by figure 22 which shows the relative enrichment of rubidium along with potassium in granite compared to the more mafic rock types. Rubidium is even more strongly enriched in biotite, but K-feldspar is much more abundant and thus more of an influence in rubidium enrichment in the more felsic rocks.

Tantalum also is somewhat enriched in the more felsic rocks, probably because of the tendency of Ta to form large complex ions which tend to concentrate in residual melts (Ringwood, 1955). Tantalum in the southern Sierra Nevada granitic rocks is somewhat less abundant than in crustal estimates of both Taylor (1965) and Turekian and Wedepohl (1961). They estimate concentrations of two to four parts per million for granodiorite and granite, whereas Sierran granitic rocks are generally about one part per million or less (fig. 13A, Tables 1-4).

Uranium and thorium both show a progressive enrichment in the more felsic rocks (fig. 13B). Like tantalum these elements also have high ionic potentials that lead to complex ion formation and concentration in residual magmas (Ringwood, 1955).

Zinc shows a slight impoverishment in the more felsic rocks (fig. 13B) and zirconium may show a slight enrichment in the felsic rocks (fig. 13B). However, both variations are subtle at best. The geochemical distribution of zinc is not well known (Taylor, 1965), but Tauson and Kravchenko (1956) suggest it enters biotite in preference to other minerals in granitic rocks. Chao and Fleischer (1960) show that Zr increases with fractionation in granitic rocks based on data from the southern California batholith. They noted that Zr is more abundant in hornblende than in biotite, but that from 50 to 100 percent of zirconium in granitic rocks is accounted for by the mineral zircon, which is generally more abundant in the more felsic rocks.

Scandium has a noticeable variation by rock type, being more concentrated in the more mafic rocks (fig. 13C). Nockolds and Mitchell (1948) noted that scandium can enter hornblende and substitute for Ti in sphene, accounting for its concentration in more mafic rocks.

Rare earth element (REE) abundance diagrams

To characterize and standardize the rare earth elements (REE) that were determined by instrumental neutron activation analysis, lanthanum to lutetium are plotted with the analytical amounts divided by the average content of each rare earth element in chondritic meteorites (Haskin and others, 1968). Each sample is plotted separately and samples are grouped together for each granitic unit (fig. 14 to 17). The standardized plots are also grouped together by rock type (figs. 18, A, B, C, and D).

These abundance diagrams emphasize the strong negative europium anomalies in some samples, particularly some of the granites. Also apparent are the gadolinium "humps" in some rocks. Most of the units that have multiple samples, for example the granodiorites of Poso Flat and Sacatar (figs. 15L, N), show similar REE patterns throughout the unit. Some units, however, show marked differences within the unit, as for example the granite of Tejon Lookout (fig. 14I), which suggests that rocks that are not related may have been grouped . Also noteworthy is the slope of the plots, a mark of their relative differentiation. This character is described in more detail later in a section dealing with the ratio of lanthanum to ytterbium.

Ratio of lanthanum to ytterbium

The ratio of lanthanum to ytterbium is a measure of the "flatness" of the REE plot. Flatter plots are thought to be more primitive and conversely those that are significantly higher on the lanthanum end are more fractionated. This ratio has been plotted against silica content for each chemically analyzed sample for which INAA data were available (fig. 19A). Also the average ratio of each granitic unit was plotted against silica content (fig. 19B). The general assumption is made that the more silica-rich rocks are more fractionated. For these plots, analytical amounts rather than chondrite normalized values of lanthanum and ytterbium are used in calculating the ratios.

As silica increases there is an increase in the La/Yb ratio, but it is not consistent or impressive. The increase makes a generally "fan-shaped" field with the highest values of the ratio falling in the intermediate silica range (fig. 19). The plot for pluton averages suggests two relatively distinct fields (fig. 19B). Most obvious is a field with a nearly horizontal trend that shows very little, if any, increase in La/Yb with increasing silica. However, there is another more diffuse trend that shows a striking increase with silica, notably for some of the granodiorites. Most of the granite bodies plot in the lower, near horizontal field. The granite of Arrastre (only one sample), however, falls well out of either field.

Chondrite normalized lanthanum and ytterbium values were also used to determine the lanthanum/ytterbium ratios for pluton averages (fig. 20) to see if there was any significant difference from the plot using absolute amounts of lanthanum and ytterbium. The normalized plot is much the same as figure 19B, only more flattened, but the same two fields are still evident.

The upper, more fractionated field consists of about half of the granodiorite bodies (Alta Sierra, Castle Rock, Gato-Montes, Lebec, Peppermint Meadow, Rabbit Island, Sorrell Peak, Wagy Flat, and Whiterock), one granite (Five Fingers) whose modal average is almost in the

granodiorite field, and two tonalite bodies of which one (Hoffman Canyon) has a modal average almost on the boundary of the granodiorite field, and one (Mount Adelaide) which plots modally well into the tonalite field. Thus, except for the tonalite of Mount Adelaide, all the bodies in the more fractionated field are essentially granodiorites.

Although the average of the Mount Adelaide mass plots well within the upper field (fig. 20), only two disparate samples are averaged for this value of La/Yb. One (4189) has a value of 7 and plots well down in the lower field. The other sample (3631) is lower in La relative to the other samples from the upper field, but much lower in Yb to give a La/Yb ration of 31. Both Mount Adelaide samples are anomalous as shown on the composite plot of the upper field (fig. 21).

Composite REE abundance diagrams were prepared for all individual samples of bodies in both the upper and lower field to see what the differences were between the two fields. Plots for the upper field (fig. 21) show no, or at best modest, Eu anomalies for most samples and a relatively narrow belt comprising most of the REE data. There is some scatter away from the main trend, but most notably anomalous are samples 3631 and 4189 of the tonalite of Mount Adelaide. They are low at both ends of the abundance diagram. The composite abundance diagram for the lower field shows a rather pronounced Eu anomaly and a much wider belt of concentrated points (fig. 22) than the upper field. When both fields are superimposed (fig. 23) there is considerable overlap but the lower field extends to lower values of La and higher values of Yb resulting in overall lower La/Yb ratios.

Europium anomaly

Most chemically analyzed samples from the southern Sierra Nevada have a negative chondrite normalized europium value (for example, abundance diagrams for Bodfish Canyon and Brush Mountain--figure 24). This negative europium anomaly is generally quantified by determining the ratio between the chondrite normalized value of europium (Eu) and the projected

point where europium is extrapolated to lie on a smoothed evolution diagram (Eu^*). Figure 24 shows that Eu^* can be estimated rather easily for the smooth curve of points for sample 3221 and that the estimate is much more subjective for an irregular trend like 5071. In a number of samples the value of gadolinium is also abnormally high relatively on a smoothed abundance diagram. This gadolinium "hump" tends to magnify the europium anomaly if Eu^* is determined based on connecting the adjacent samarium (Sm) and gadolinium (Gd) points (fig. 25). Therefore, for those samples with prominent gadolinium humps, Eu^* was determined from a line connecting samarium (Sm) and terbium (Tb).

Based on data from the southern Sierra Nevada, anomalously low Eu values and anomalously high Gd values are characteristic in many of these granitic rocks -- if a smooth REE evolution diagram is indeed the norm.

Most samples have Eu/Eu^* ratios from 0.6 to 0.9 with most of the granite samples much lower (fig. 26). The histogram (fig. 27) shows this relationship even more clearly.

One granite sample (3752 of the Tejon Lookout mass) has a positive Eu anomaly in contrast to the other two samples from this mass that have pronounced negative Eu anomalies. It may be significant that sample 3752 is from a small isolated mass east of the main Tejon Lookout outcrops. Possibly the smaller 3752 mass is not correlative with the main Tejon Lookout outcrops, although three samples are a rather limited sample from which to draw conclusions.

Three tonalite samples also have positive Eu anomalies. Two are the only samples analyzed from the Mount Adelaide mass (3631 and 4189) and the other anomalous tonalite is from the Walt Klein mass (6088). The latter tonalite has a very slightly positive anomaly and does not have a much different pattern from two other samples from that mass (6281A and 6314-1) that have essentially no Eu anomalies. Three of the six samples from this mass (6321, 6096, and 6061) do have negative Eu anomalies. One quartz diorite sample from the Walker Pass mass (6220) also has a positive Eu anomaly. Other samples from this mass have no Eu anomalies or very modest negative ones.

On composite REE evolution diagrams by rock type, the granite field is relatively narrow with a pronounced negative Eu anomaly (fig. 18A). The granodiorite and tonalite fields are grossly similar, both being rather broad, particularly at the light REE end and both showing a somewhat modest negative Eu anomaly (figs. 18B, C). The tonalite field is somewhat lower on the light REE end, suggesting a slightly more "primitive" diagram. The quartz diorite field is decidedly narrower (perhaps because of fewer samples) and it is also decidedly flatter and more "primitive" (fig. 18D).

Barium-rubidium relations

Taylor (1965) noted that rubidium (Rb) increased with a decrease in barium (Ba) in some feldspars. To test whether such a fractionation would occur in whole rock granitic samples from the southern Sierra Nevada, Rb (in ppm) was plotted against Ba (in ppm) for each rock type separately and with a composite plot of all samples (fig. 28). The resulting composite plot shows a somewhat blob-like concentration of points and the only rock type that shows a negative correlation as Taylor reported for feldspar is granite. Conversely, tonalite and to some extent quartz diorite show a possible positive correlation, but with a very weak trend.

If the granite samples and the granodiorites richer in Ba and Rb are combined there is a fair negative correlation for these samples that make a "mushroom cap" over the rest of the samples that define a gross positive correlation trend. Admittedly, the split of granodiorite samples is arbitrary, but there is a hint of two fields on the composite plot (fig. 28). The trends, except for granite, however, may be largely illusory -- being enhanced by dashed lines around the "fields" of the composite plot.

If only average values of Ba and Rb for each granodiorite body are plotted, the field is somewhat tightened but still retains its blob-like outline that has no evident separation into two fields. Using the arbitrary boundary shown in figure 28 there is no significant difference modally between the two resulting groups of plutons for most minerals. K-feldspar is on the average 3.5

percent richer in the upper group of plutons and plagioclase and mafic minerals are only slightly lower in the upper group. Individual samples have significant variations in both Ba and Rb in some plutons, so individual sample variations are apparently more significant than are the differences between plutons.

Barium and rubidium were also plotted against silica. Both increase with increasing silica, but the trends are rather diffuse (fig. 29). As both elements tend to be concentrated in K-feldspar, it is predictable that they would be more abundant in the more silicic rocks. The wide spread of values in both elements for any given silica value is also evident.

Potassium-rubidium relations

Plots of potassium against rubidium have been made for all the chemically analyzed samples (fig. 30) and for averages for each granitic unit (fig. 31, table 11). Both these plots show a well confined relatively linear trend. Most samples plot somewhat on the rubidium depleted side of the K/Rb ratio of 230 that has been the commonly accepted ratio for igneous rocks (Shaw, 1968). A comparable average value of 231 has been determined by Dodge et al. (1970) for 44 analyzed samples from the central Sierra Nevada. Contrastingly, the average for chemically analyzed samples from the southern Sierra Nevada is 271 (Table 11). These samples show a pronounced rubidium enrichment in the granites (the rubidium "hook"). This is expectable in "late stage" granites (Taylor, 1965), where considerable K-feldspar but less biotite is concentrated.

The potassium-rubidium plot of unit averages (fig. 31) shows a grouping into a granite field, a granodiorite field, and a tonalite-quartz diorite field. However, these fields do not exclusively separate rock types. For example, two granite bodies (Five Fingers and Arrastre), anomalously low in Rb for their K values, both plot in the granodiorite field. There is also some overlap of granodiorite with the tonalite-quartz diorite field. The most "enriched" tonalite (Hoffman Canyon) plots well into the granodiorite field. The tonalite of Antimony Peak is

considerably lower in both K and Rb than all other plutons. This body, associated with the mafic gneiss in the San Emigdio Mountains, is probably not closely related to the other analyzed granitic samples. Other than these two exceptions, all the tonalite and quartz diorite averages plot in a fairly concise field. Two granodiorite averages (Poso Flat and Wagy Flat) nestle in the tonalite-quartz diorite field, but both bodies texturally, and to some extent in mineral content, resemble two of the tonalite bodies (Bear Valley Springs and Mount Adelaide). The modal averages of both the Poso Flat and Wagy Flat masses plot near the tonalite field (Ross, 1987c) suggesting that they are "calcic" granodiorites closely related to tonalite. The K-Rb plot tends to confirm this.

A histogram showing the K/Rb ratio for each granitic unit (fig. 32) shows wide ranges for each rock type. Granite bodies definitely have the lowest ratios reflecting higher Rb values, with the granodiorites somewhat higher, but on the average close to granite. The tonalite and quartz diorite masses have a considerable range in K/Rb ratios -- to 400 and higher, but also down to about 200, overlapping with the granites and granodiorites. The tonalite and quartz diorite bodies as a group have higher average K/Rb ratios of about 300. Without the influence of the anomalous Antimony Peak ratio of 497, the tonalite average is 271, intermediate between granodiorite and quartz diorite.

In minerals analyzed from granitic rocks in the central Sierra Nevada (Dodge et al., 1970) K-feldspar contains a little over 325 ppm Rb, whereas biotite contains nearly 600 ppm Rb. These are the principal sources of Rb in granitic rocks. In the granitic rocks of the southern Sierra Nevada, K-feldspar probably has more influence on rubidium values in the granites and sodic granodiorite bodies, whereas biotite is a greater influence in the more mafic rocks.

Cobalt-magnesium relations

Carr and Turekian (1961) noted a strong positive correlation between Co and Mg for granitic rocks suggesting that most cobalt in granitic rocks is in the ferromagnesian minerals.

This relation is borne out in the southern Sierra Nevada where a similar plot (fig. 33) shows a strong linear trend with only five anomalous granite samples (3005 and 3221 from Brush Mountain, 3401 and 3752 from Tejon Lookout, and 4100A from Tehachapi Airport). Compared with other modal samples from the same units these chemically analyzed samples are not unusual, except for 3752 which is anomalously low in biotite. With all the other samples so close to the trend line, it is tempting to suggest that there are some discrepancies in analytical amounts that account for these granite anomalies.

Figure 33 reflects the general increase in cobalt by rock type from granite to quartz diorite shown by the histograms (fig. 13A), but there is considerable overlap between the various rock types. Granite samples are concentrated on the low end, tonalite and quartz diorite together are relatively high, and granodiorite overlaps considerably with the other fields.

Modal data for chemically analyzed rocks

How valid a sample of the granitic rocks of the southern Sierra Nevada are the rocks selected for chemical analysis?

The modal field for 123 of the chemically analyzed samples are plotted on a standard Q-A-P triangular diagram (fig. 34). To test how representative these modes are of the total modal field, figure 34 has been superimposed with a plot showing modal averages for all the granitic bodies (Ross, 1987c). The coincidence of the two modal fields is generally good (fig. 35A). Another comparison superposed the areas of densest concentration of each field (fig. 35B). This figure suggests that granites, particularly the more sodic ones, are somewhat undersampled.

Another test compared chemically analyzed and total modal samples for each individual major mineral, by rock type. The modal differences are rarely more than 1 percent for each mineral for each rock type (table 12). Considering the accuracy of modal analyses, these two

groups of modes are practically the same. Only quartz diorite has somewhat more variations for some minerals (quartz, plagioclase, and hornblende). This is summarized by figure 36, a modal plot of the data of table 12. Quartz diorite is the only rock type where the two groups are not virtually superposed and it makes up only a small proportion of the total area of granitic rocks.

Modal mineral content as a key to silica abundance

Each modal mineral has been plotted against silica (fig. 37). Such S_iO_2 plots can serve as guides to roughly estimating the silica content of rocks in this region if modal data are available, but no chemical data. These plots suggest that quartz and biotite are particularly useful for estimating silica content from modal data. Biotite or color index are probably the best indicators -- it is relatively easy to identify and quantify, even in the field without a modal analysis. For some rocks where biotite is difficult to distinguish from hornblende (fortunately rare in this region), one can at least estimate the color index and from this estimate the silica content of the rock, albeit not as precisely.

REFERENCES CITED

- Bailey, E.H., and Blake, M.C., Jr., 1974, Major chemical characteristics of Mesozoic Coast Range ophiolite in California: U.S. Geological Survey Journal of Research, v. 2, no. 6, p. 637-656.
- Barker, Fred, 1979, Trondhjemite: definition, environment and hypotheses of origin in Barker, Fred (ed.), Trondhjemites, dacites, and related rocks: Developments in Petrology 6, Elsevier, Amsterdam, p. 1-12.
- Bateman, P.C., Dodge, F.C.W., and Bruggman, P.E., 1984, Major oxide analyses, CIPW norms, modes, and bulk specific gravities of plutonic rocks from the Mariposa 1° x 2° sheet, central Sierra Nevada, California: U.S. Geological Survey Open-File Report 84-162, 50 p.
- Carr, M.H., and Turekian, K.K., 1961, The geochemistry of cobalt: Geochemica et Cosmochimica Acta, vol. 23, n. 1-2, p. 9-60.
- Chao, E.C.T., and Fleischer, M., 1960, Abundance of zirconium in igneous rocks: Report of the International Geologic Congress XXI, Session (Norden) I, p. 106-131.
- Davis, G.A., 1963, Structure and mode of emplacement of Caribou Mountain pluton, Klamath Mountains, California: Geological Society of America Bulletin, vol. 74, p. 331-348.
- Dodge, F.C.W., Fabbi, B.P., and Ross, D.C., 1970, Potassium and rubidium in granitic rocks of central California, in Geological Survey Research, 1970: U.S. Geological Survey Professional Paper 700-D, p. D-108-115.

Fox, L.K., 1981, Compositional variations and implications of petrogenesis of the Kernville pluton, southern Sierra Nevada, California: Unpublished senior thesis, Princeton University, 77 p.

Goldschmidt, V.M., 1916, Geologisch-petrographische Studien im Nachgebirges des Südlichen Norwegens, IV Übersicht der Eruptivegesteine im Kaledonischen Gebirge zwischen Stavanger und Trondhjem: Vid. Selsk. Skrifter, Kristiana, no. 2, 140 p.

Hamilton, Warren, 1962, Trondhjemite in the Riggins quadrangle, western Idaho, in Geological Survey Research 1962: U.S. Geological Survey Professional Paper 450E, p. E98-E101.

Haskin, L.A., Haskin, M.A., Frey, F.A., Wildeman, T.R., 1968, Relative and absolute terrestrial abundances of the rare earths in L.H. Ahrens, ed., Origin and distribution of the elements: Oxford, England and New York Pergamon Press, p. 889-911.

Hietanen, Anna, 1951, Metamorphic and igneous rocks of the Merrimac area, Plumas National Forest, California: Geological Society of America Bulletin, v. 62, p. 565-608.

Hotz, P.E., 1971, Plutonic rocks of the Klamath Mountains, California and Oregon: U.S. Geological Survey Professional Paper 684-B, p. B1-B20.

Kistler, R.W., and Peterman, Z.E., 1973, Variations in Sr, Rb, K, Na, and initial $\text{Sr}^{87}/\text{Sr}^{86}$ in Mesozoic granitic rocks and intruded wall rocks in central California: Geological Society of America Bulletin, v. 84, no. ?, p. 3489-3512.

Kistler, R.W., and Peterman, Z.E., 1978, Reconstruction of crustal blocks of California on the basis of initial strontium isotopic compositions of Mesozoic granitic rocks: U.S. Geological Survey Professional Paper 1071, 17 p.

Larsen, L.H., and Poldervaart, Arie, 1961, Petrologic study of Bald Rock batholith, near Bidwell Bar, California: Geological Society of America Bulletin, v. 72, p. 69-92.

Lipman, P.W., 1963, Gibson Peak pluton: a discordant composite intrusion in the southeastern Trinity Alps, northern California: Geological Society of America Bulletin, v. 74, p. 1259-1280.

Nockolds, S.R., and Mitchell, R.L., 1948, The geochemistry of some Caledonian plutonic rocks: A study in the relationship between the major and trace elements of igneous rocks and their minerals: Transactions, Royal Society of Edinburgh, v. 61, p. 533-575.

Olmsted, F.H., 1971, Pre-Cenozoic geology of the south half of the Auburn 15-minute quadrangle, California: U.S. Geological Survey Bulletin 1341, 30 p.

Peacock, M.A., 1931, Classification of igneous rock series: Journal of Geology, v. 39, no. 1, p. 54-67.

Ringwood, A.E., 1955, The principles governing trace element behavior during magmatic crystallization, Part II: The role of complex formation: Geochimica et Cosmochimica Acta, v. 7, no. 5-6, p. 242-254.

Ross, D.C., 1987a, Generalized geologic map of the basement rocks of the southern Sierra Nevada, California: U.S. Geological Survey Open-File Report 87-276, 28 p., scale 1:250,000.

Ross, D.C., 1987b, Mafic plutonic rocks of the southern Sierra Nevada, California: U.S. Geological Survey Open-File Report 87-275, 42 p.

Ross, D.C., 1987c, Granitic rock modal data from the southern Sierra Nevada, California: U.S. Geological Survey Open-File Report 87-373, 276 p.

Sams, D.B., 1986, U/Pb geochronology, petrology, and structural geology of the crystalline rocks of the southernmost Sierra Nevada and Tehachapi Mountains, Kern County, California: Pasadena, California Institute of Technology, Ph.D. thesis, 315 p.

Shaw, D.M., 1968, A review of the K-Rb fractionation trends by covariance analysis: *Geochimica et Cosmochimica Acta*, v. 32, no. 6, p. 573-602.

Streckeisen, A.L., 1967, Classification and nomenclature of igneous rocks: *Neues Jahrbuch für Mineralogie Abhandlungen*, v. 107, p. 144-214.

Streckeisen, A.L., and Le Maitre, R.W., 1979, A chemical approximation to the modal Q A P F classification of the igneous rocks: *Neues Jahrbuch für Mineralogie Abhandlungen*, v. 136, p. 169-206.

Tauson, L.V., and Krauchenko, L.A., 1956, Characteristics of lead and zinc distribution in minerals of Caledonian granitoids of the Susamyr batholith in central Tian-Shan: *Geochimiya*, no. 8, p. 819-824.

Taylor, S.R., 1965, The application of trace element data to problems in petrology, in Physics and Chemistry of the Earth, v. 6, Pergamon Press, Oxford, p. 133-213.

Turekian, K.K., and Wedepohl, K.H., 1961, Distribution of the elements in some major units of the Earth's crust: *Geological Society of America Bulletin*, v. 72, no. 2, p. 175-191.

Turner, H.W., 1894, Rocks of the Sierra Nevada: U.S. Geological Survey Annual Report 14, part 2, p. 435-495.

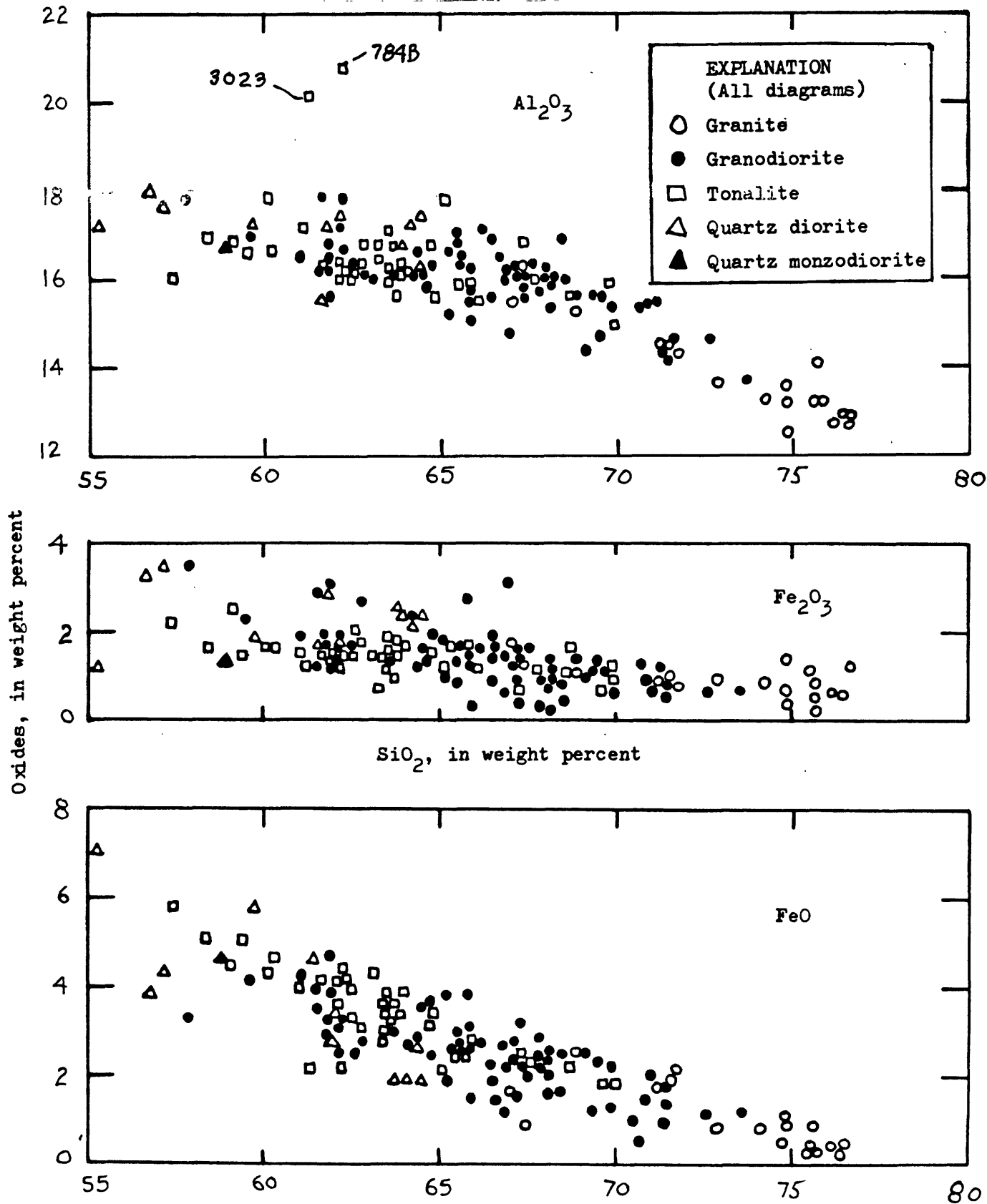


Figure 1. Silica variation ("Harker") diagrams.

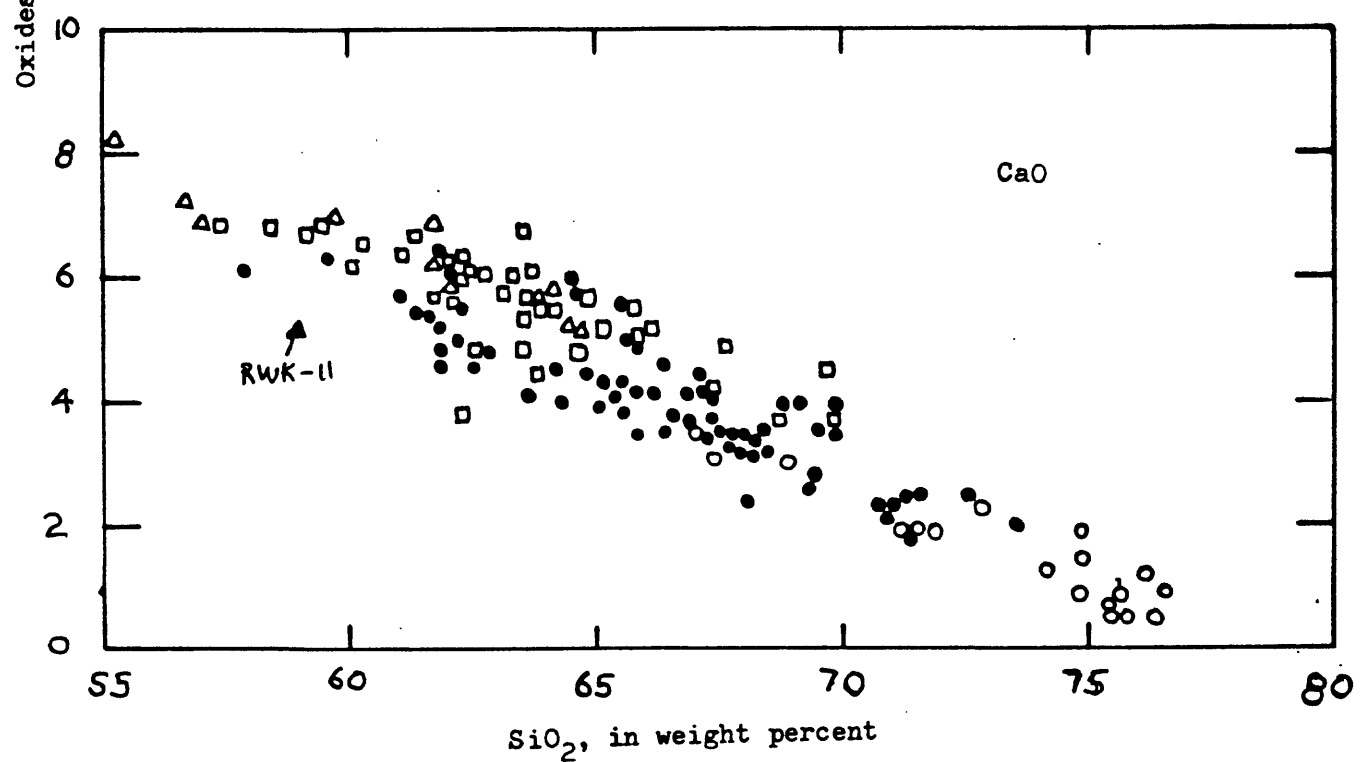
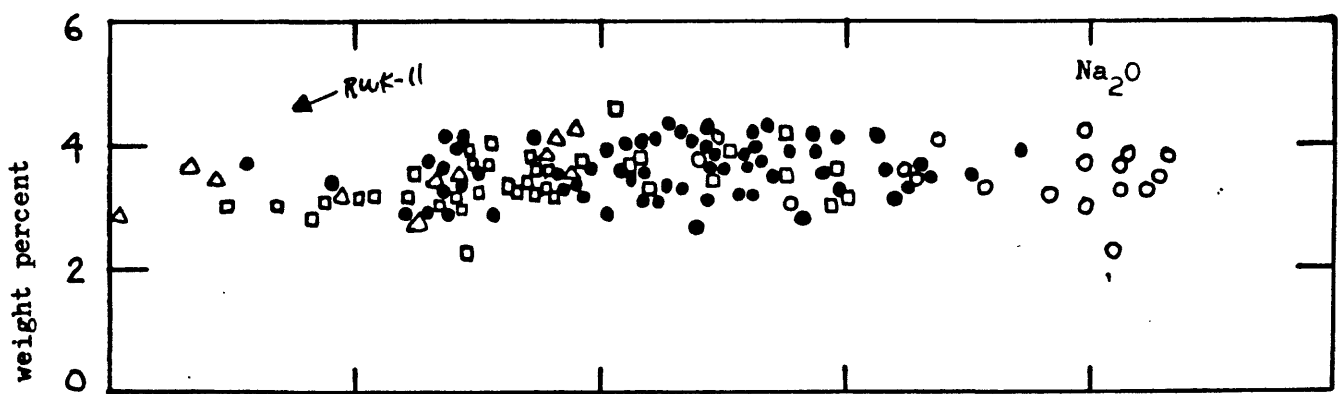
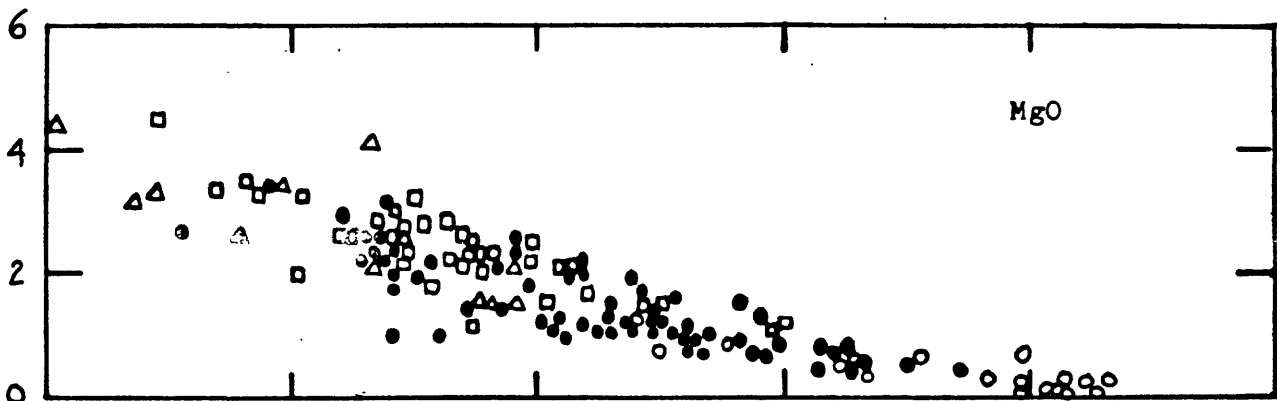


Figure 1 . (cont.)

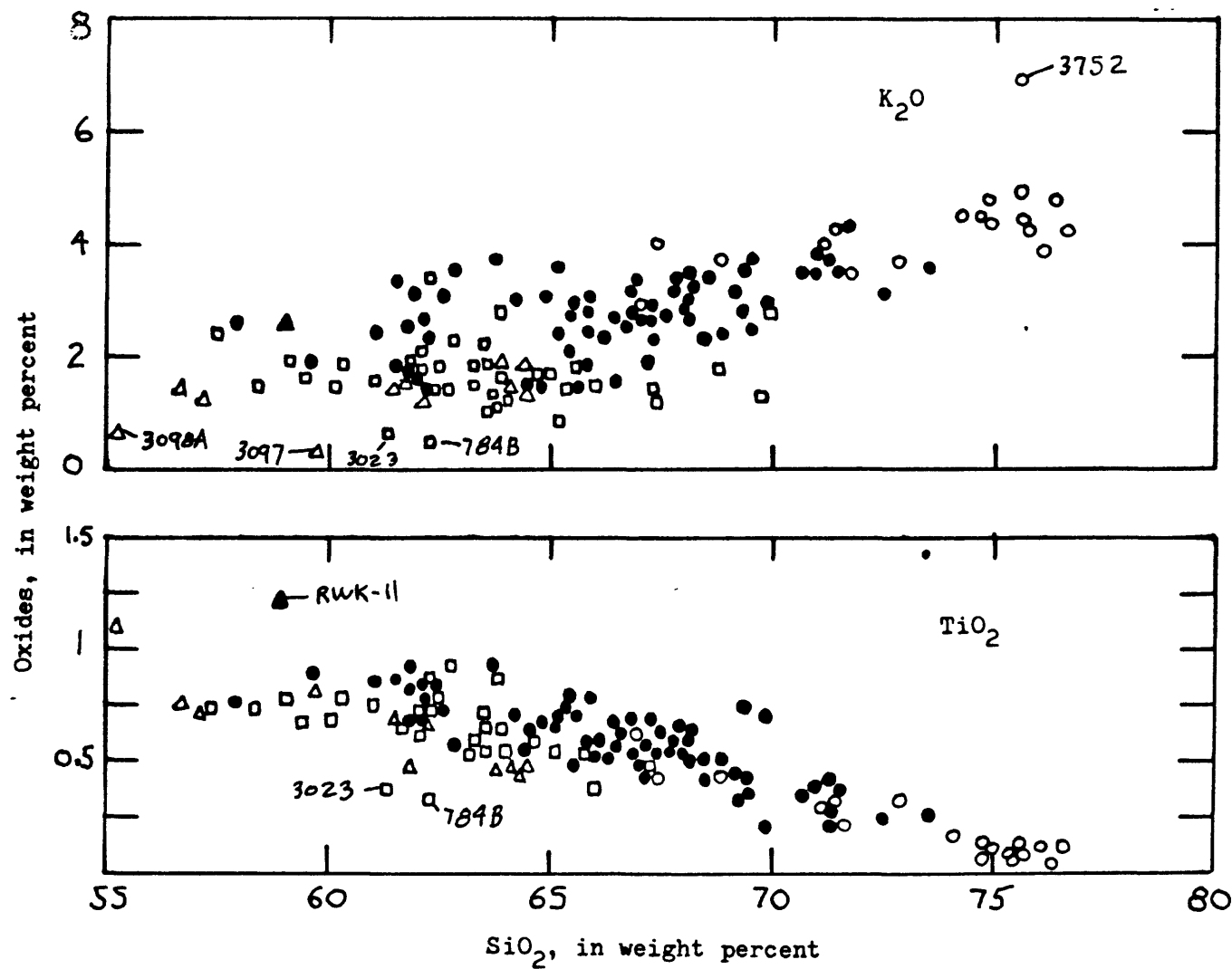


Figure 1 . (cont.)

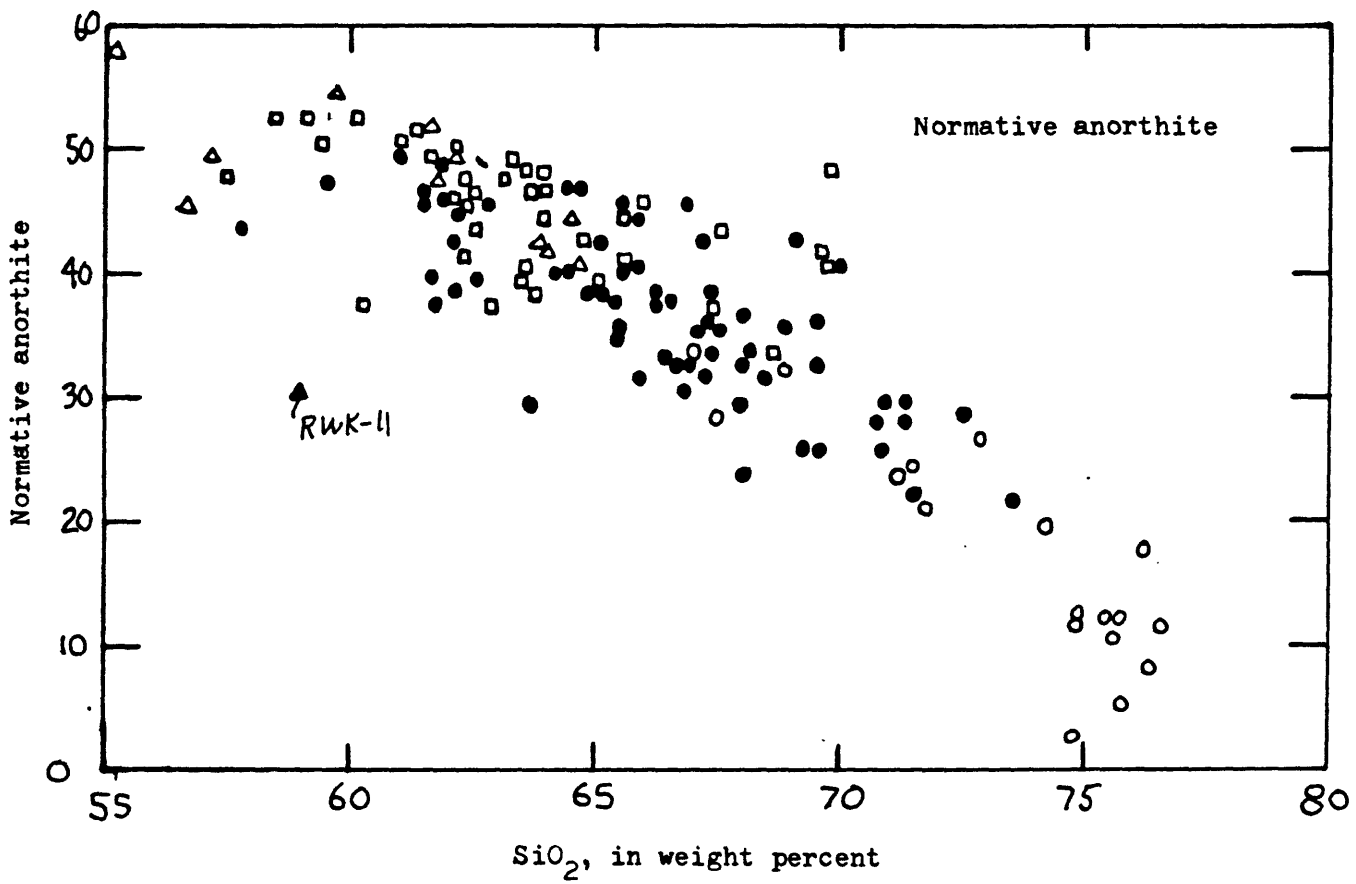


Figure 1 . (cont.)

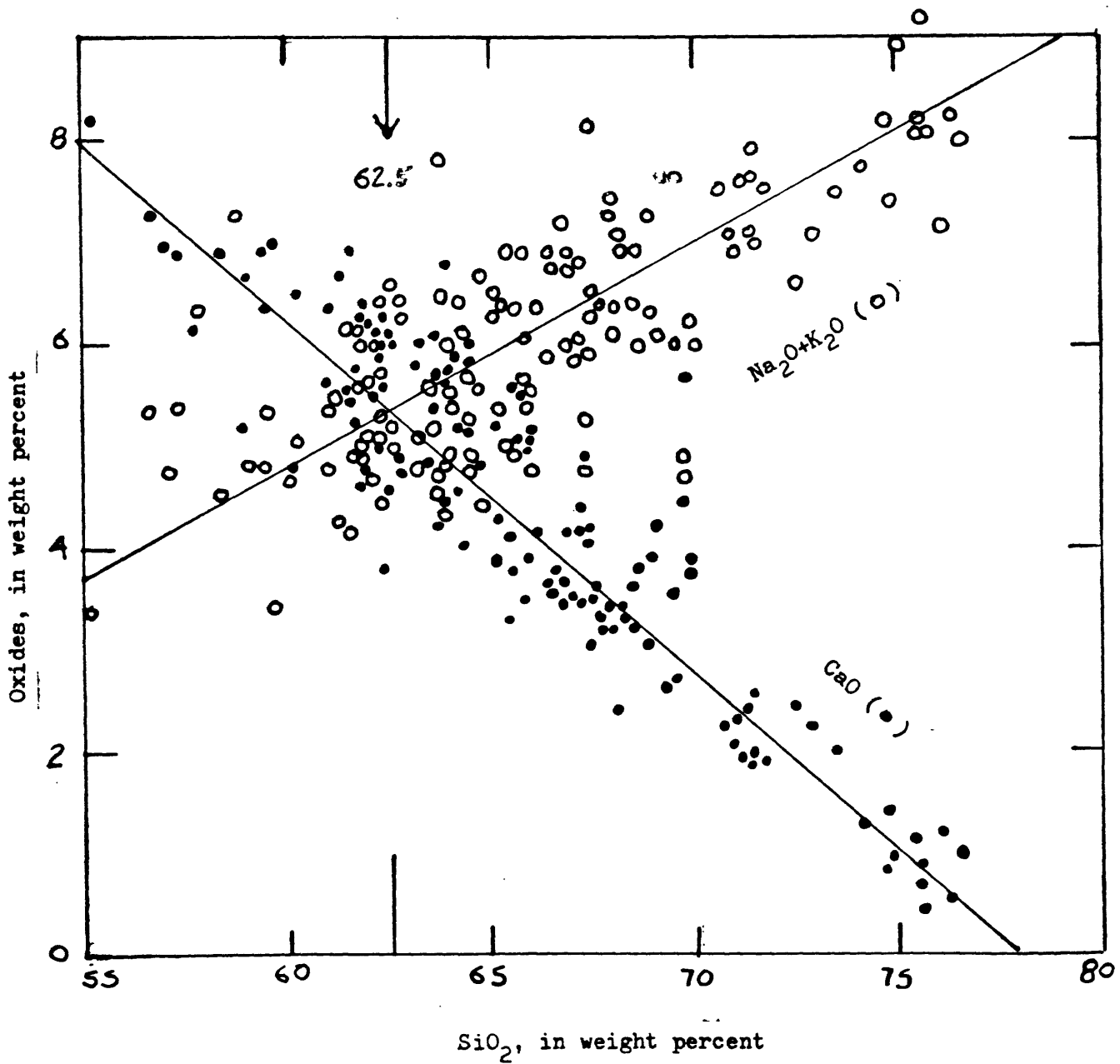


Figure 2. Plot of CaO and $\text{Na}_2\text{O} + \text{K}_2\text{O}$ against SiO_2 . Intersection of the two trends is the Peacock Index. Trend-lines are visually estimated.

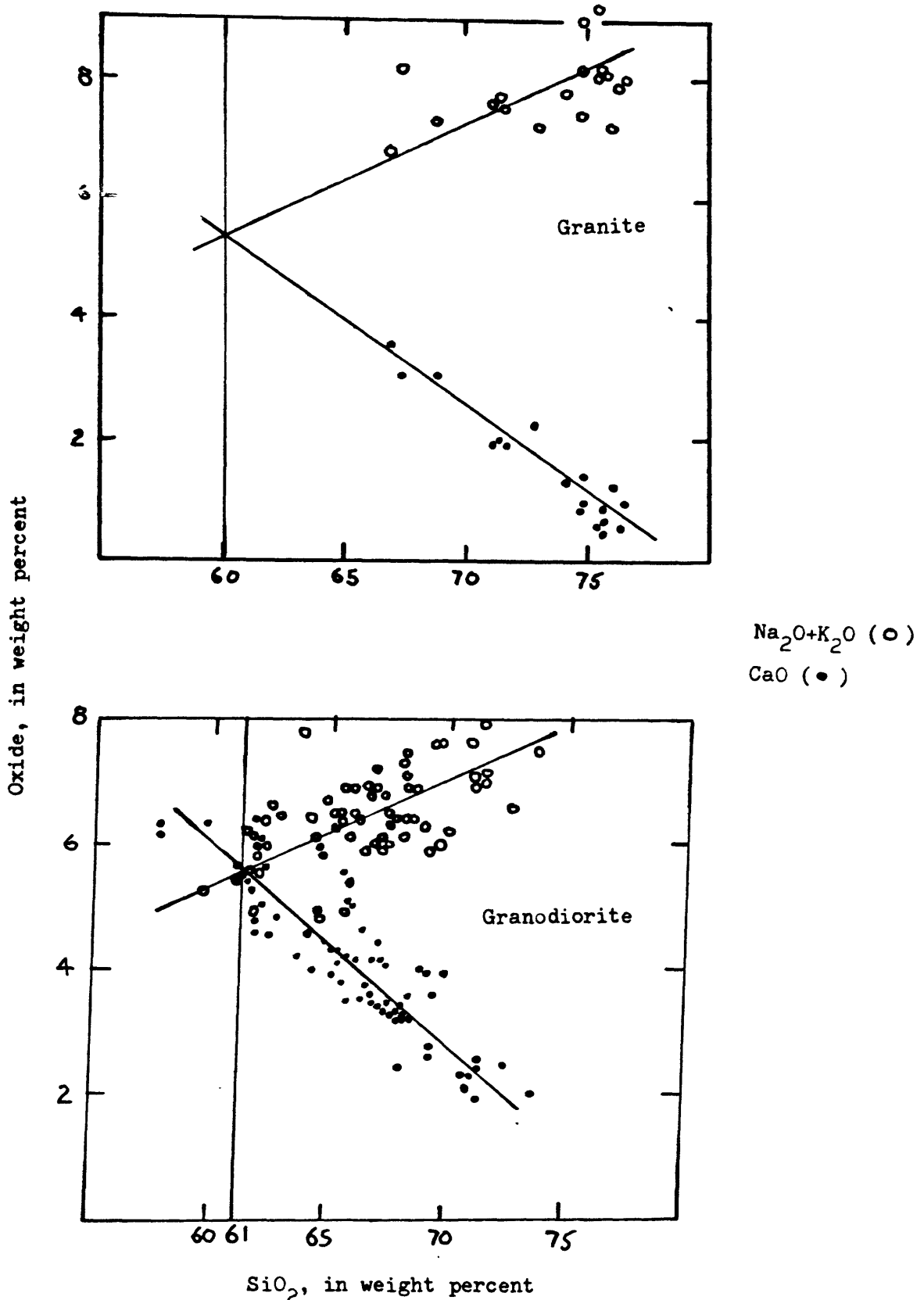


Figure 3. Peacock index, by rock type for granitic rocks of the southern Sierra Nevada. Trend lines, whose intersection is the Peacock index, were determined by visual estimates.

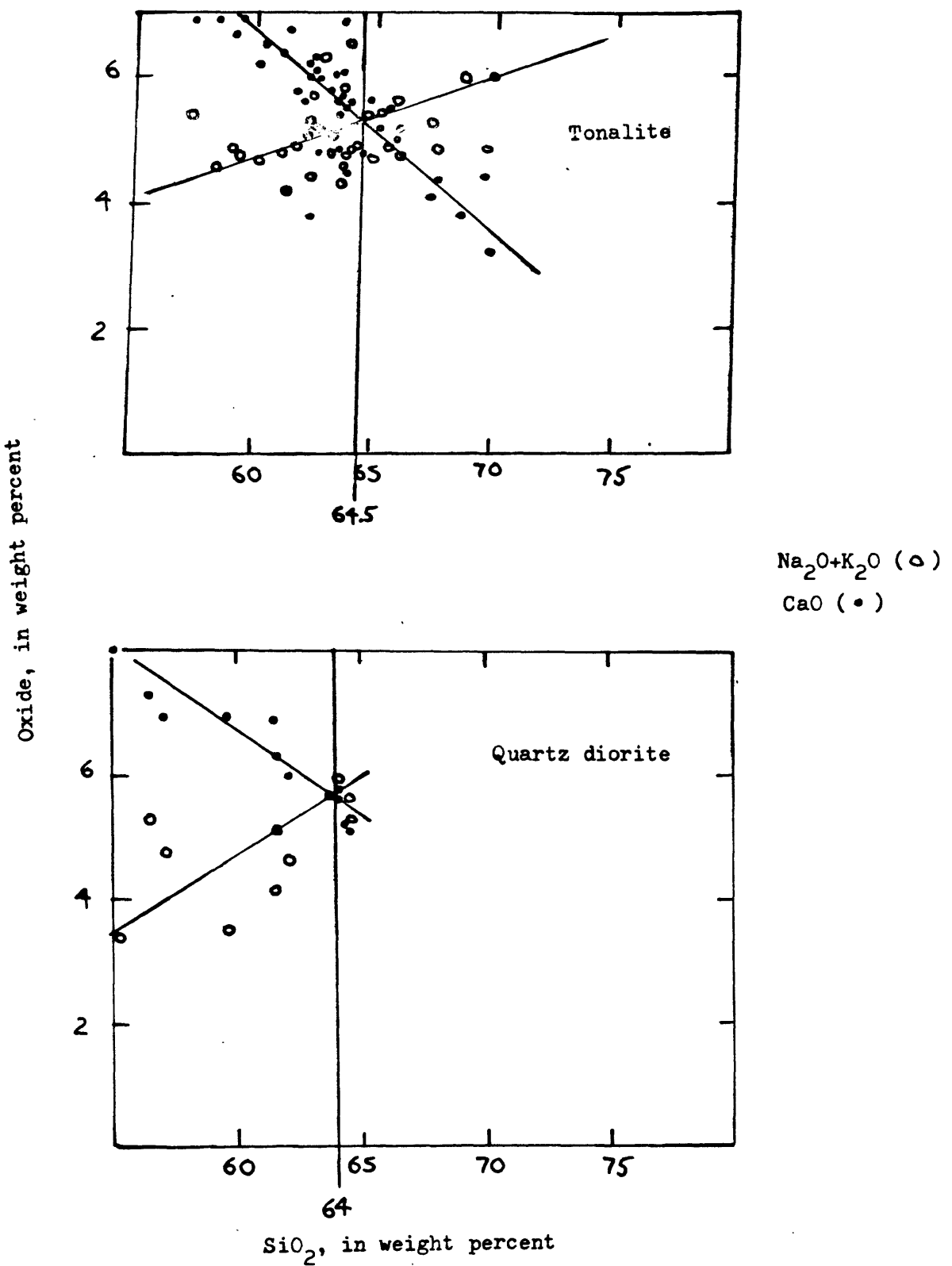


Figure 3. (cont.)

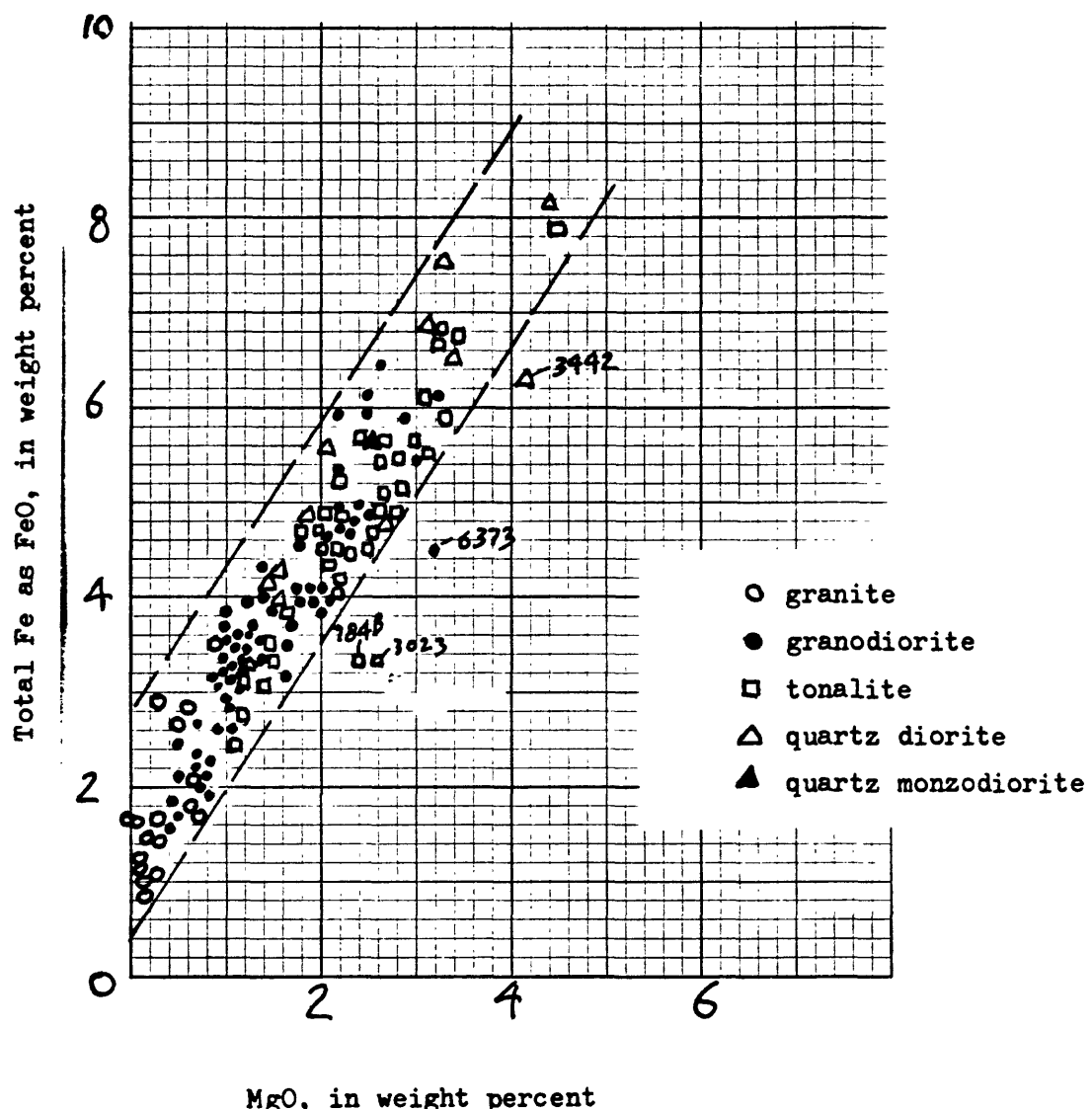


Figure 4. Total Fe as FeO^* ($0.9 \text{ Fe}_2\text{O}_3$ plus FeO) plotted against MgO for chemically analyzed samples of the southern Sierra Nevada. Numbered samples are discussed in text.

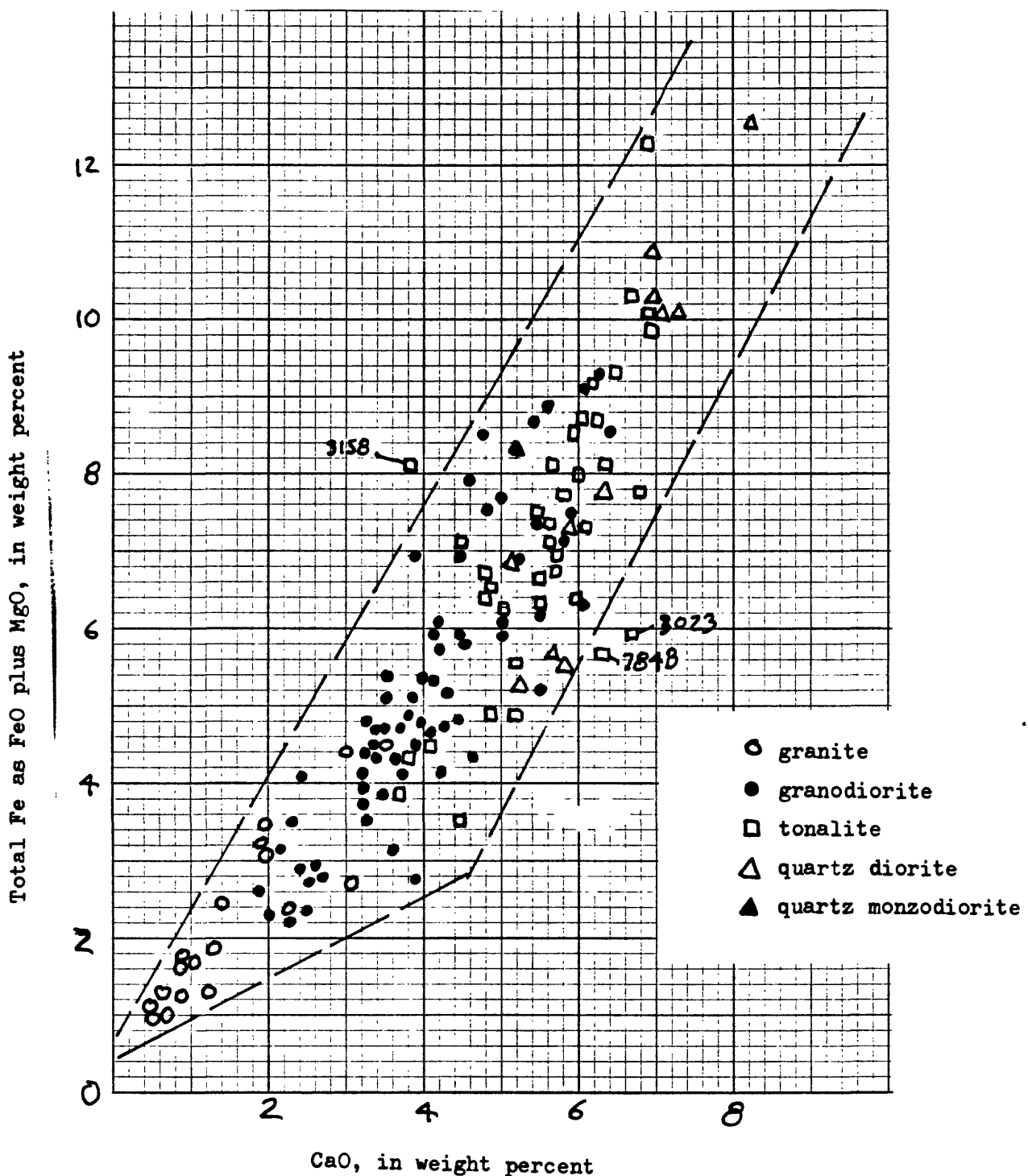


Figure 5. Total Fe as FeO plus MgO plotted against CaO for chemically analyzed samples of the southern Sierra Nevada. Numbered samples are discussed in text.

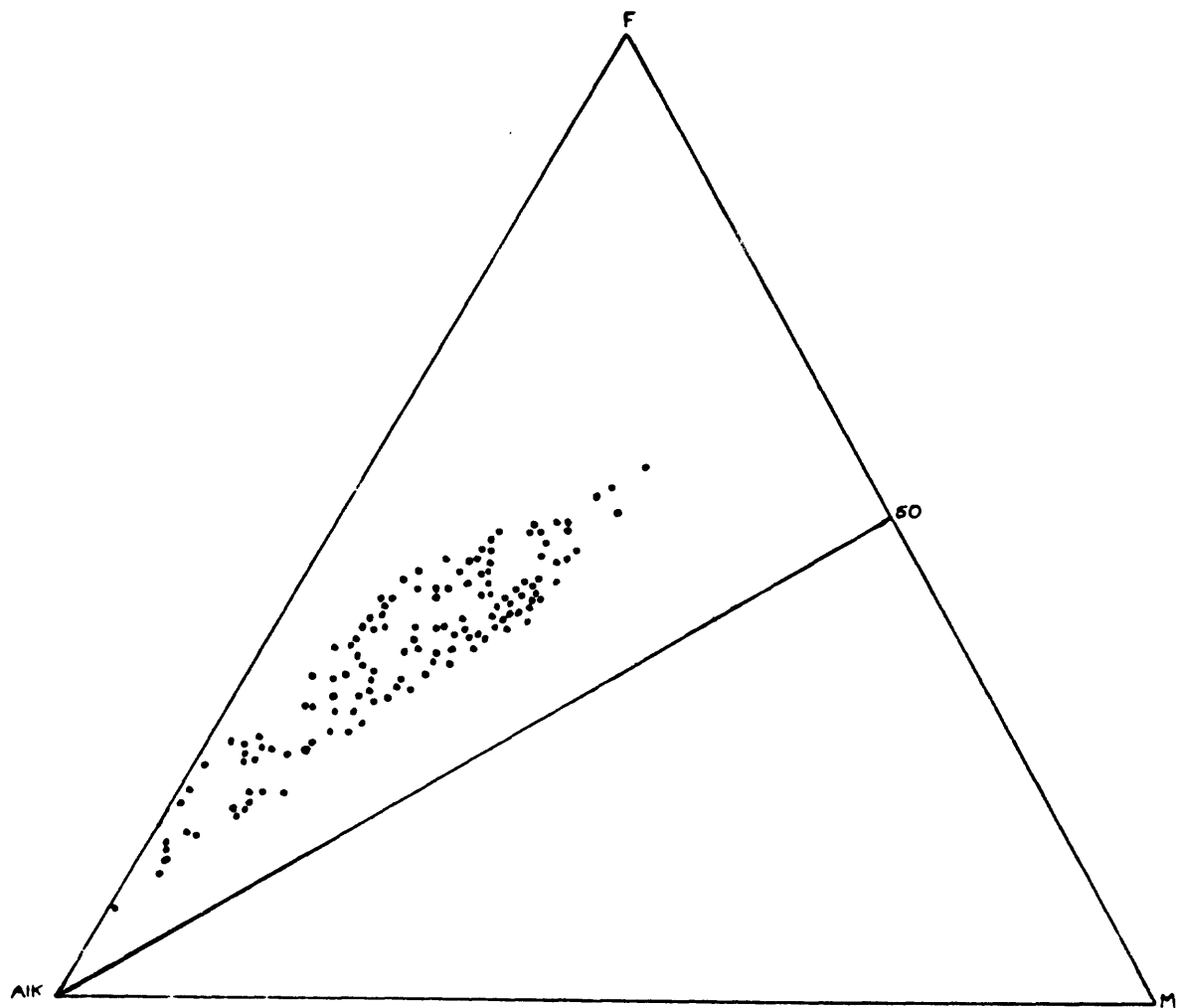


Figure 6. Triangular Alk-F-M plot for granitic rocks from the southern

Sierra Nevada, California

*
 Alk=Na₂O + K₂O
 F=FeO + 2Fe₂O₃ + MnO
 M=MgO

*
 3 components are normalized to total 100 percent using
 analytical amounts (not mole amounts as some Alk-F-M plots use)

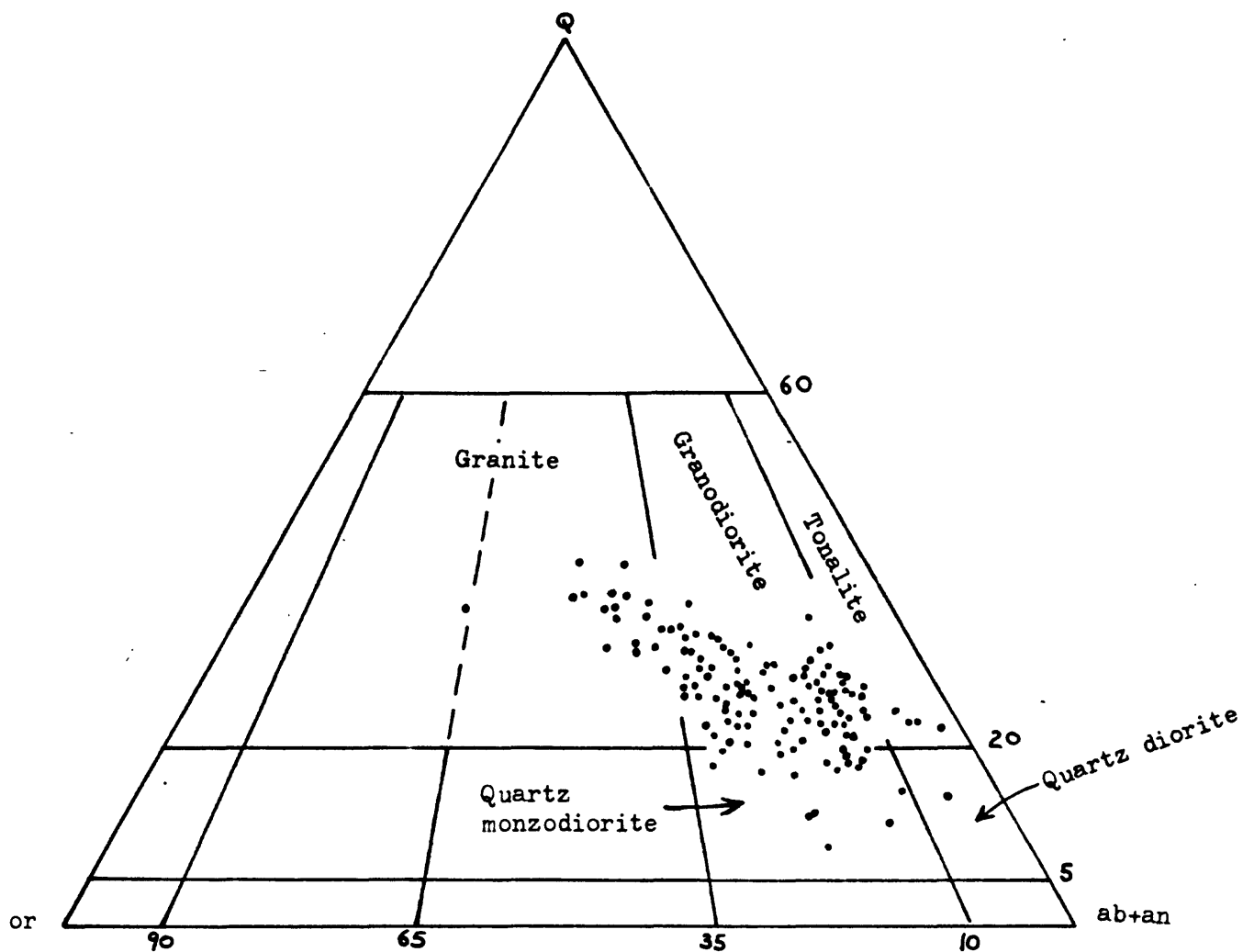
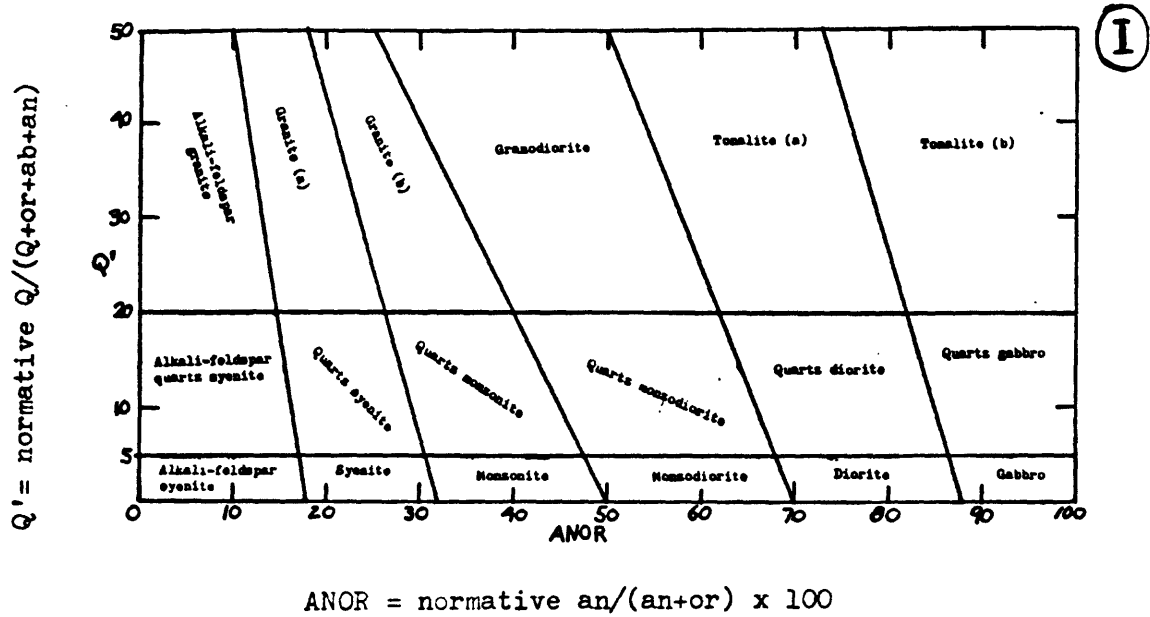


Figure 7 . Triangular plot of normative quartz (Q), orthoclase (or), and albite plus anorthite (ab + an) for granitic rocks of the southern Sierra Nevada, California. Superimposed on the triangle is the IUGS granitic rock modal classification.



$$\text{ANOR} = \text{normative an} / (\text{an} + \text{or}) \times 100$$

Figure 7A. Diagrams showing CIPW normative approximation to modal classification of chemically analyzed granitic rocks from the southern Sierra Nevada by the method of Streckeisen and LeMaitre (1979).

- I). Classification scheme of Streckeisen and Le Maitre
- II). Granite
- III). Granodiorite
- IV). Tonalite
- V). Quartz diorite and quartz monzodiorite

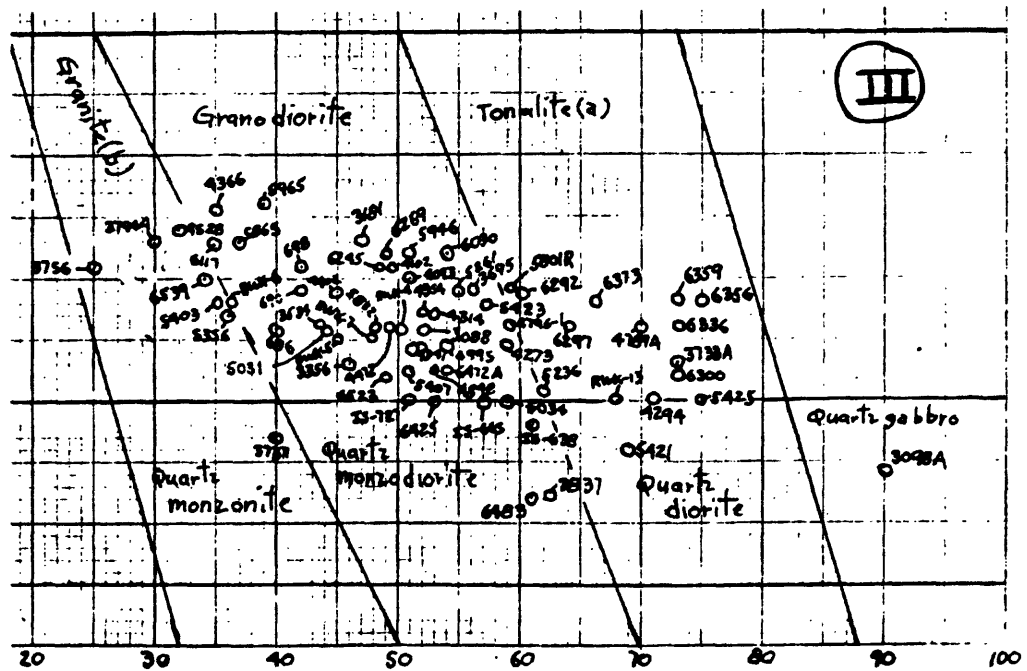
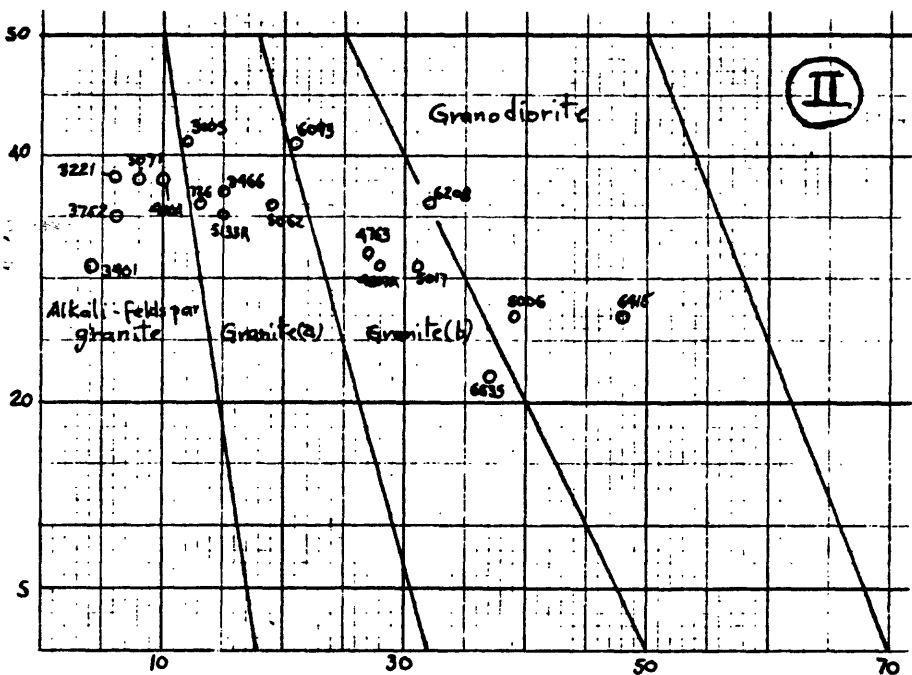


Figure 7A (cont.).

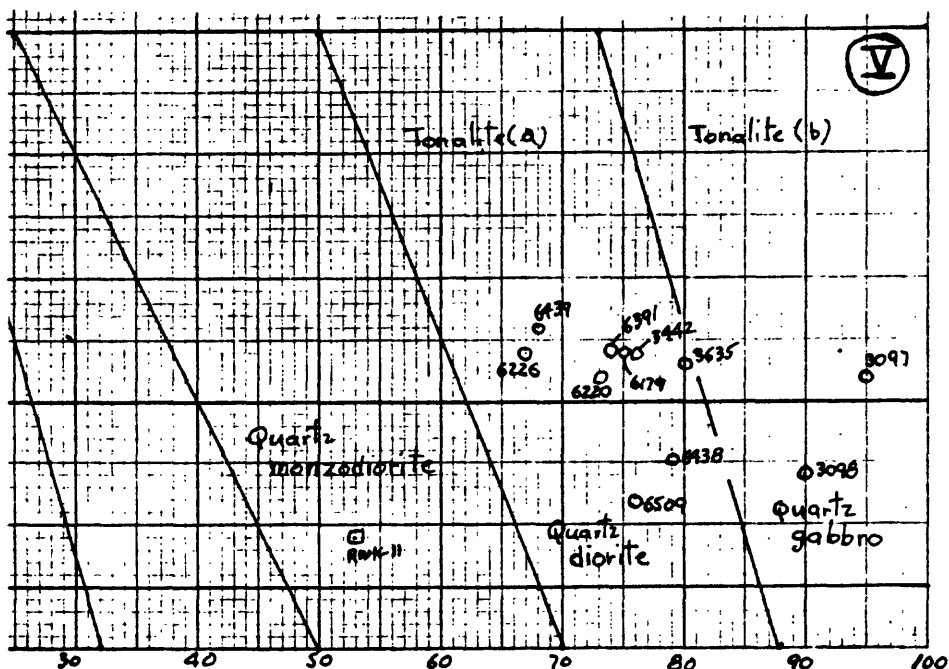
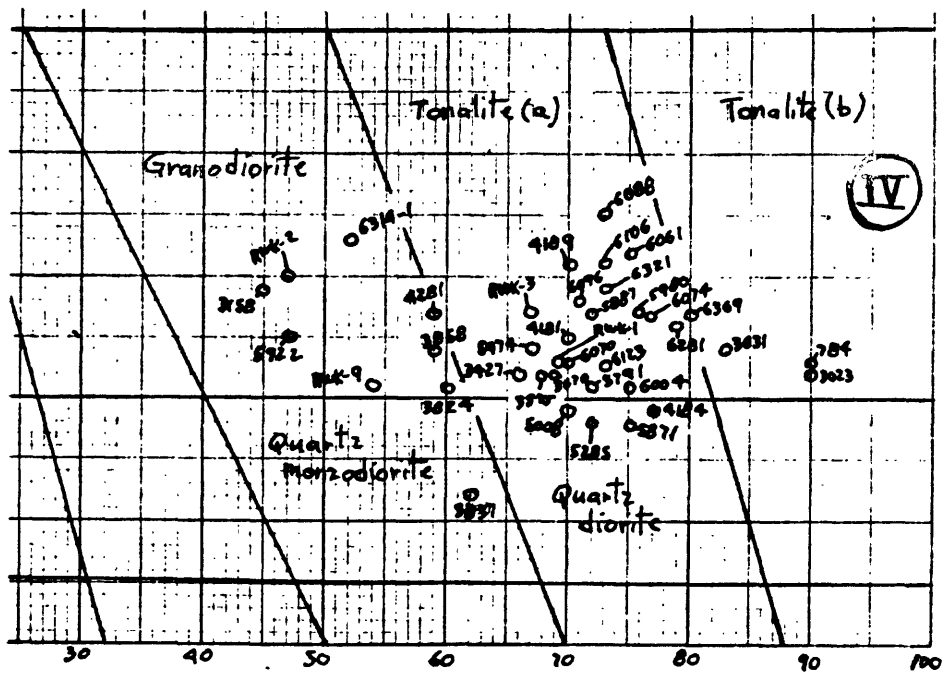


Figure 7A (cont.)

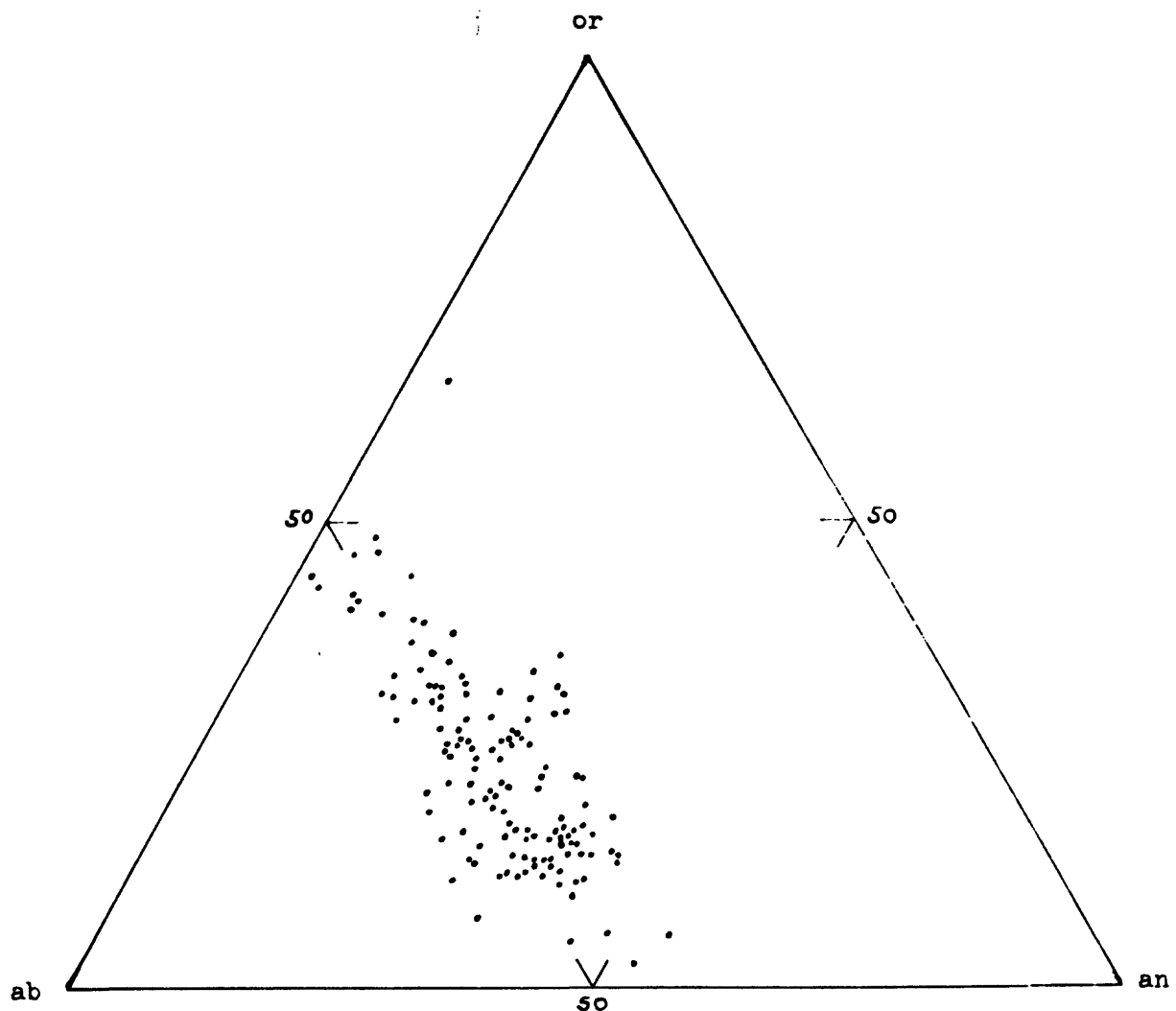


Figure 8. Triangular plot of normative orthoclase (or), albite (ab), and anorthite (an) for granitic rocks of the southern Sierra Nevada, California

EXPLANATION

Samples from the southern Sierra Nevada

Trondhjemite samples from the central Sierra Nevada (Ward Mountain, Butteman and others, 1964)

O Trondhjemite samples from the northern Sierra Nevada (Rocklin pluton, Olmsted, 1971; and the Bald Rock batholith, Hietanen, 1951; Larsen and Poldergaard, 1961; and Turner, 1994)

▲ Trondhjemite samples from the Klamath Mountains (Caribou Mountain pluton, Davis, 1963; Craggy Peak and White Rock plutons, Hotz, 1971; and Gibson Peak pluton, Lipman, 1963)

□ Trondhjemite samples from Idaho (Riggins area, Hamilton, 1962)

■ Trondhjemite samples from Norway (Goldschmidt, 1916)

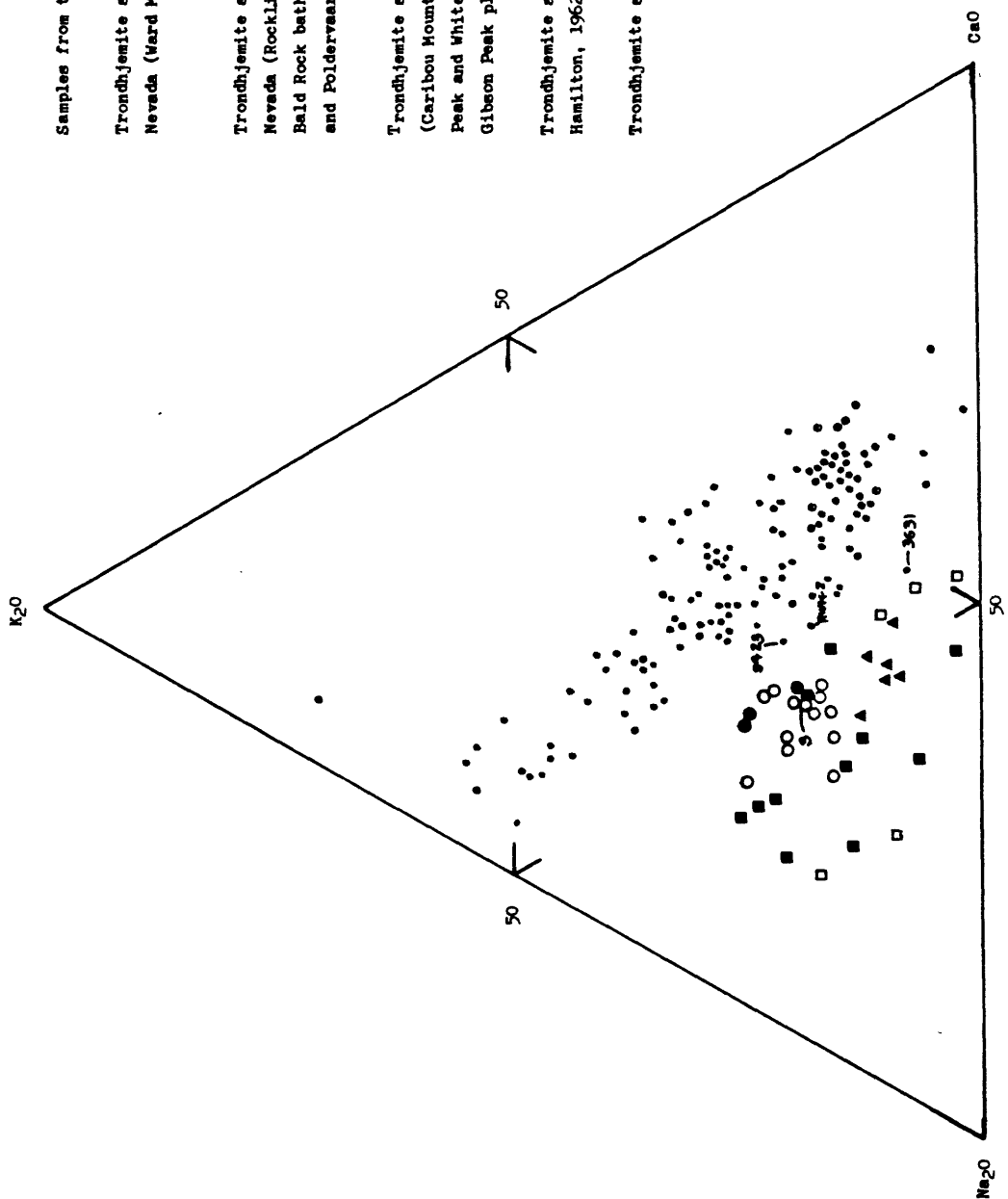


Figure 9A. $\text{CaO-Na}_2\text{O-K}_2\text{O}$ plot comparing samples from the southern Sierra Nevada with selected trondhjemites.

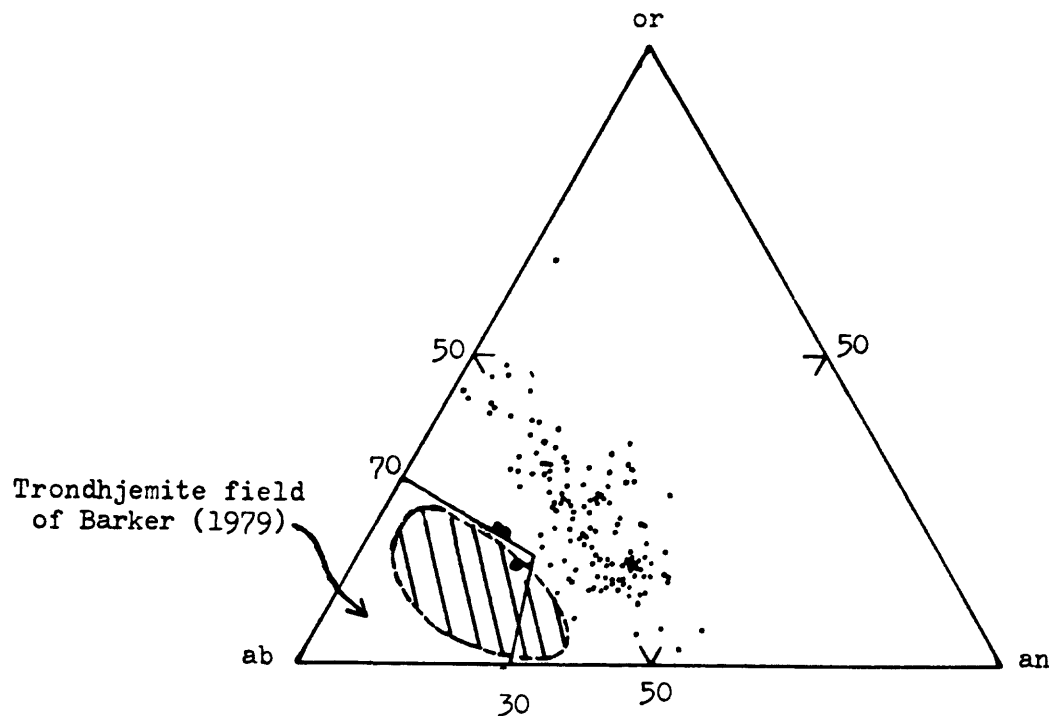


Figure 9B. Trondhjemite field of Barker (1979) superposed on or-ab-an triangular diagram. Cross-lined field encloses trondhjemites of figure 9A except for trondhjemites of Ward Mountain (Bateman and others, 1984), which are shown by three large dots. Small dots are chemically analyzed granitic rocks from the southern Sierra Nevada.

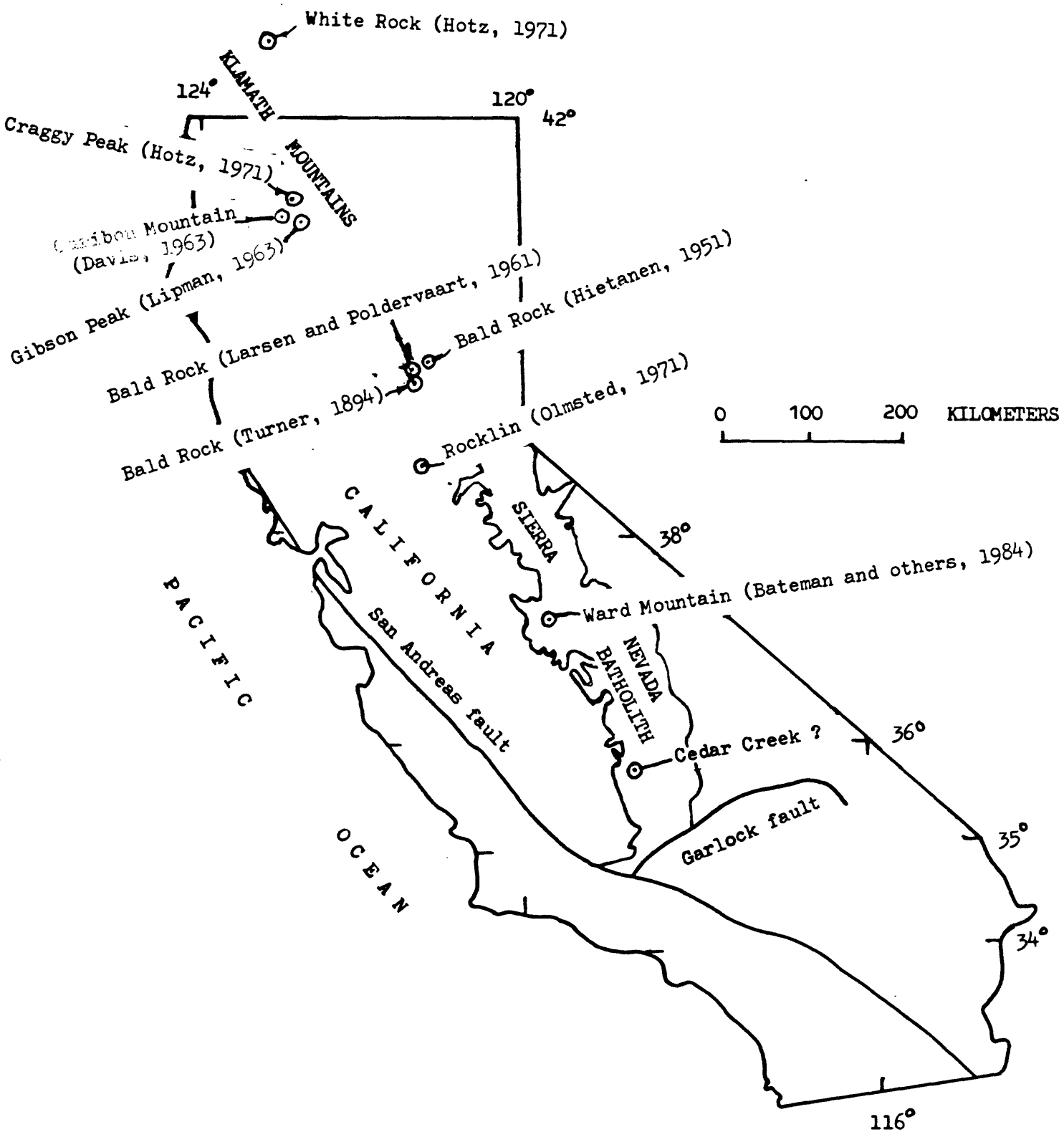


Figure 10. Index map showing some trondhjemite localities in the Sierra Nevada and Klamath Mountains.

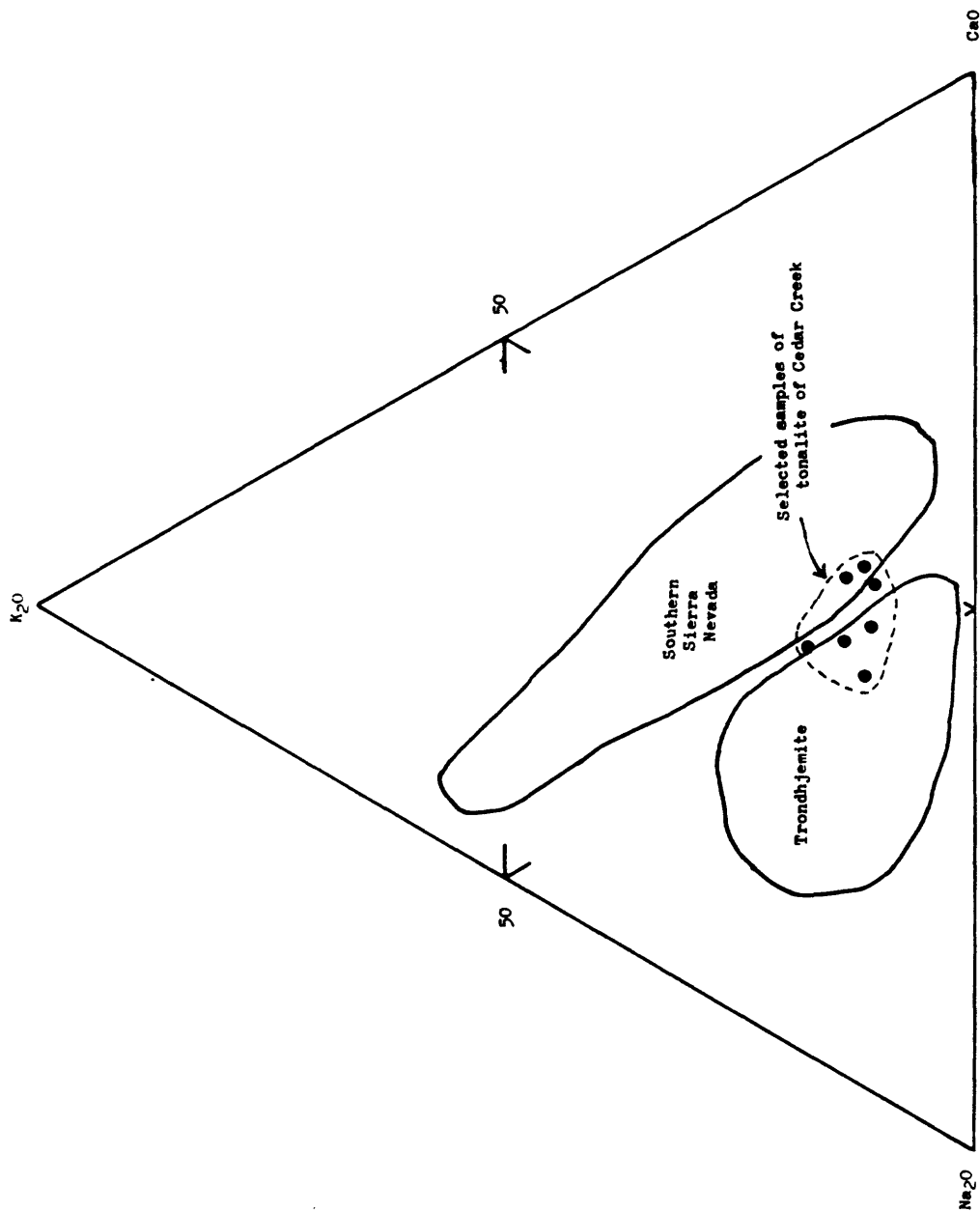


Figure 11. CaO-Na₂O-K₂O plot showing relation of some Cedar Creek tonalitic samples to trondhjemites and other southern Sierra Nevada samples (fields based on figure 9A). Chemical data from Cedar Creek samples estimated from modes.

118°22'30"

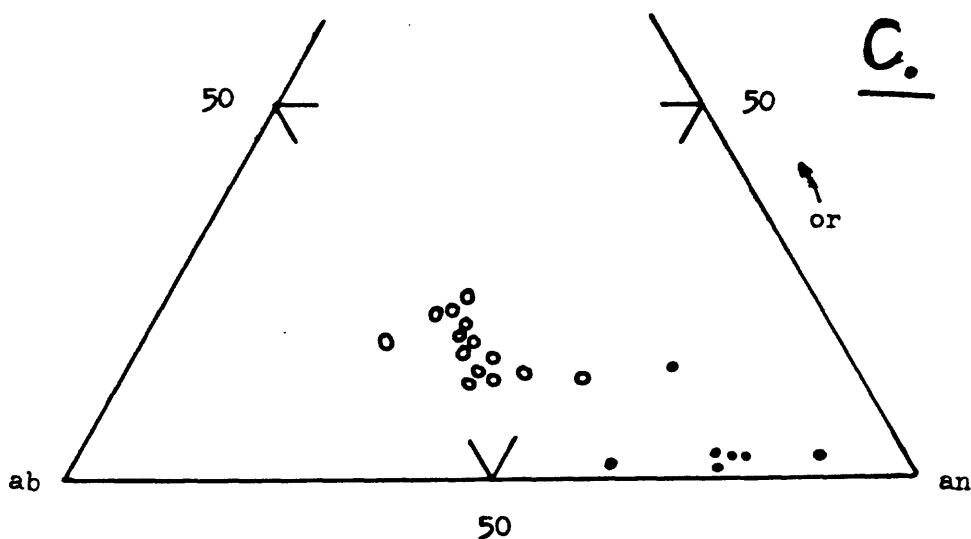
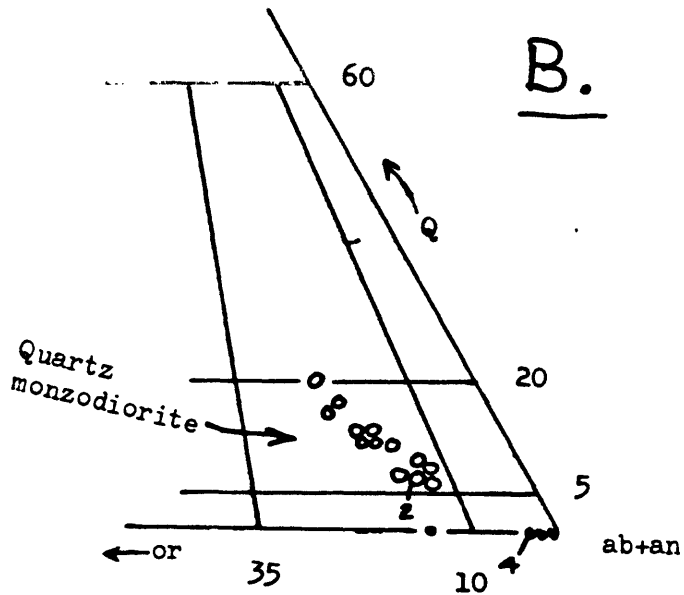
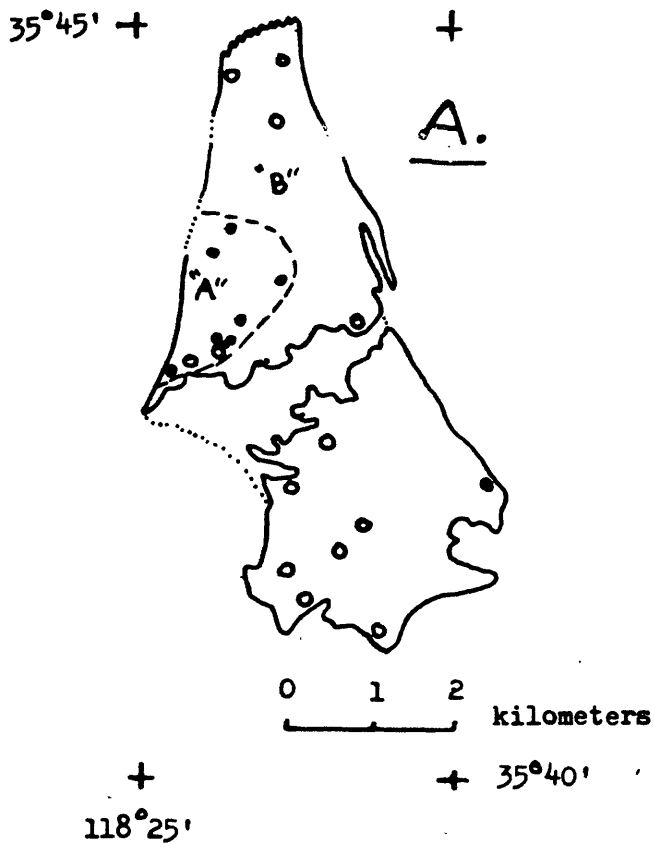


Figure 12. Kernville pluton of Fox (1981)

A. Index map showing location of chemically analyzed samples and outline of units "A" and "B"

B. Triangular plot of normative quartz (Q), orthoclase (or), and plagioclase (ab+an)

C. Triangular plot of normative orthoclase (or), albite (ab), and anorthite (an)

Figure 13. Histograms showing trace element abundances. For some elements abundance range shown by rock type. Average crustal abundances values for granite and granodiorite (arrows) taken from Taylor (1965), except for some of the Lanthanides which are based on Turekian and Wedepohl's (1961) estimates.

- A. Ba, Co, Cr, Cs, Hf, Rb, and Tl
- B. Th, U, Zn, and Zr
- C. Sc, La, Ce, Nd, and Sm
- D. Eu, Gd, Tb, Tm, Yb, and Lu

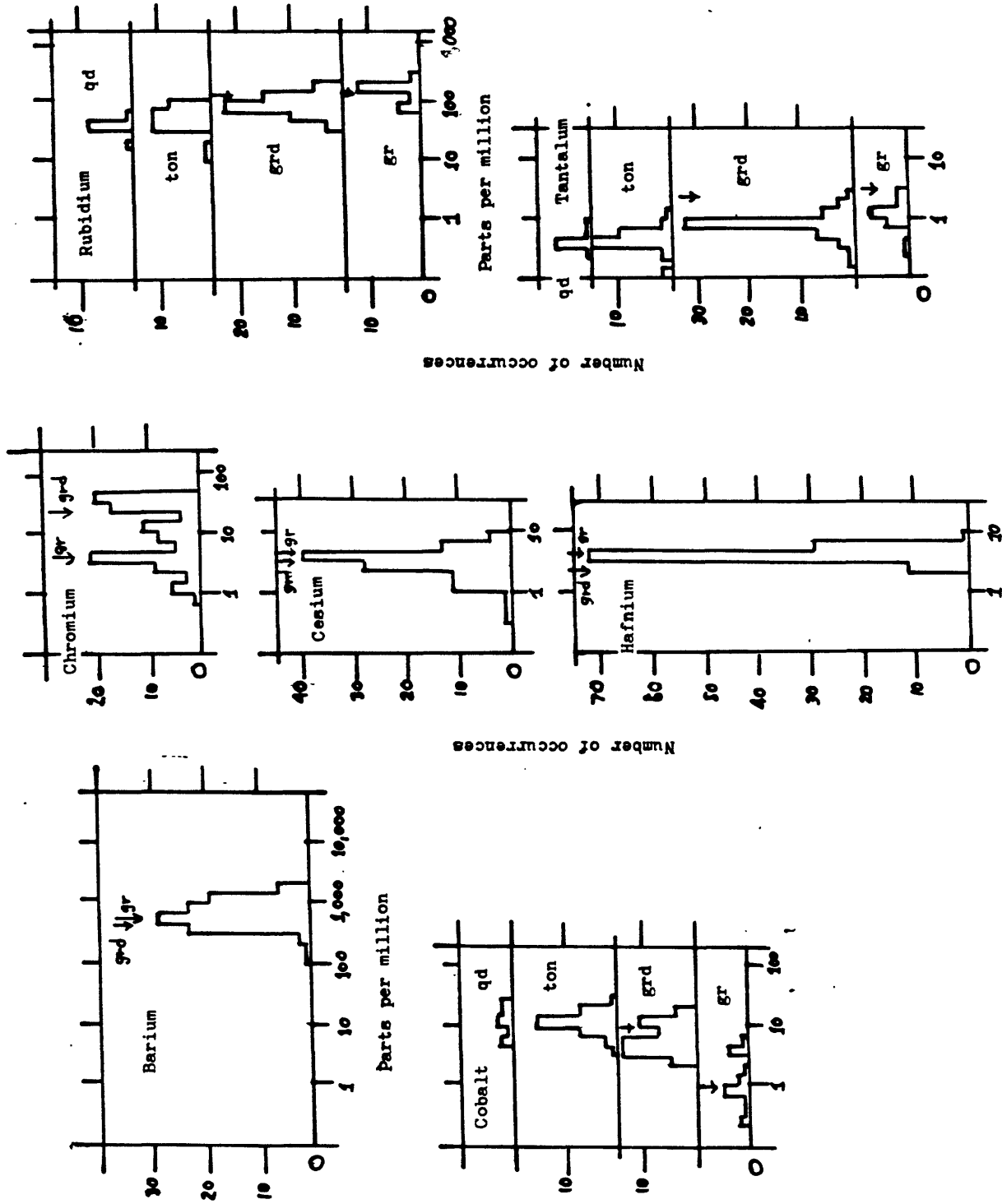
A

Figure 13A. Histograms for Ba, Co, Cr, Cs, Hf, Rb, and Tl.

B

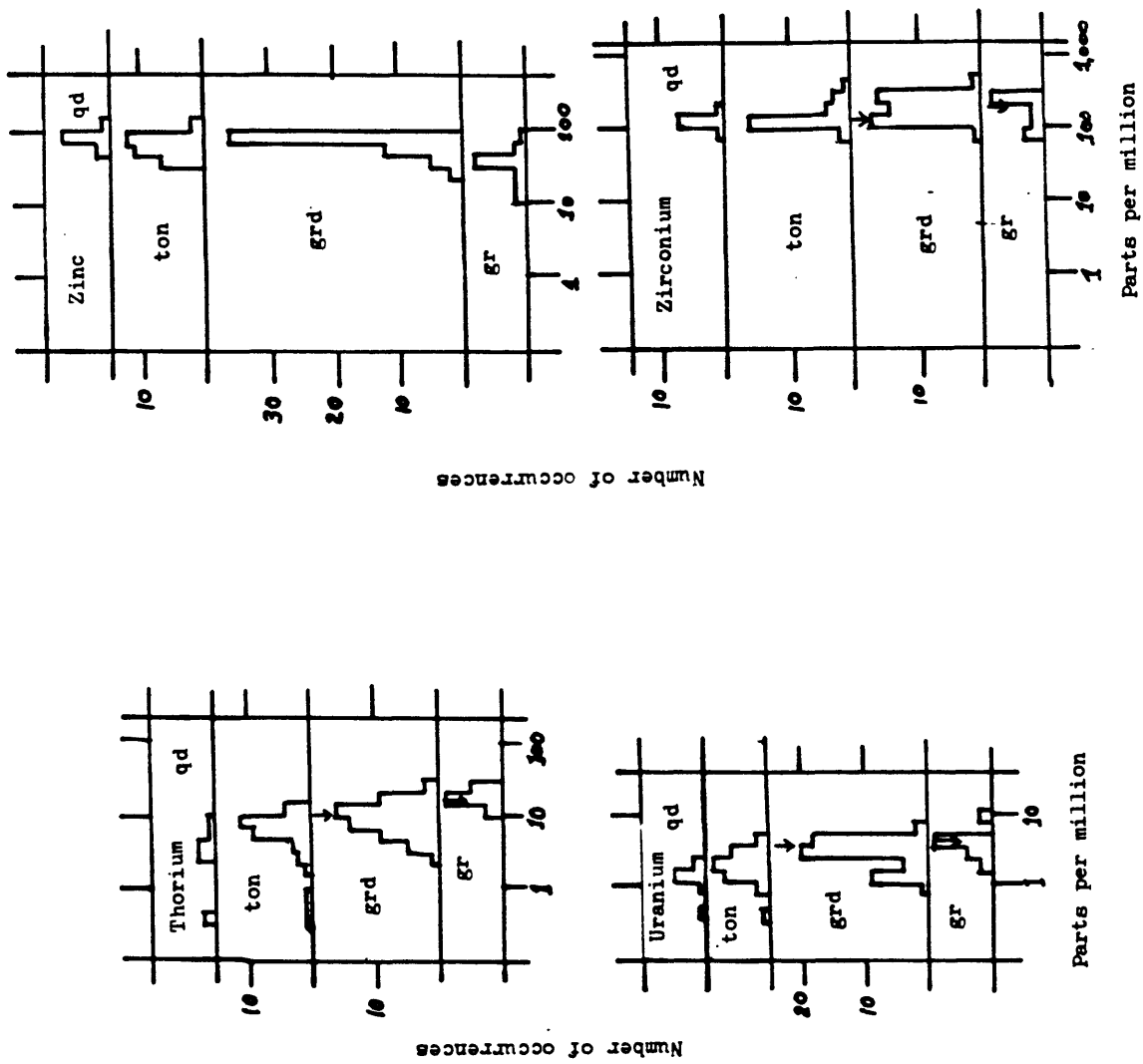


Figure 13B. Histograms for Th, U, Zn, and Zr.

C

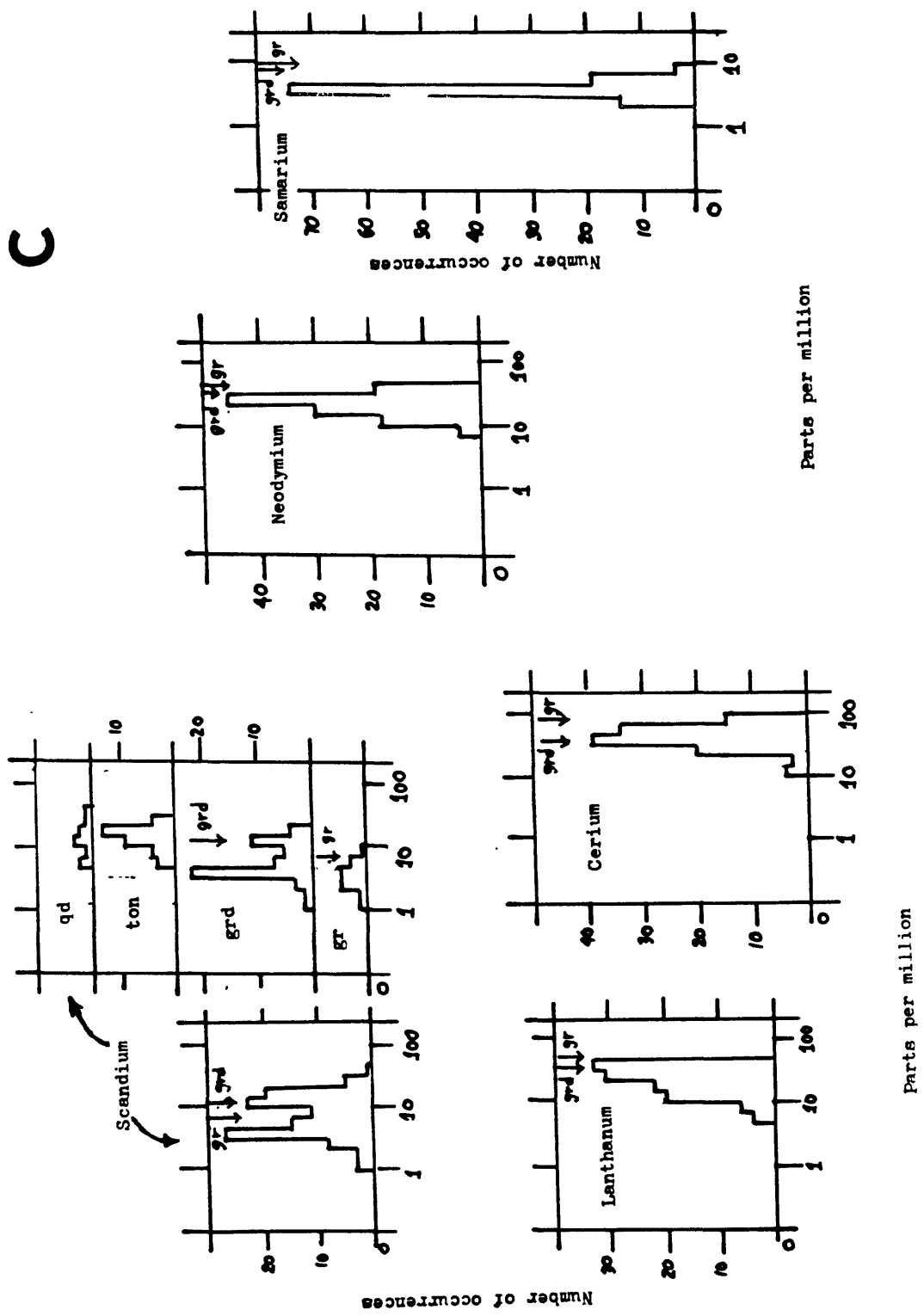


Figure 13 C. Histograms for Sc, La, Ce, Nd, and Sm.

D

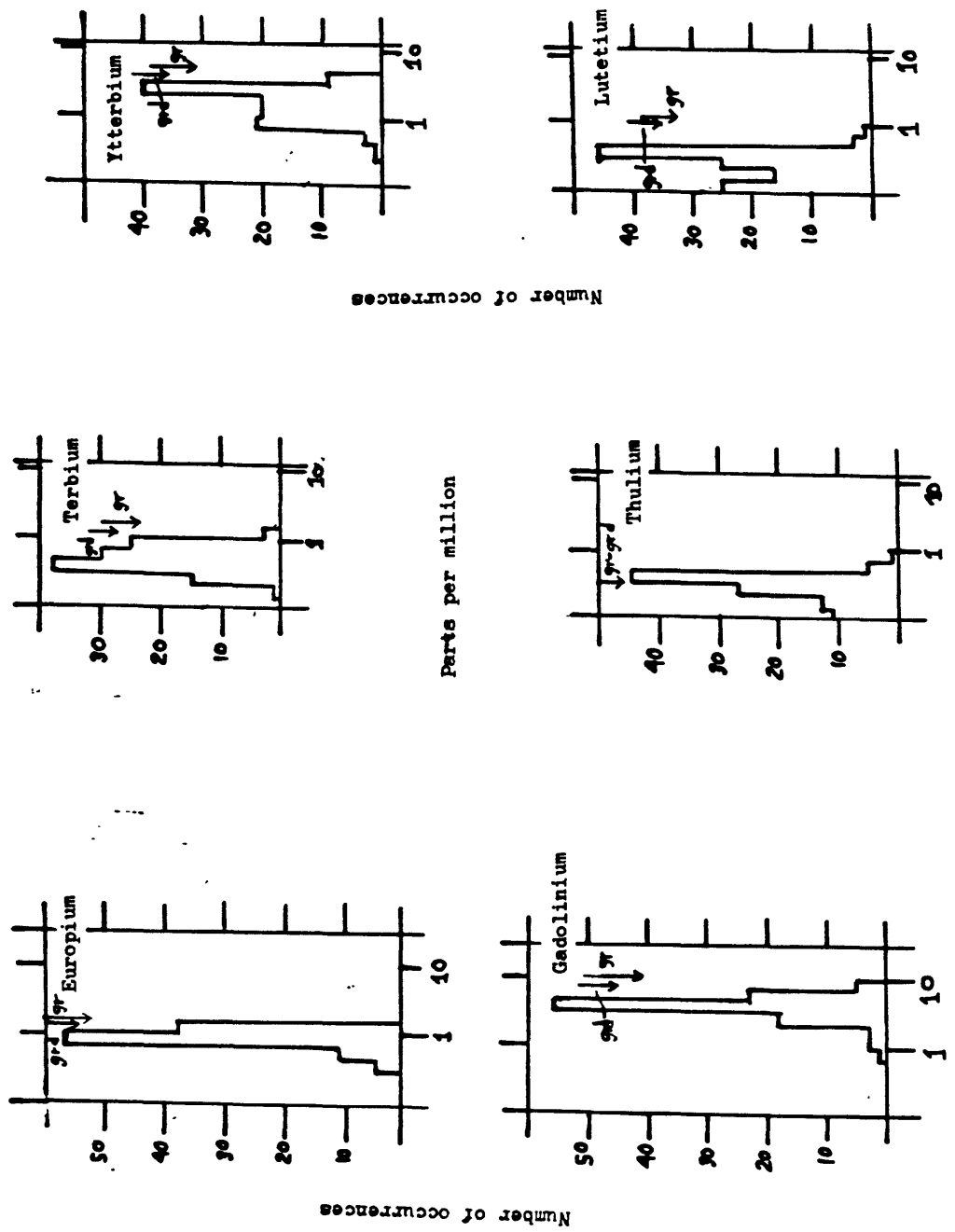


Figure 13 D. Histograms for Eu, Gd, Tb, Tm, Yb, and Lu.

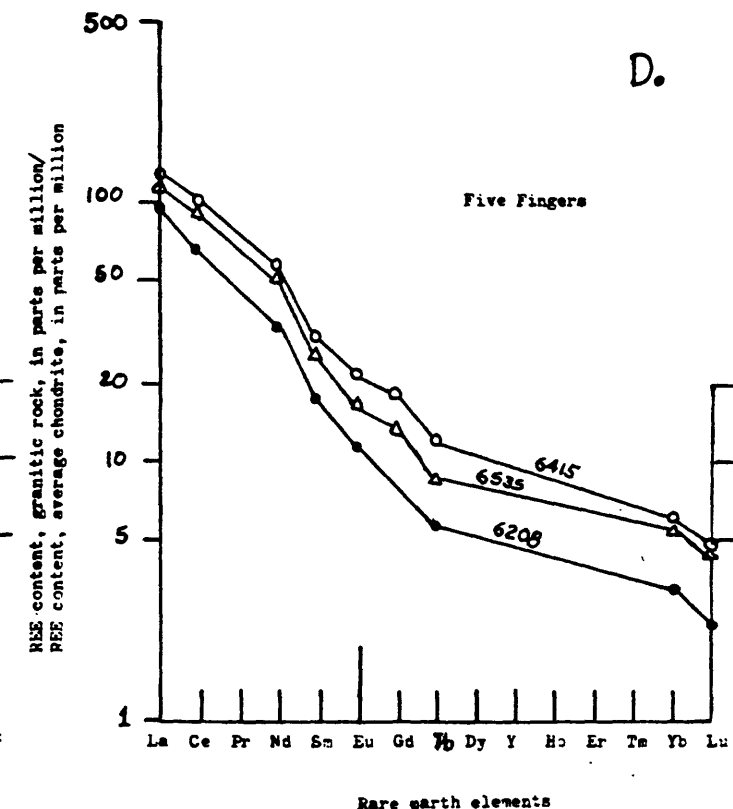
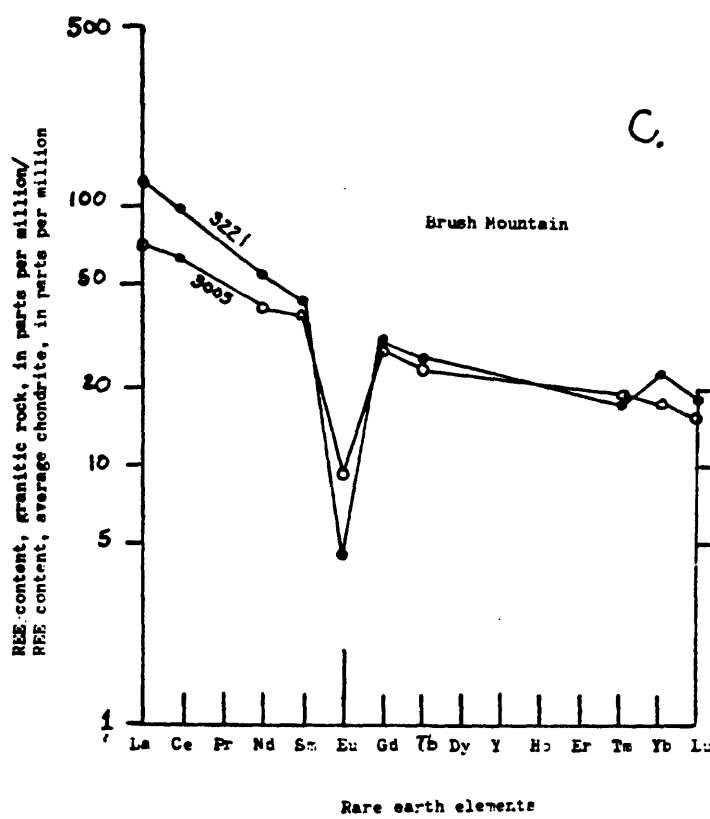
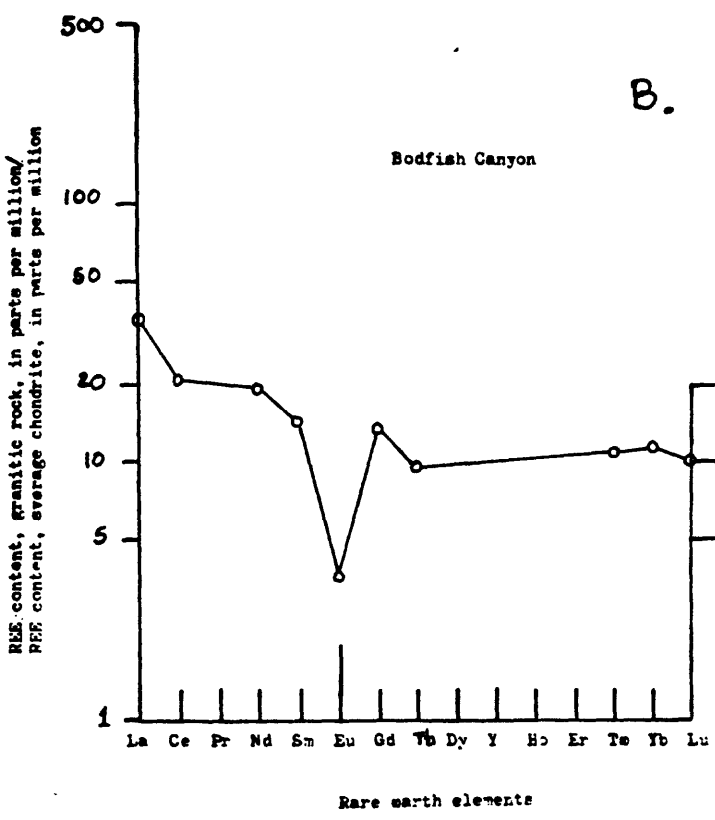
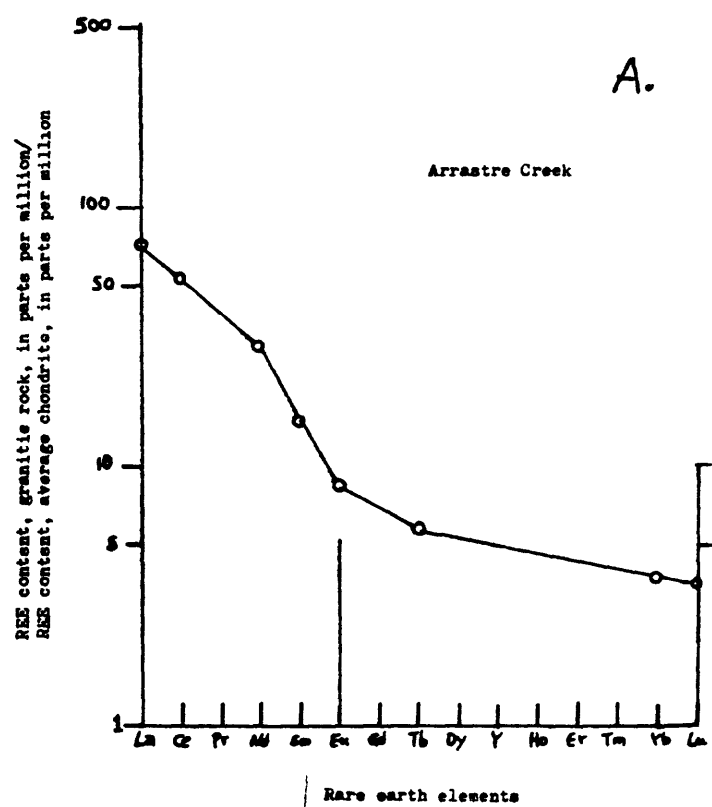


Figure 14. Rare earth element (REE) chondrite normalized abundance diagrams for granite bodies.

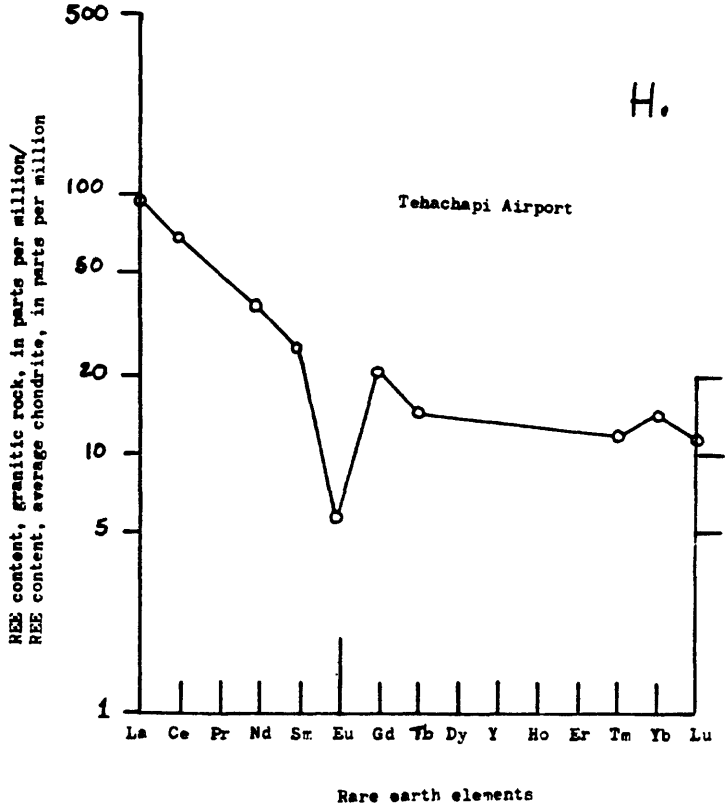
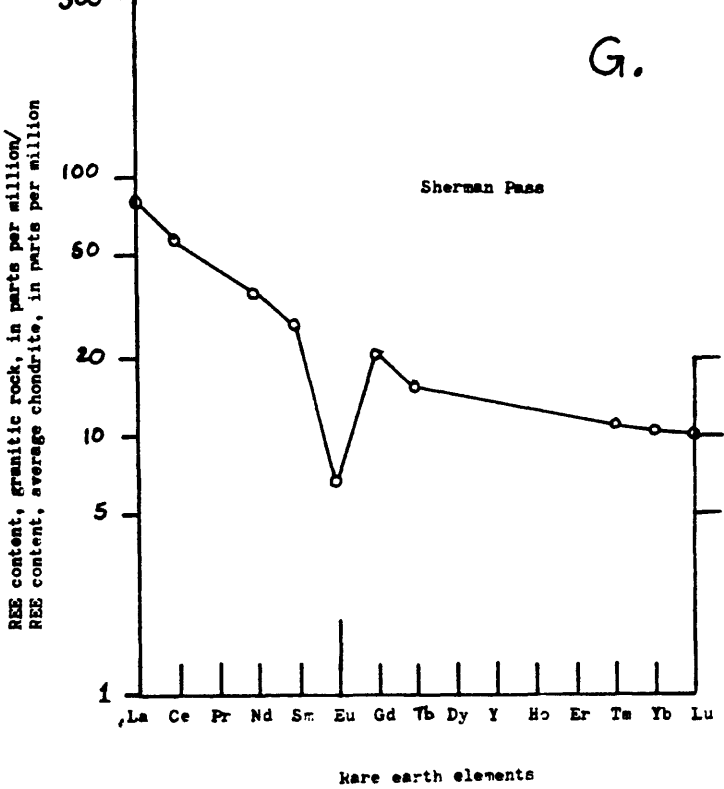
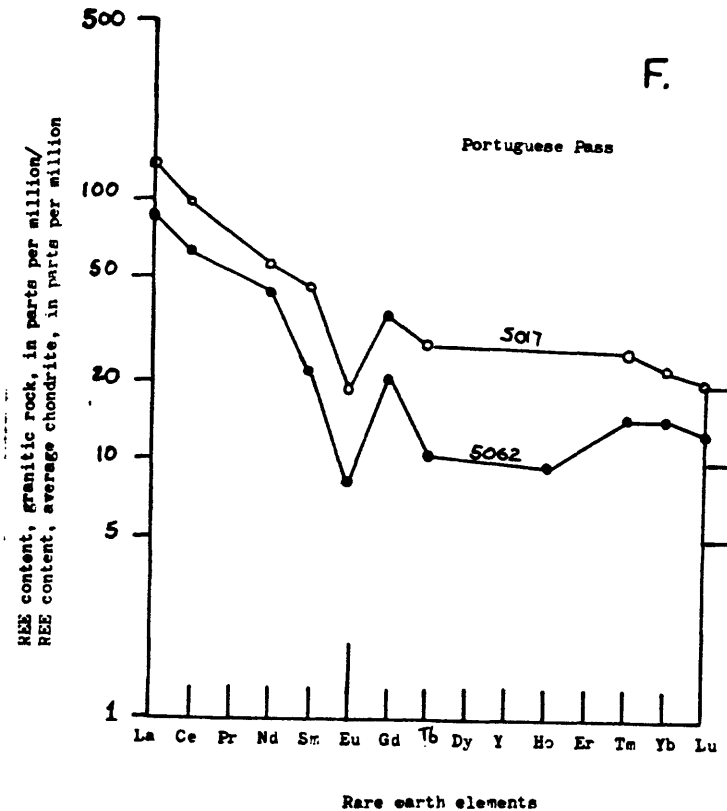
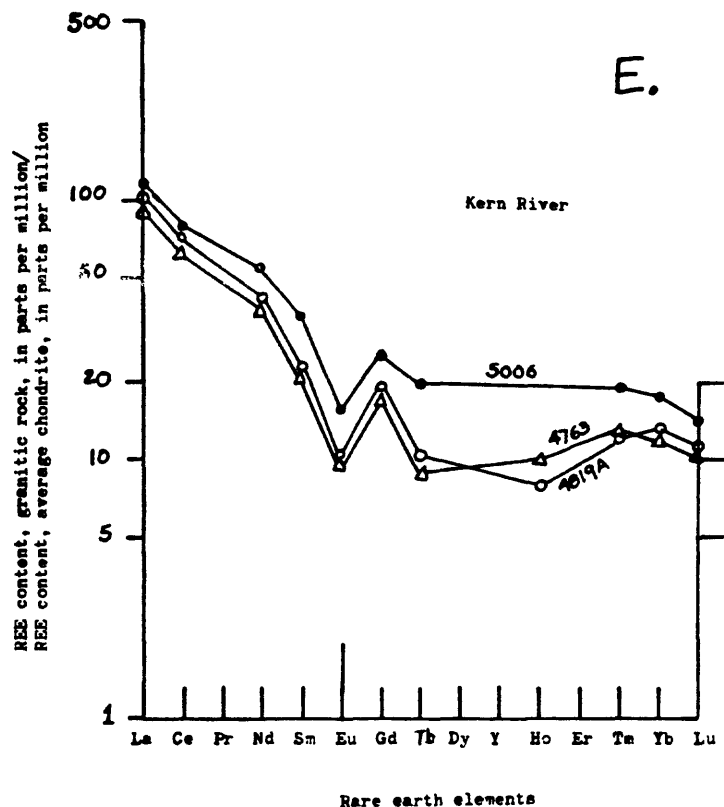


Figure 14. (cont.)

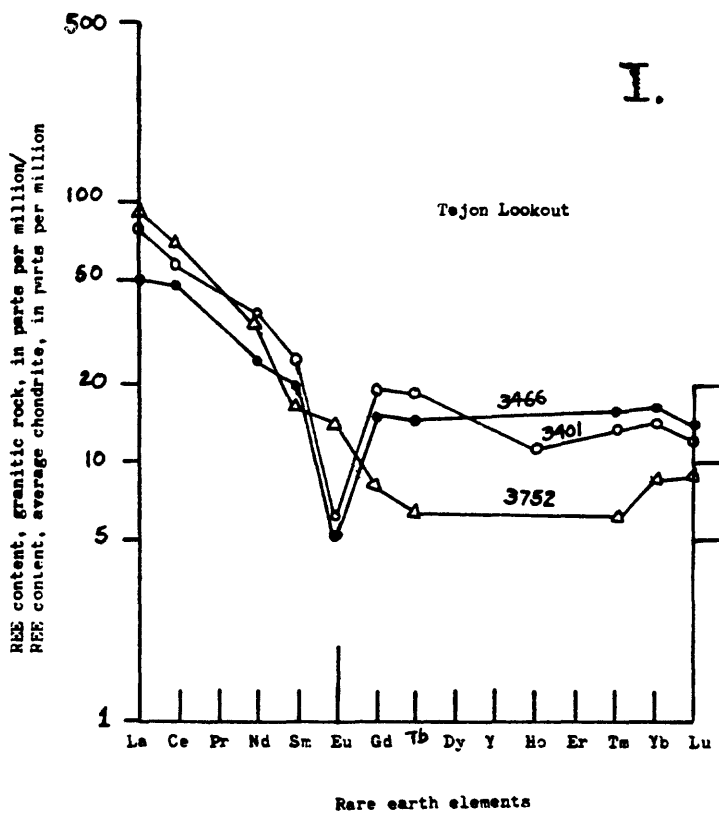


Figure 14. (cont.)

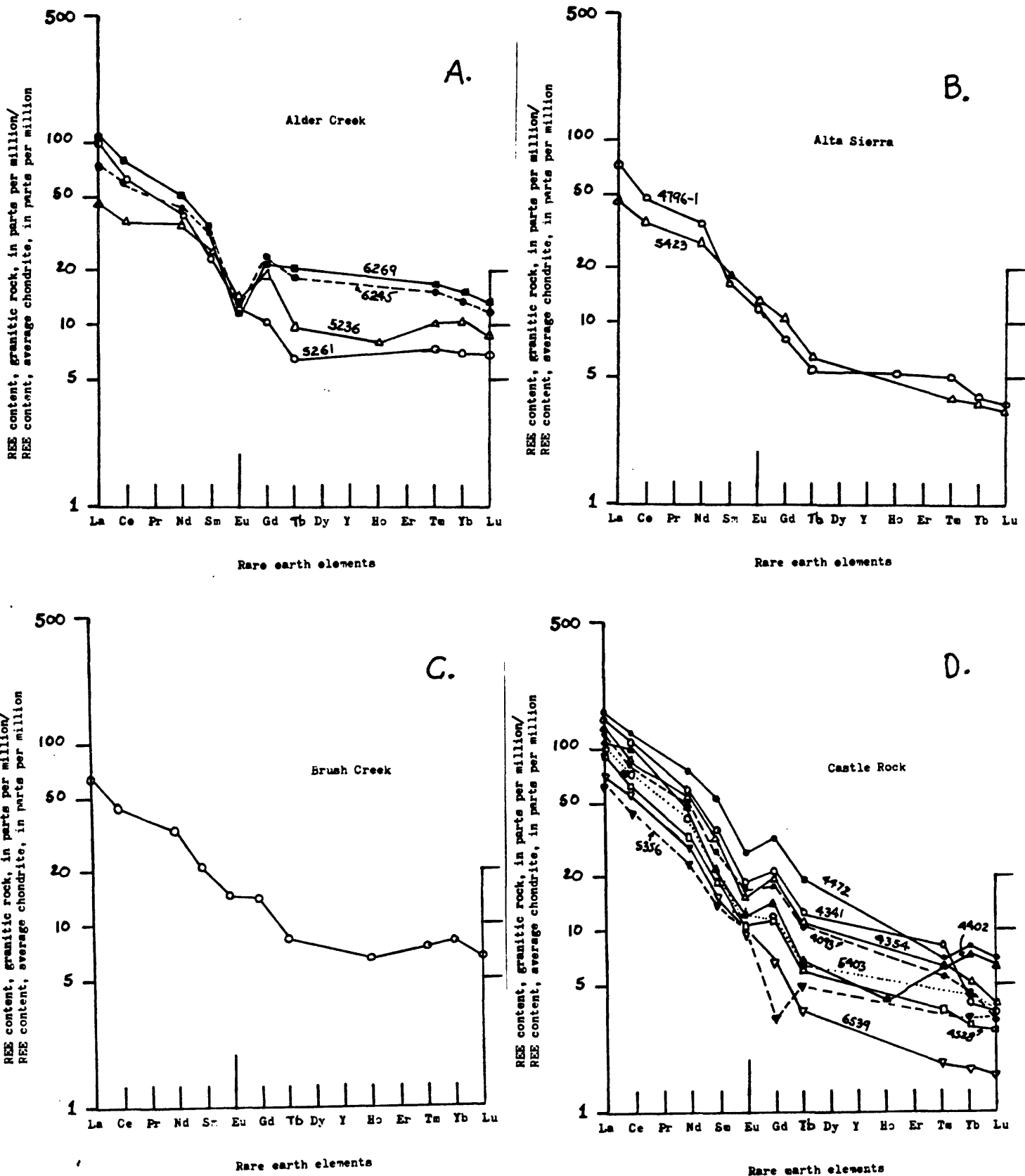


Figure 15. Rare earth element (REE) chondritic normalized abundance diagrams for granodiorite bodies.

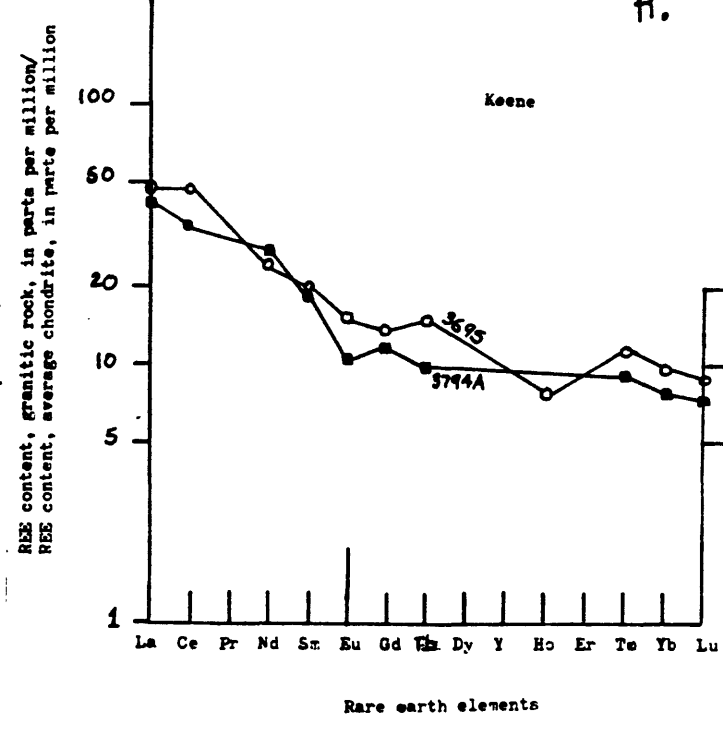
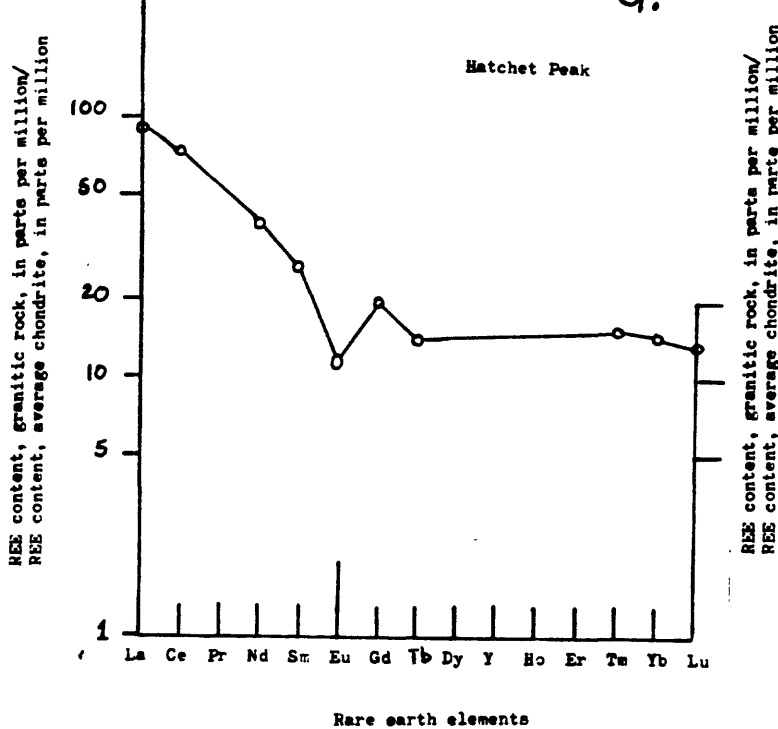
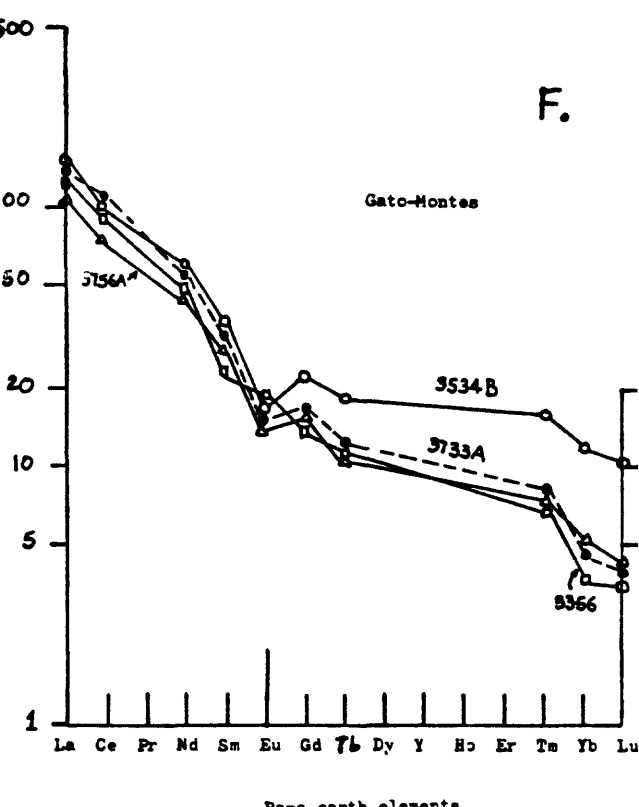
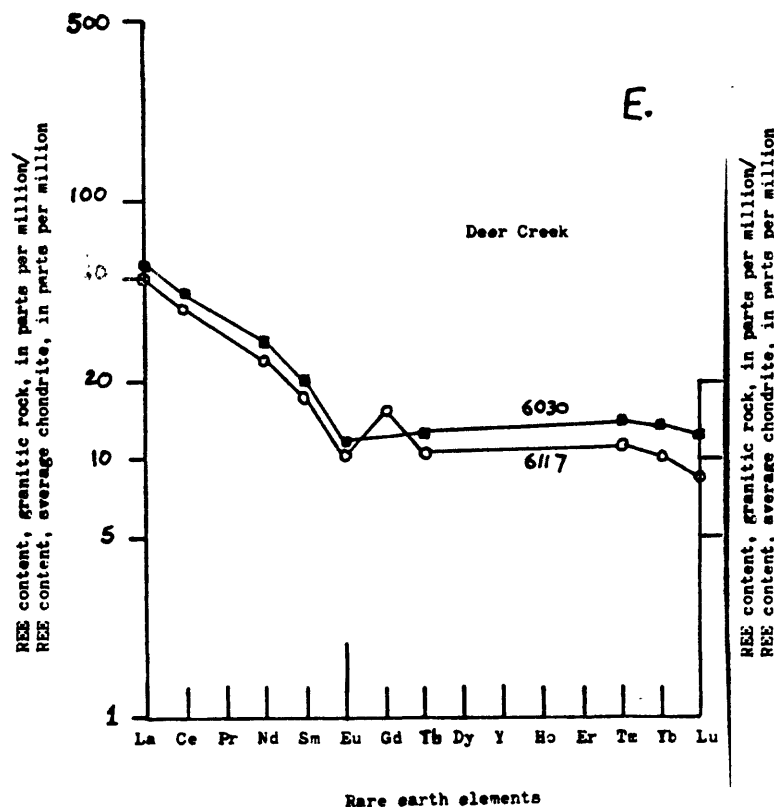


Figure 15. (cont.)

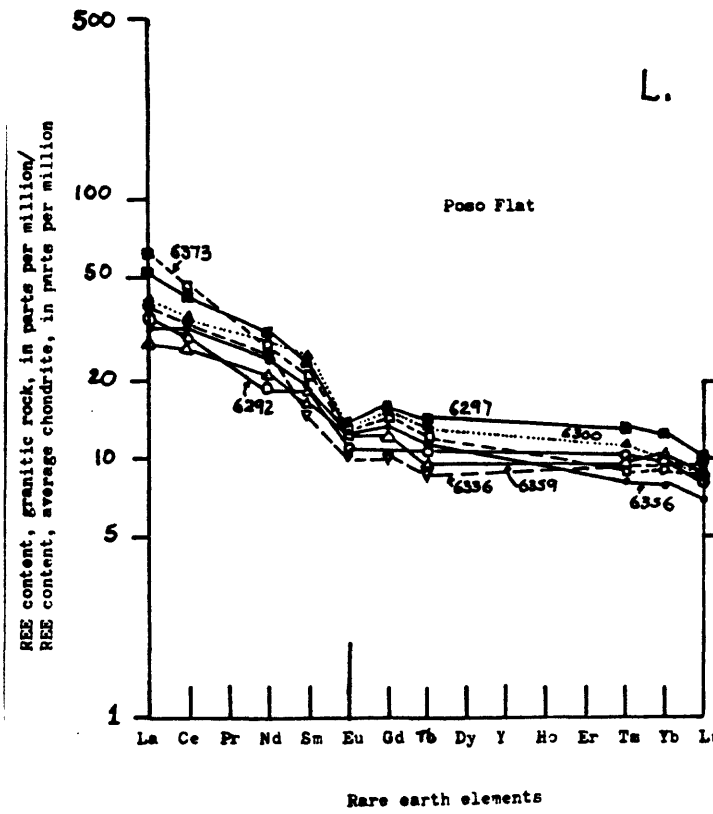
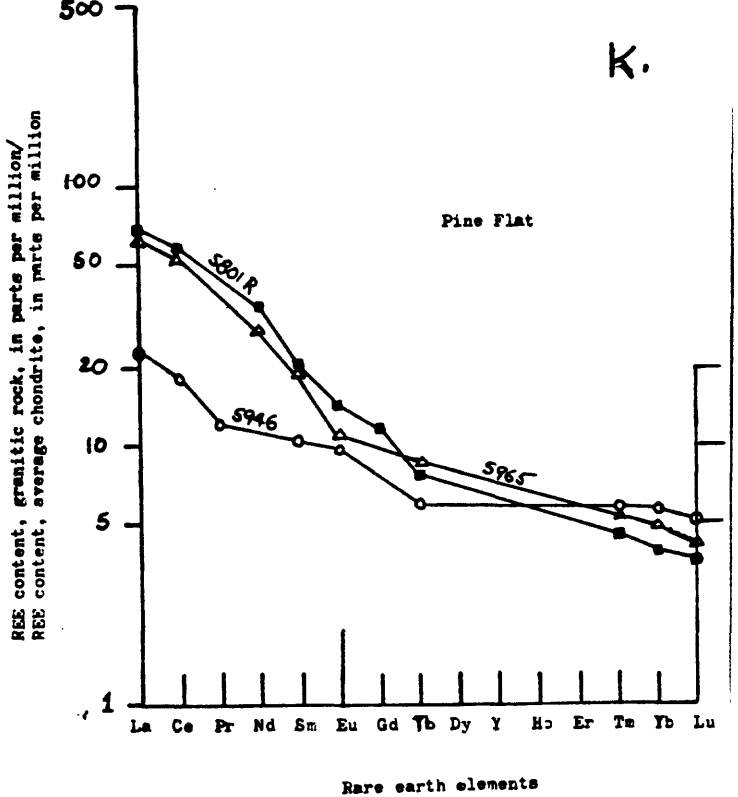
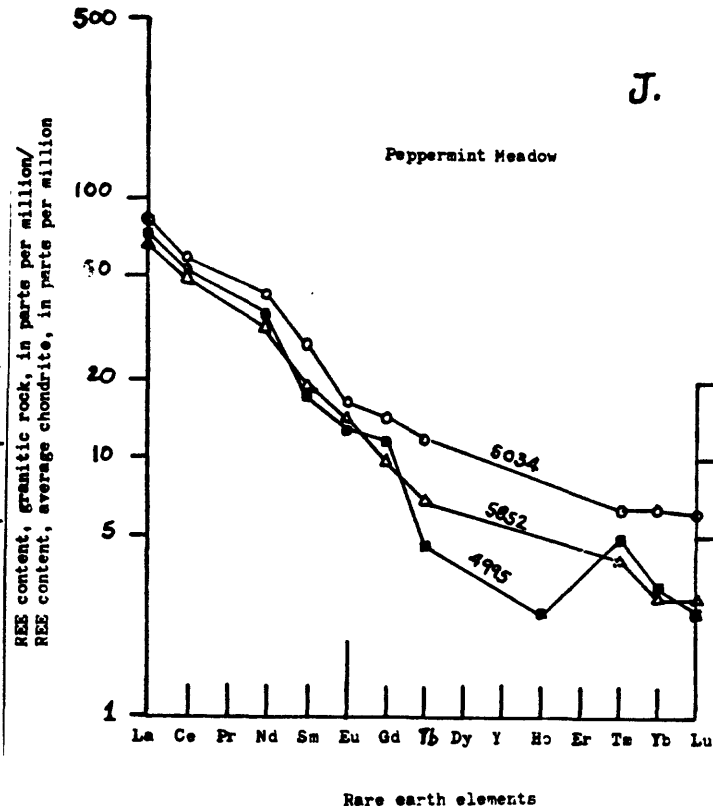
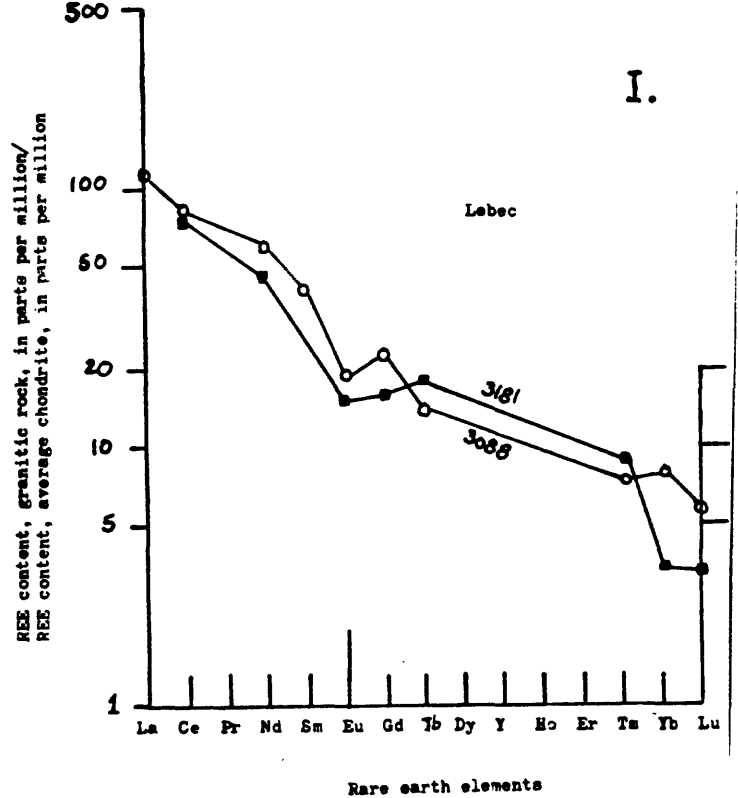


Figure 15. (cont.)

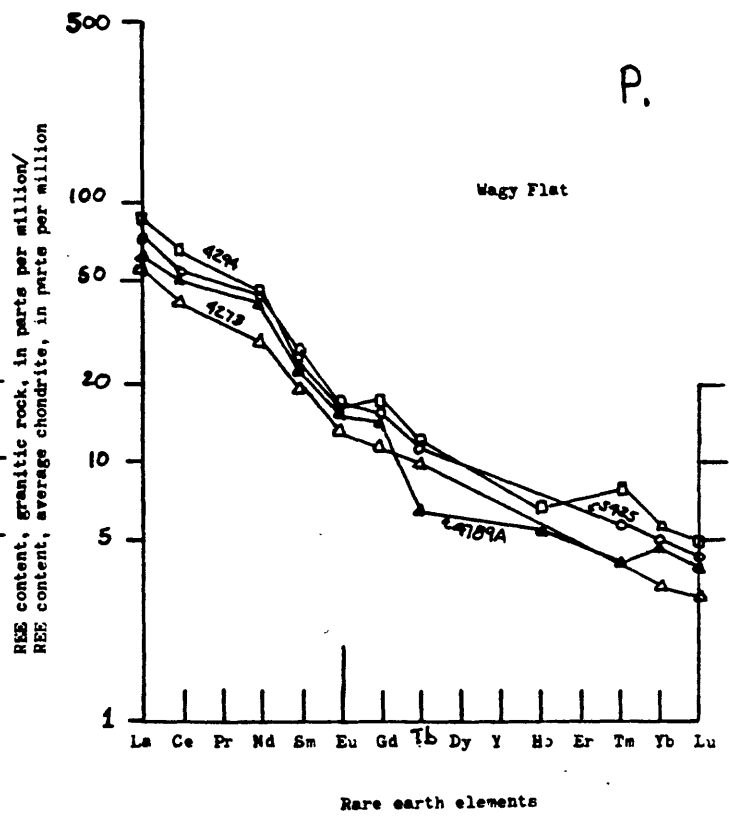
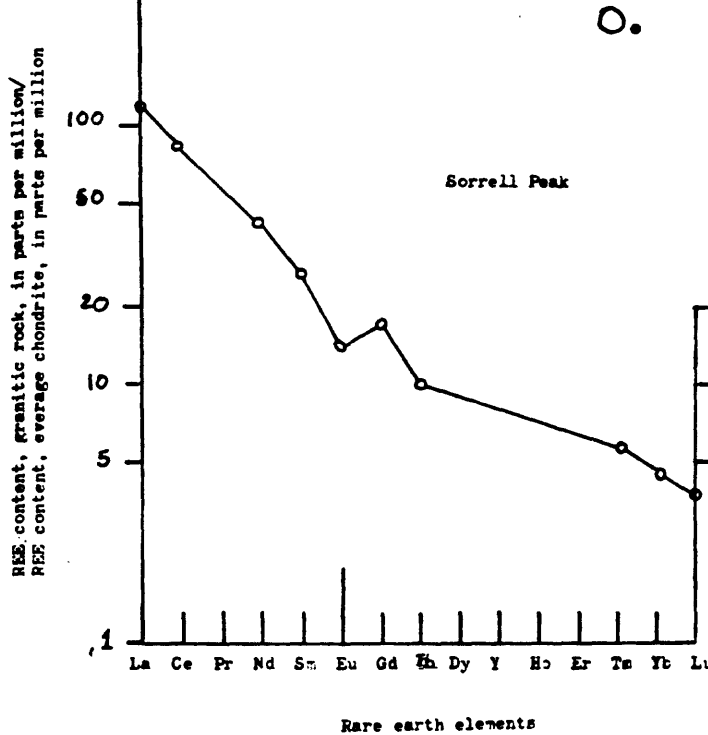
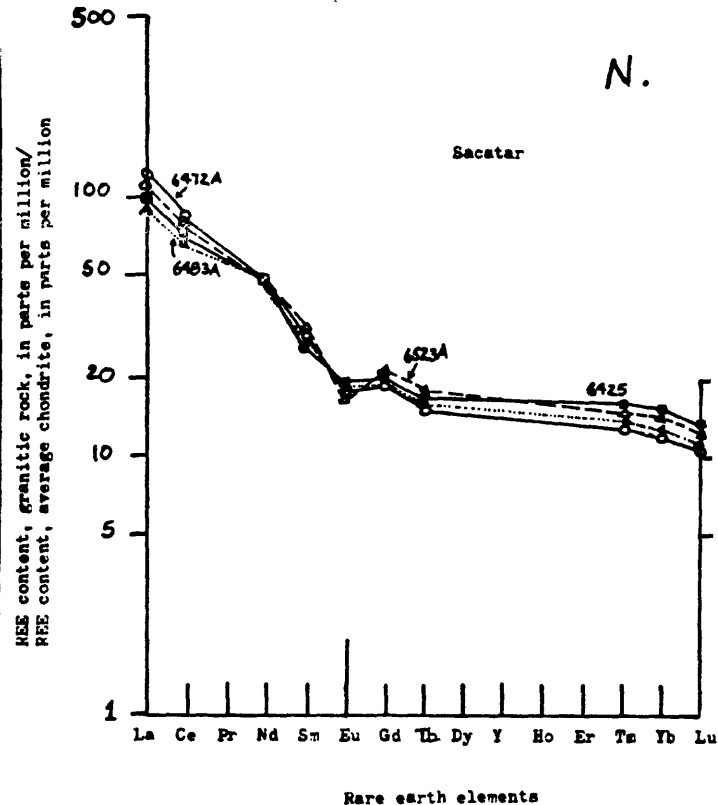
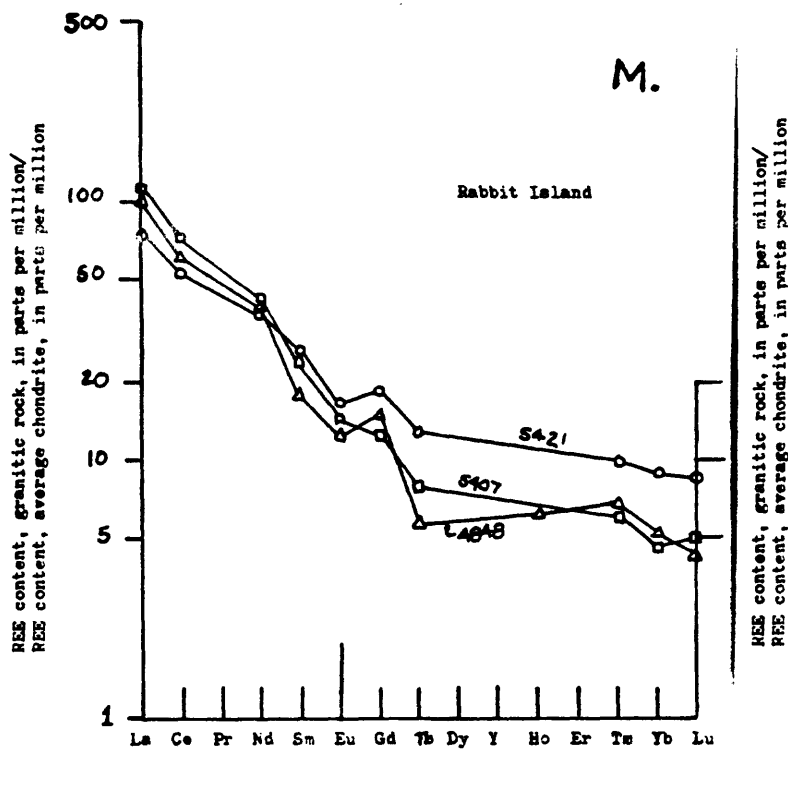


Figure 15. (cont.)

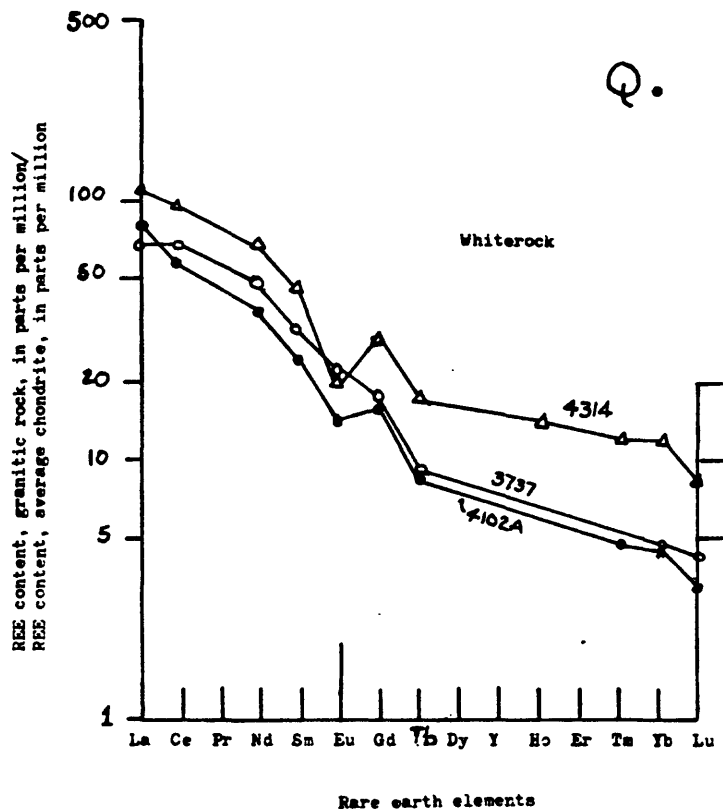


Figure 15. (cont.)

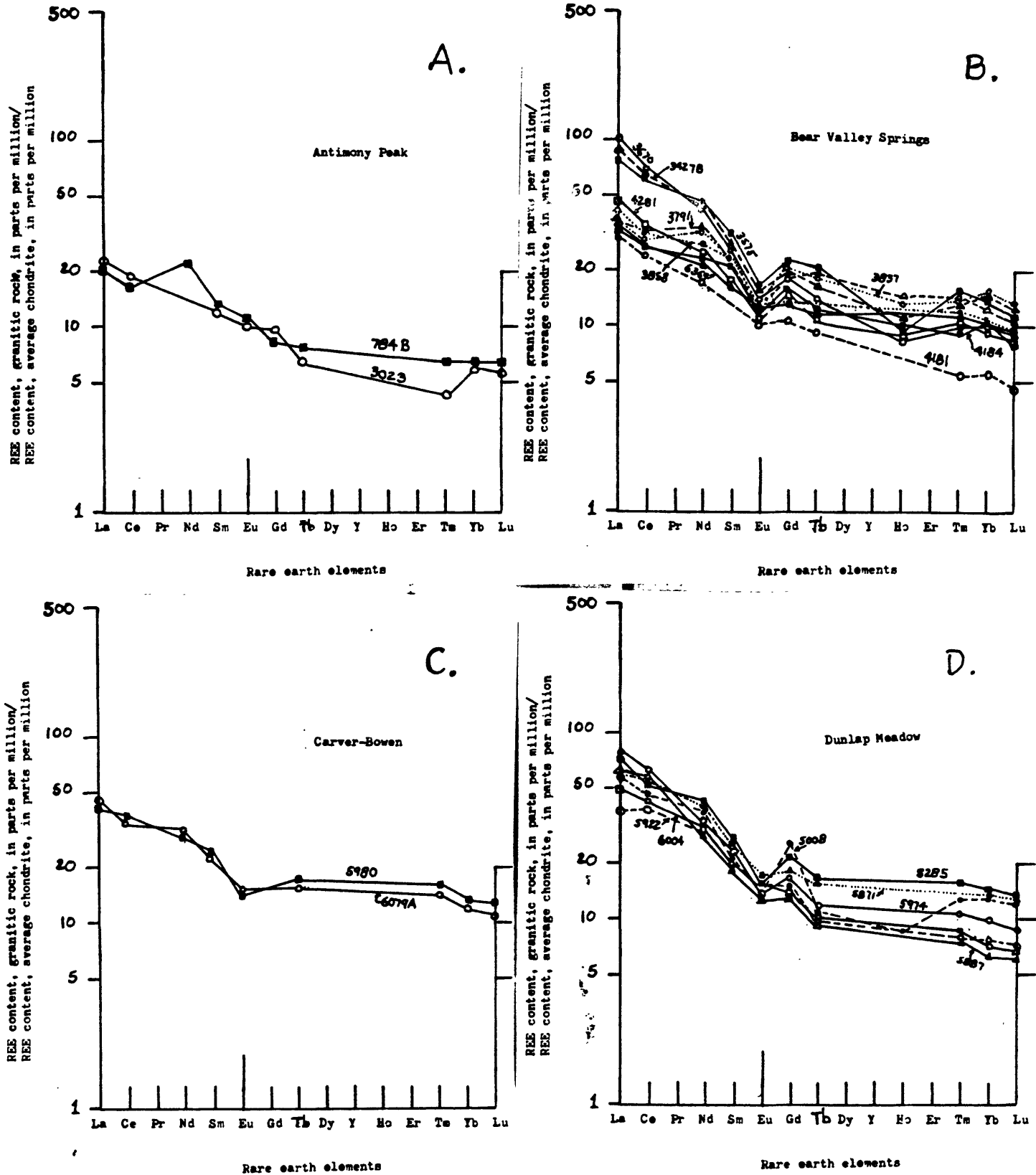


Figure 16. Rare earth element (REE) chondritic normalized abundance diagrams for tonalite bodies.

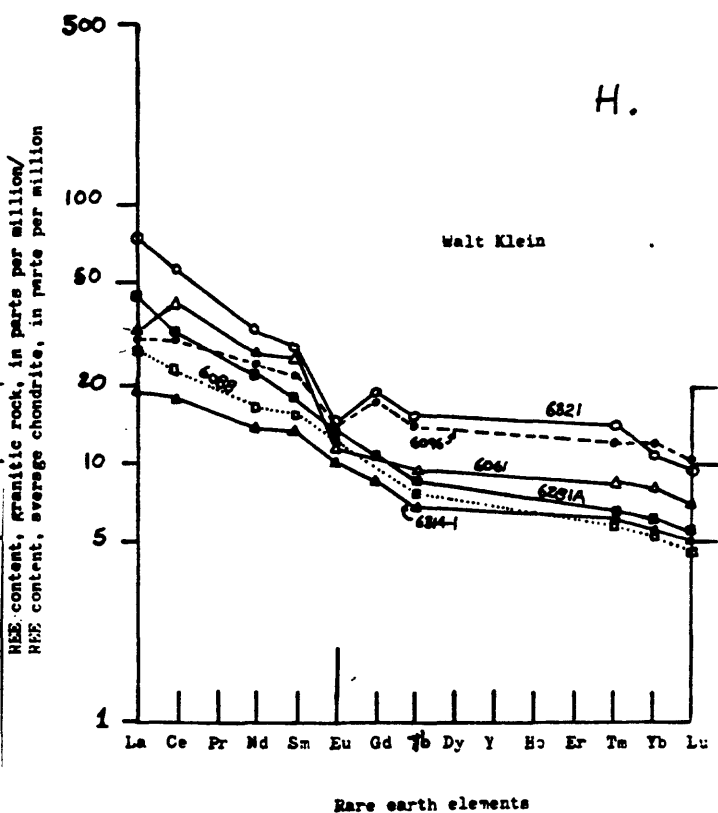
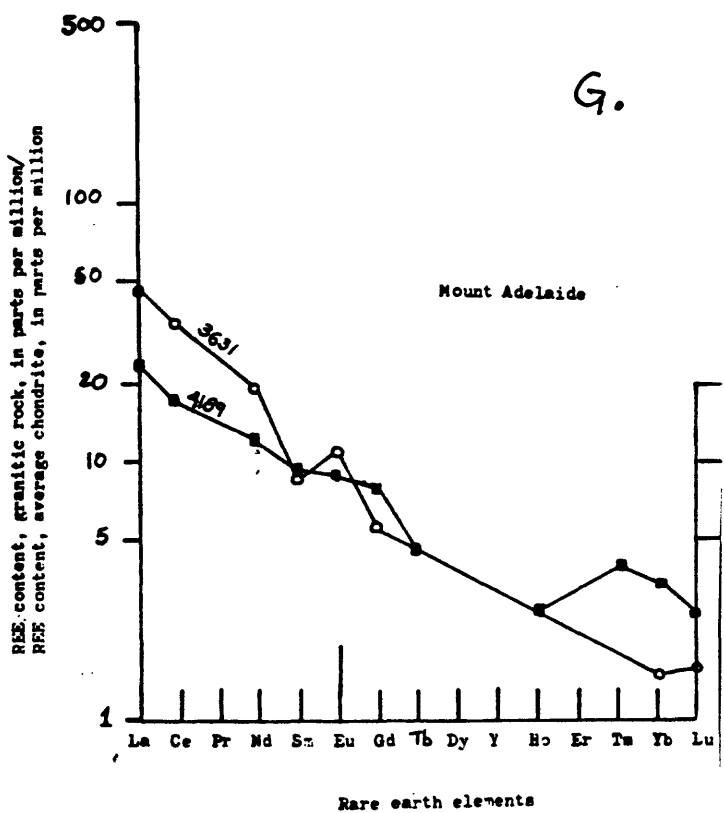
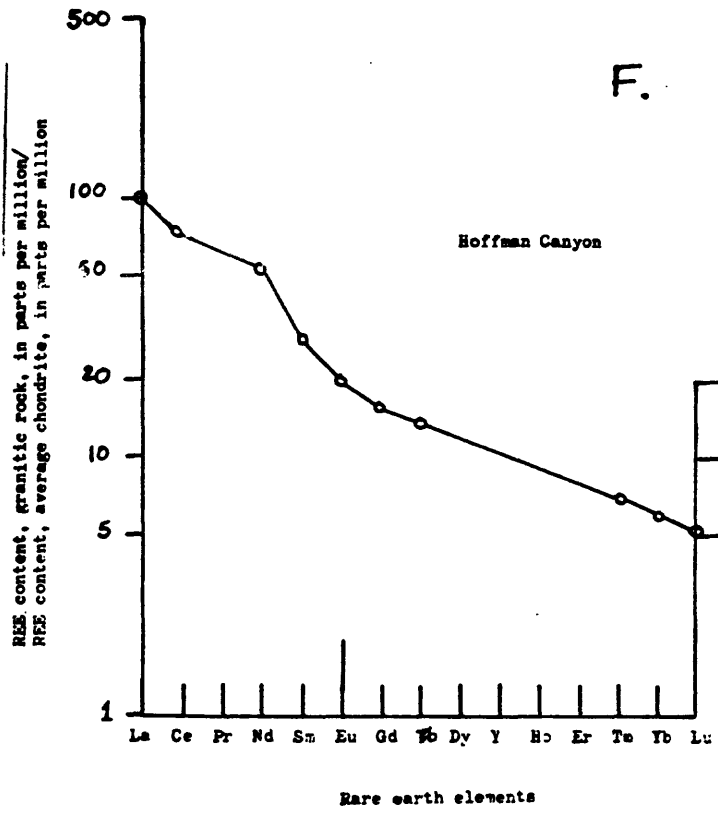
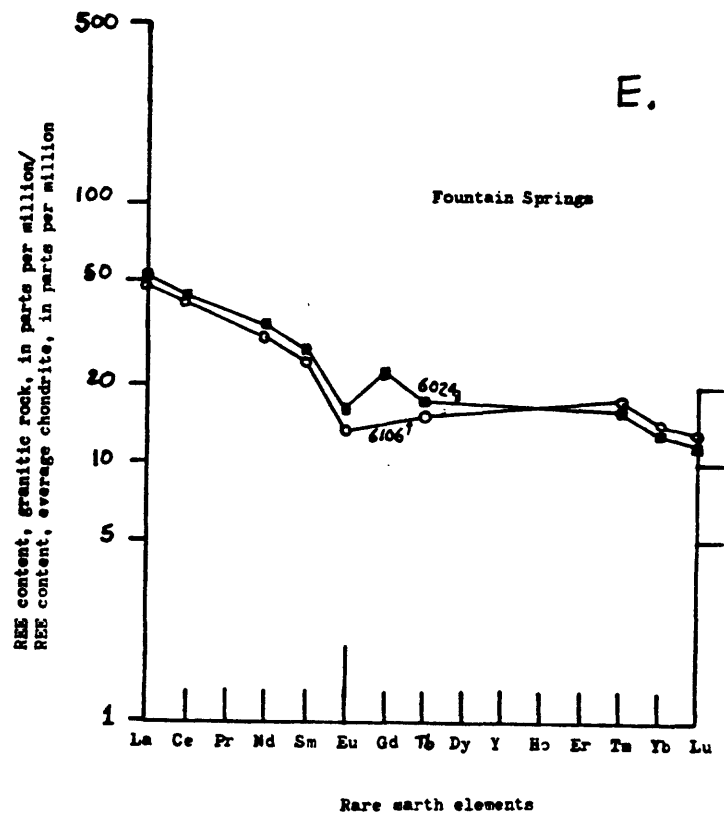


Figure 16. (cont.)

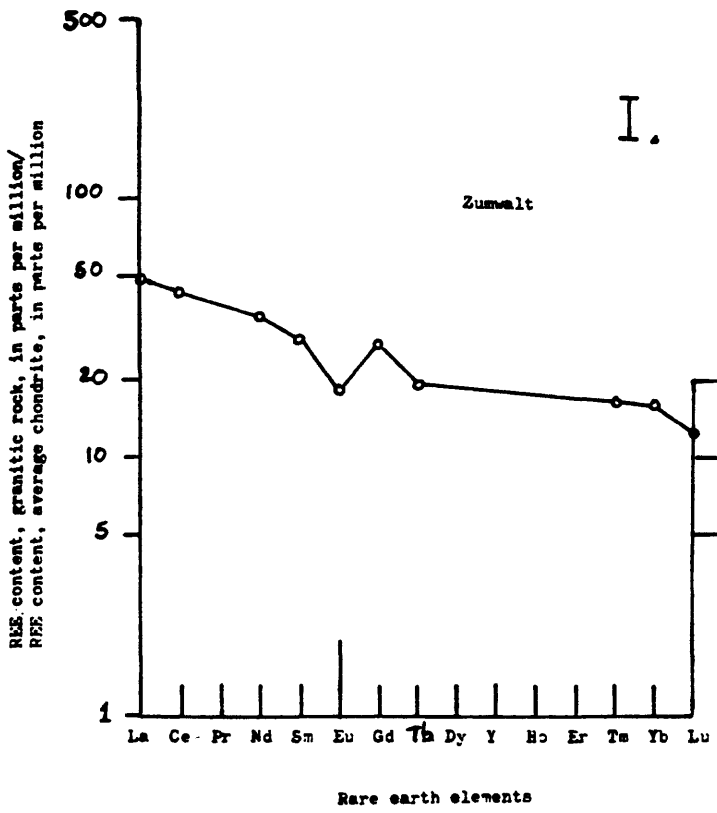


Figure 16. (cont.)

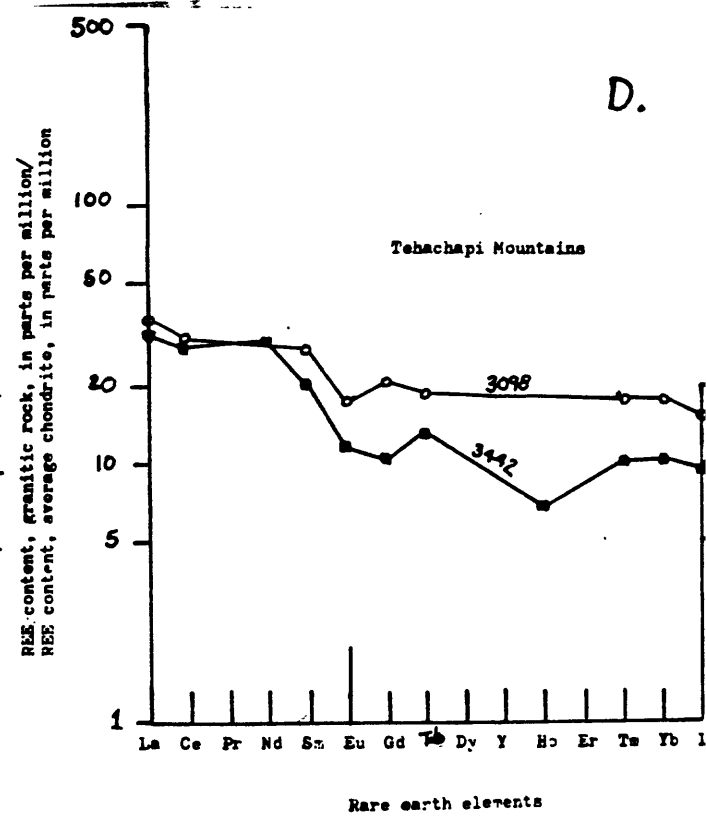
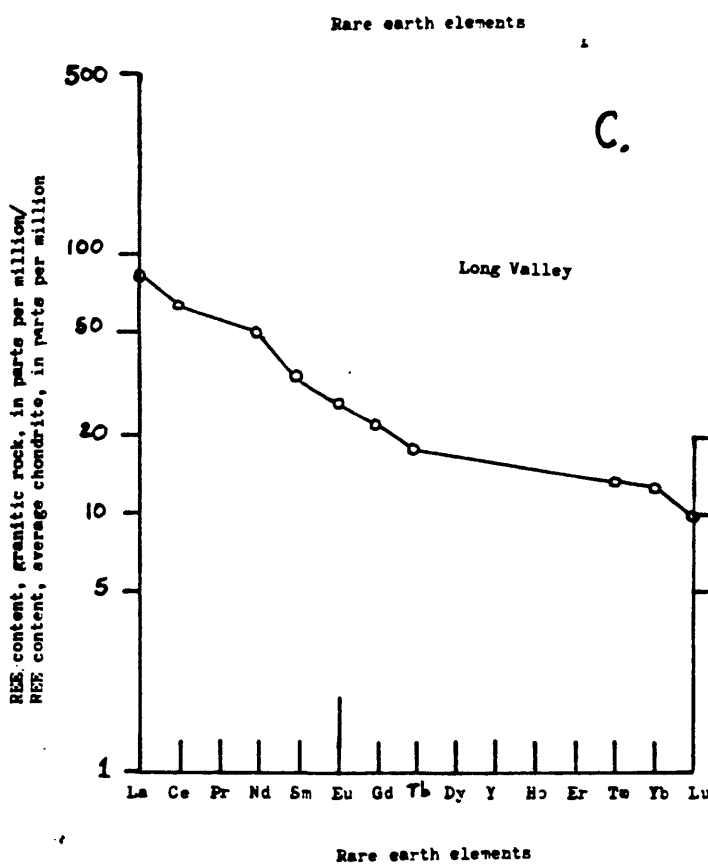
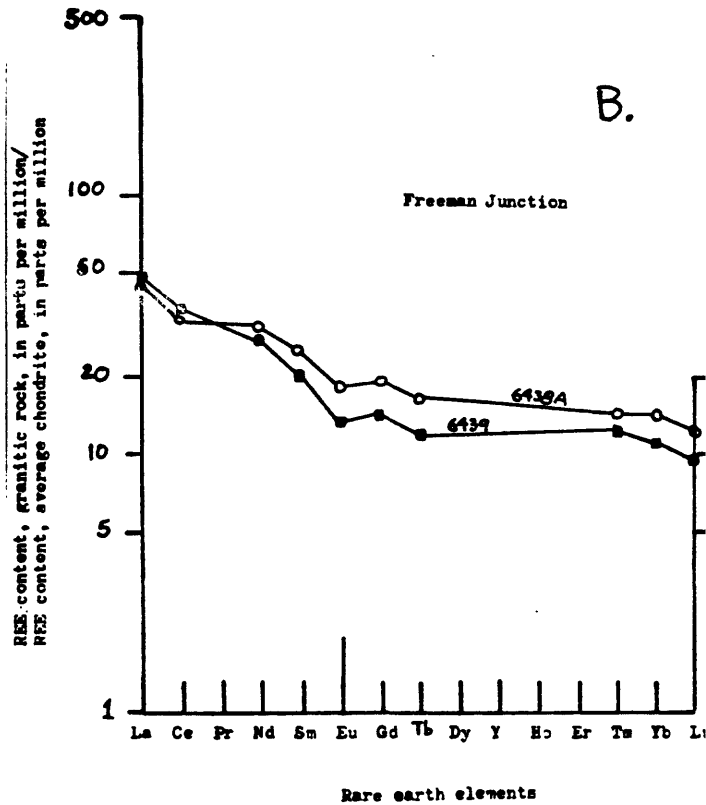
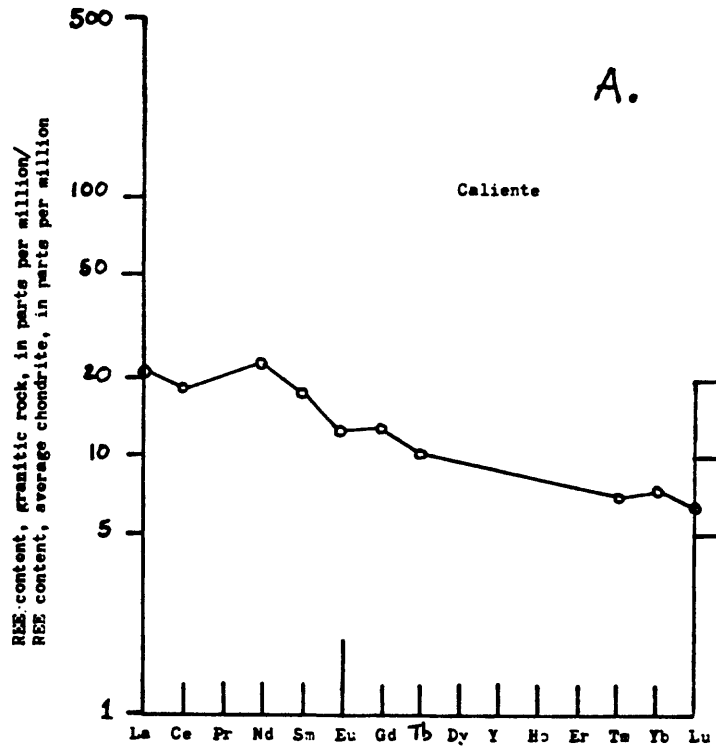


Figure 17. Rare earth element (REE) chondritic normalized abundance diagrams for quartz diorite bodies.

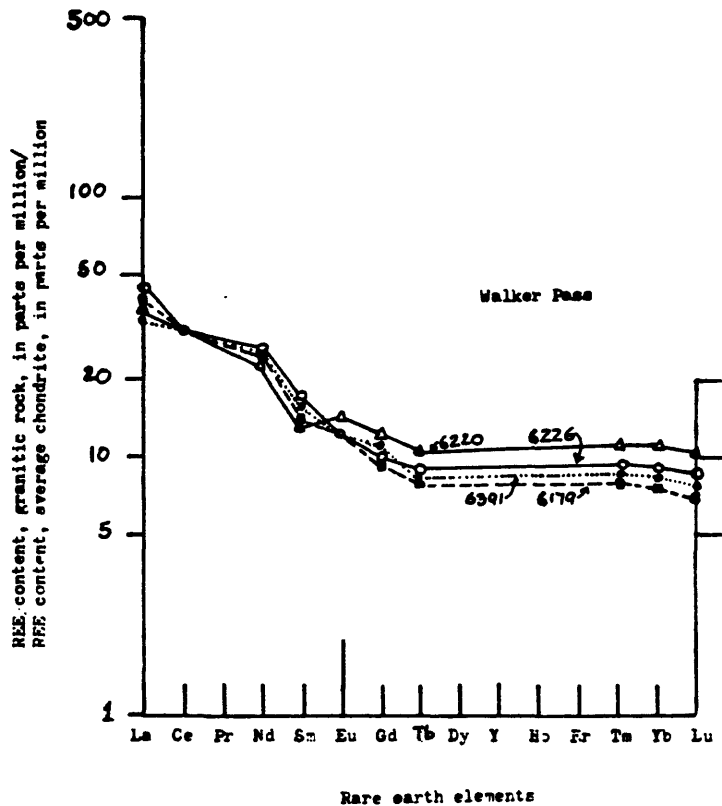


Figure 17. (cont.)

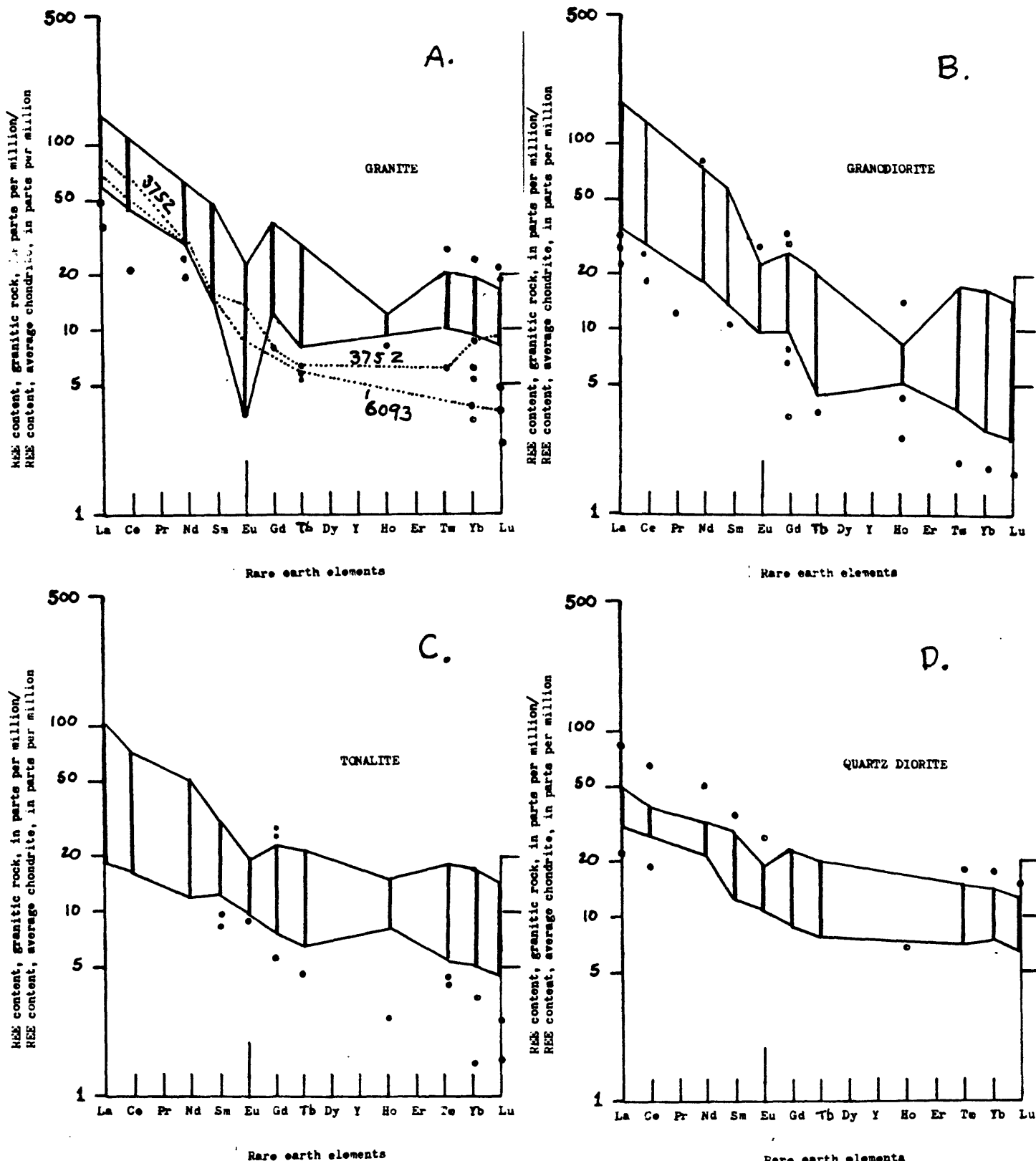


Figure 18. Composite REE abundance diagrams for: A) granite, B) granodiorite, C) tonalite, and D) quartz diorite. Ranges of most values shown by vertical black bars. Individual values outside of main ranges shown by black dots. Trend of two granite samples (6093 and 3752) without pronounced negative Eu anomalies shown by dot pattern.

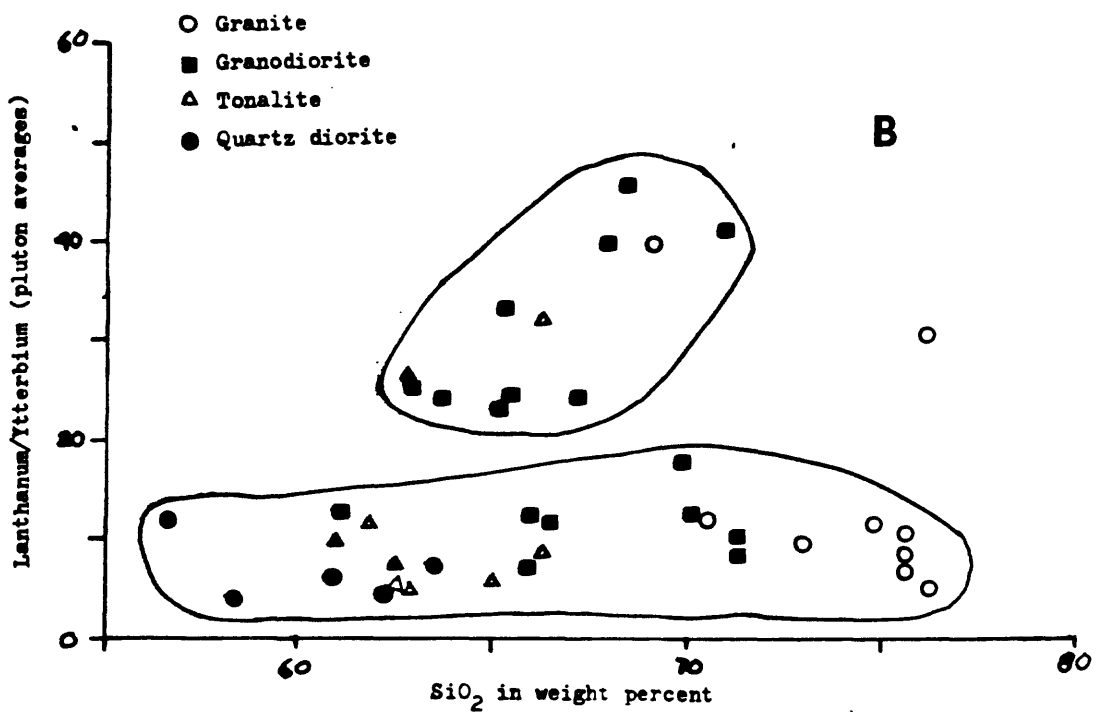
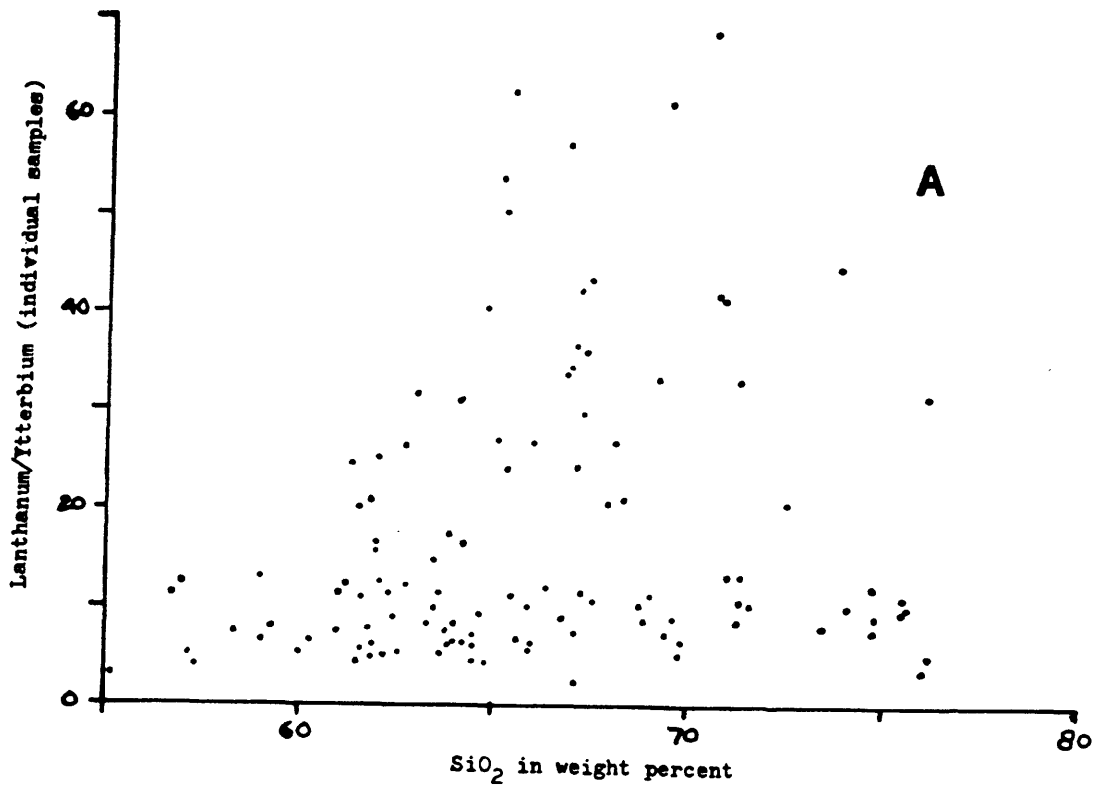


Figure 19. Lanthanum/Ytterbium ratio plotted against SiO_2 .

A. Individual samples

B. Average of each granitic unit

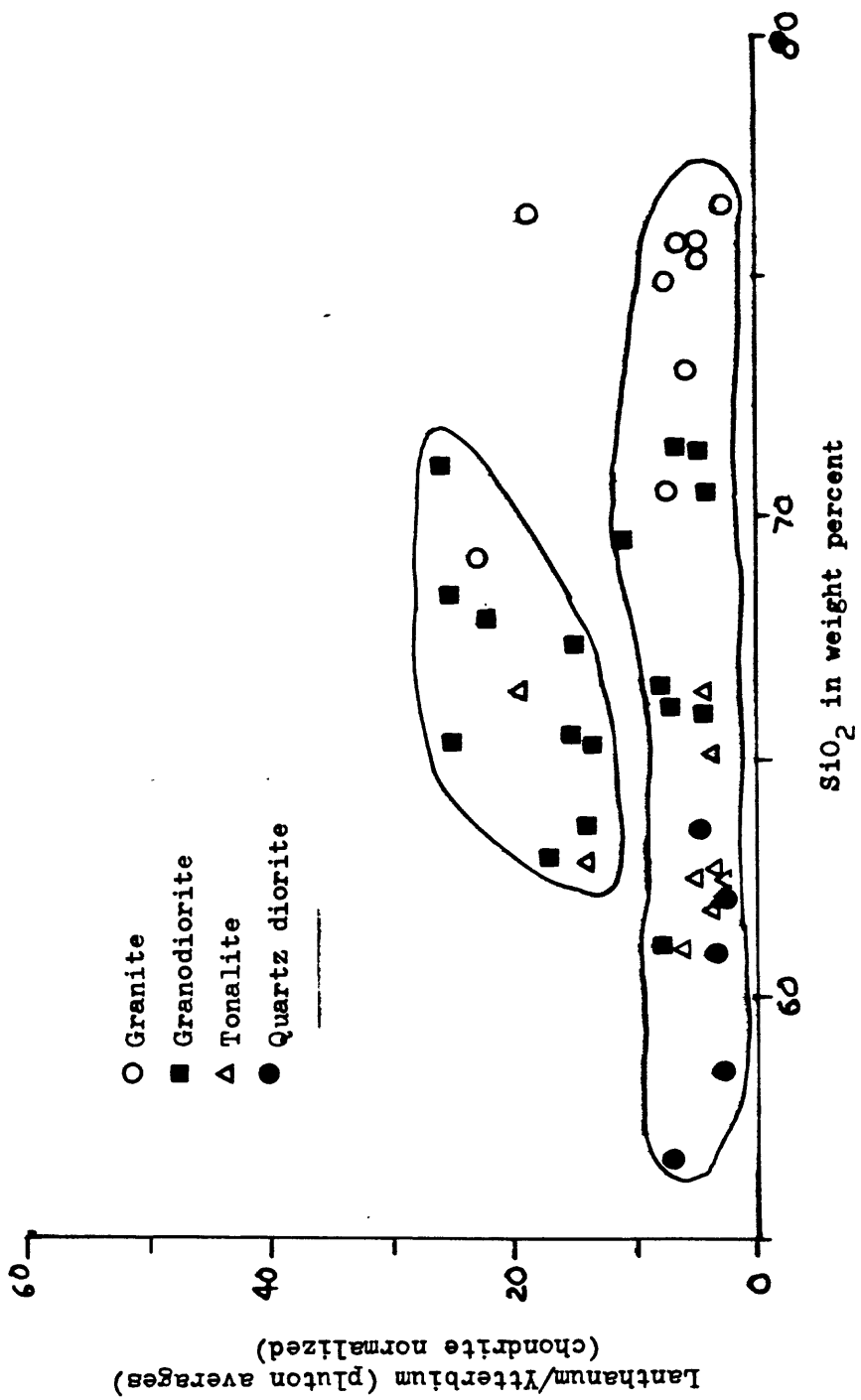


Figure 20. Ratio of chondrite normalized lanthanum to ytterbium plotted against SiO_2 .

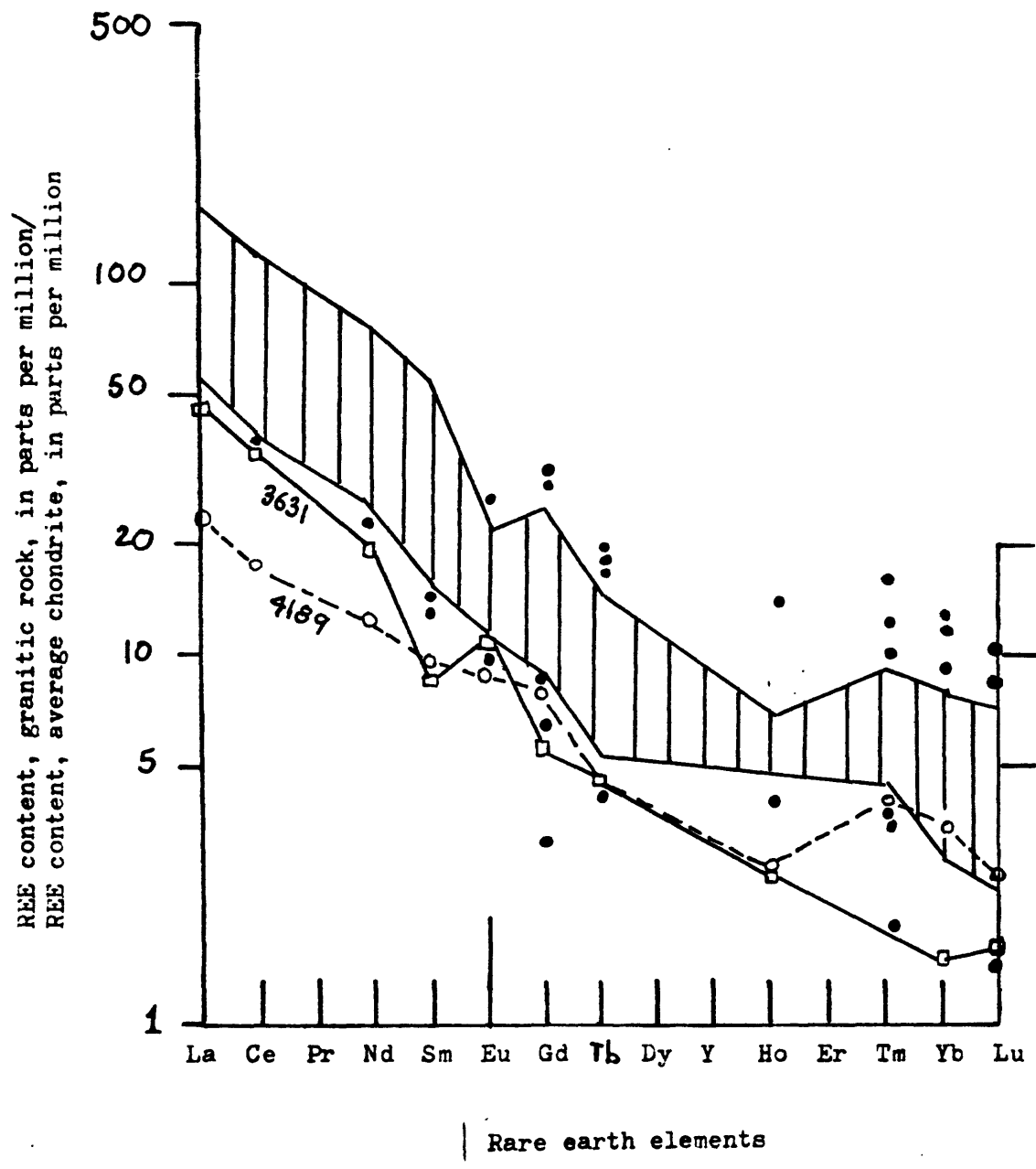


Figure 21. REE abundance diagram showing belt of individual sample concentration for bodies whose average La/Yb is in the upper field of figure 19, 20. Individual samples points only shown outside of belt of major concentration. Trends also shown for individual samples from Mount Adelaide mass.

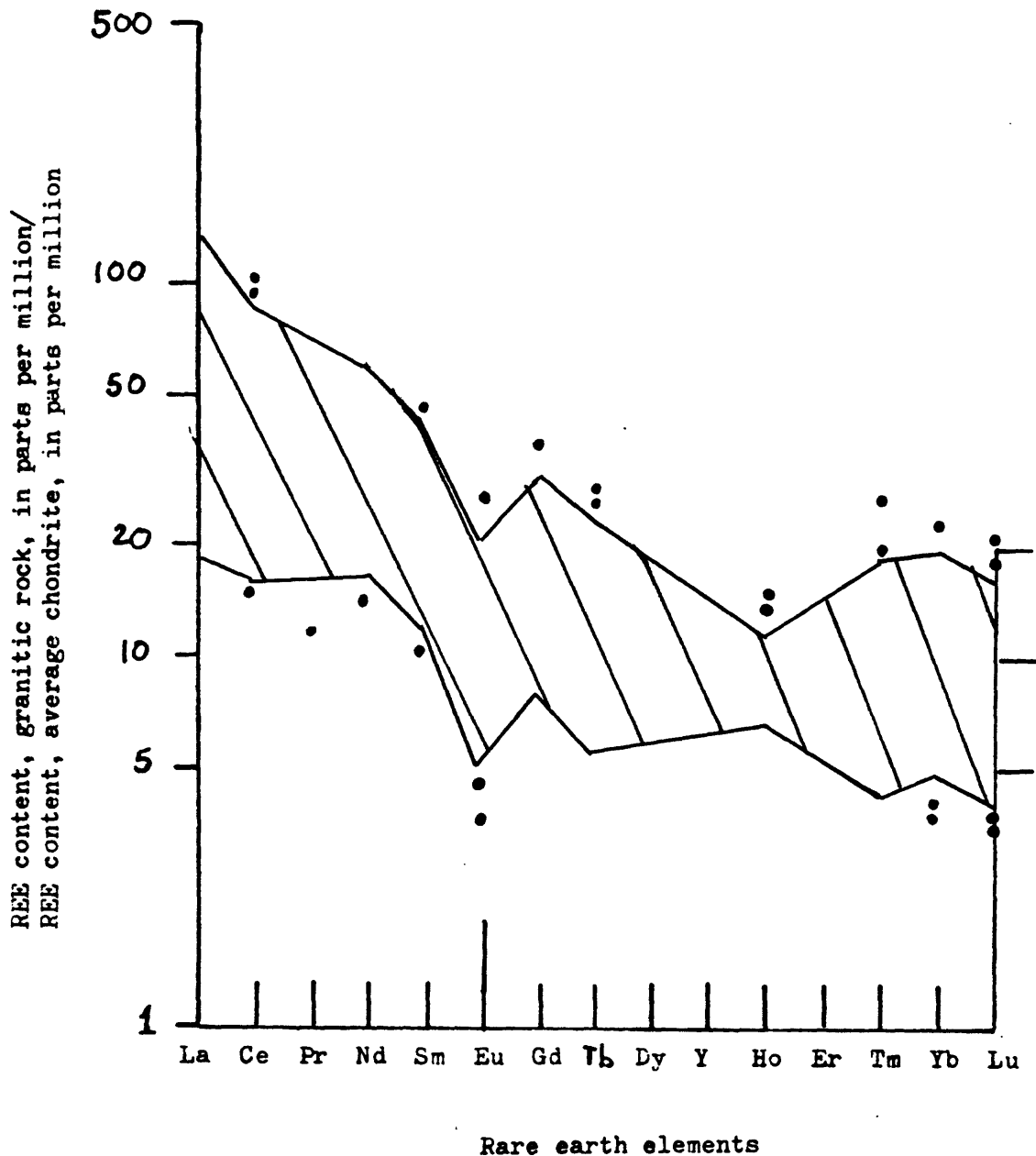


Figure 22. REE abundance diagram showing belt of individual sample concentration for bodies whose average La/Yb is in the lower field of figures 19 & 20. Individual sample points only shown outside of belt of major concentration.

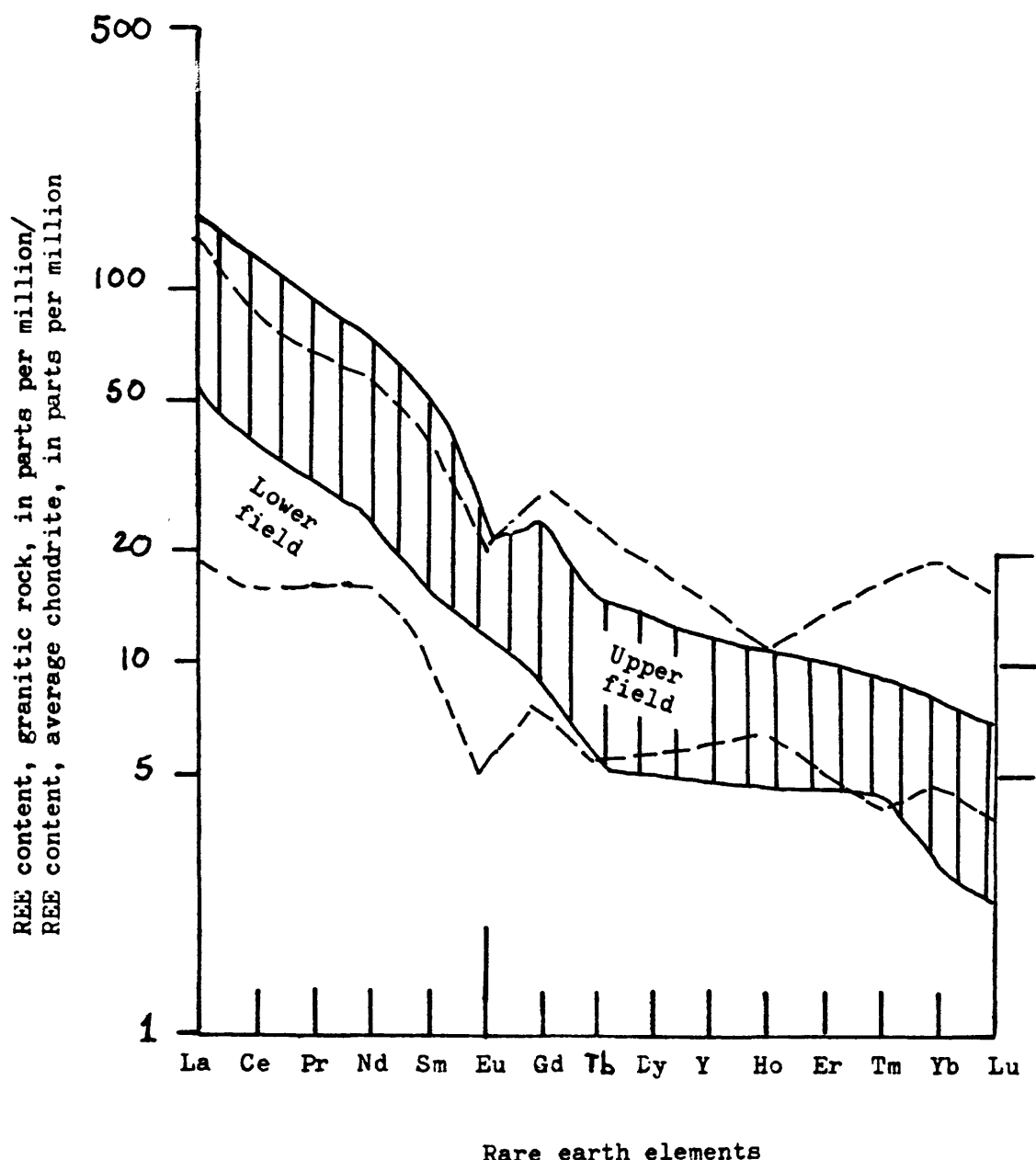


Figure 23. Superimposed upper and lower fields from figures 21 and 22.

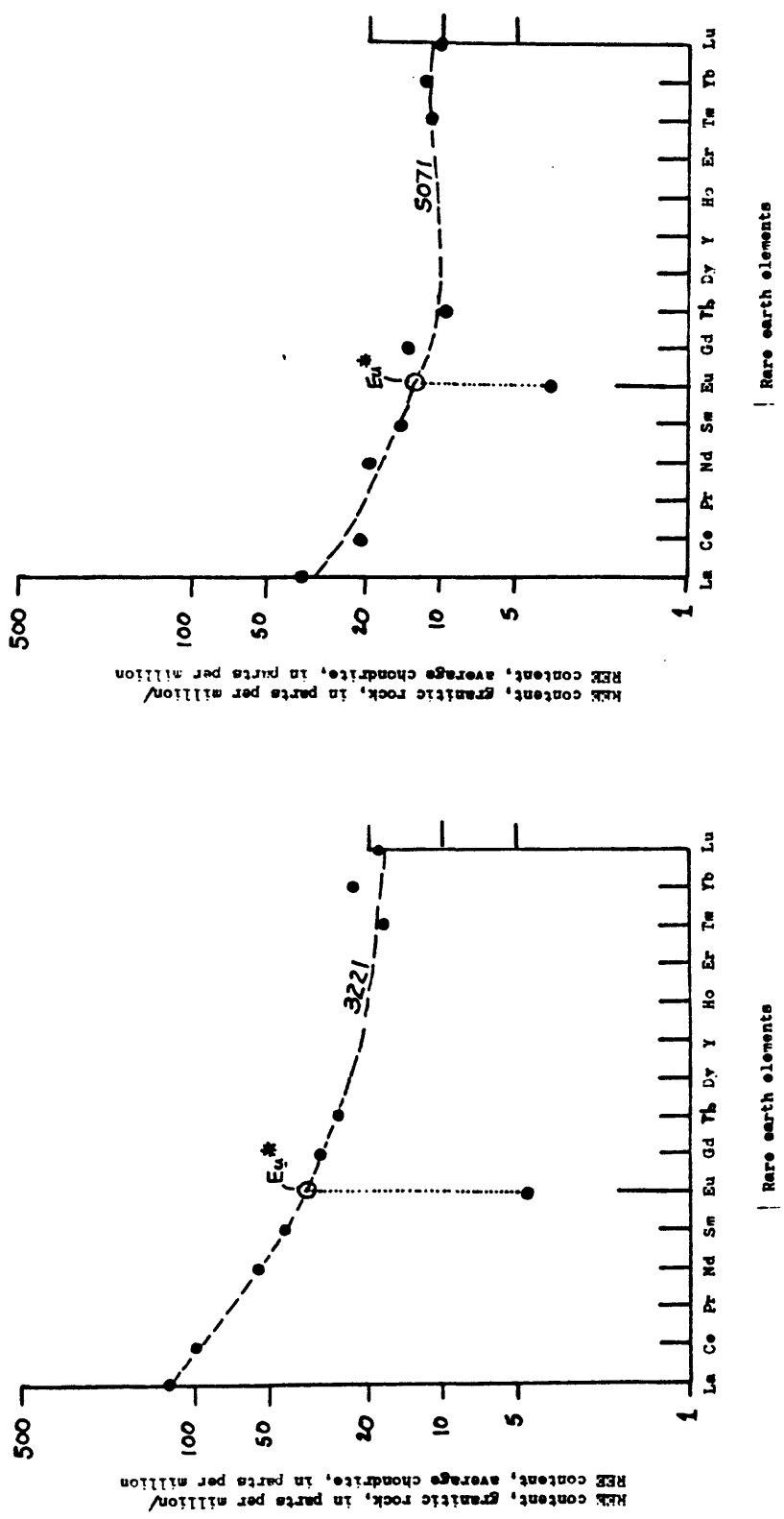


Figure 24. Examples of how Eu^* is determined

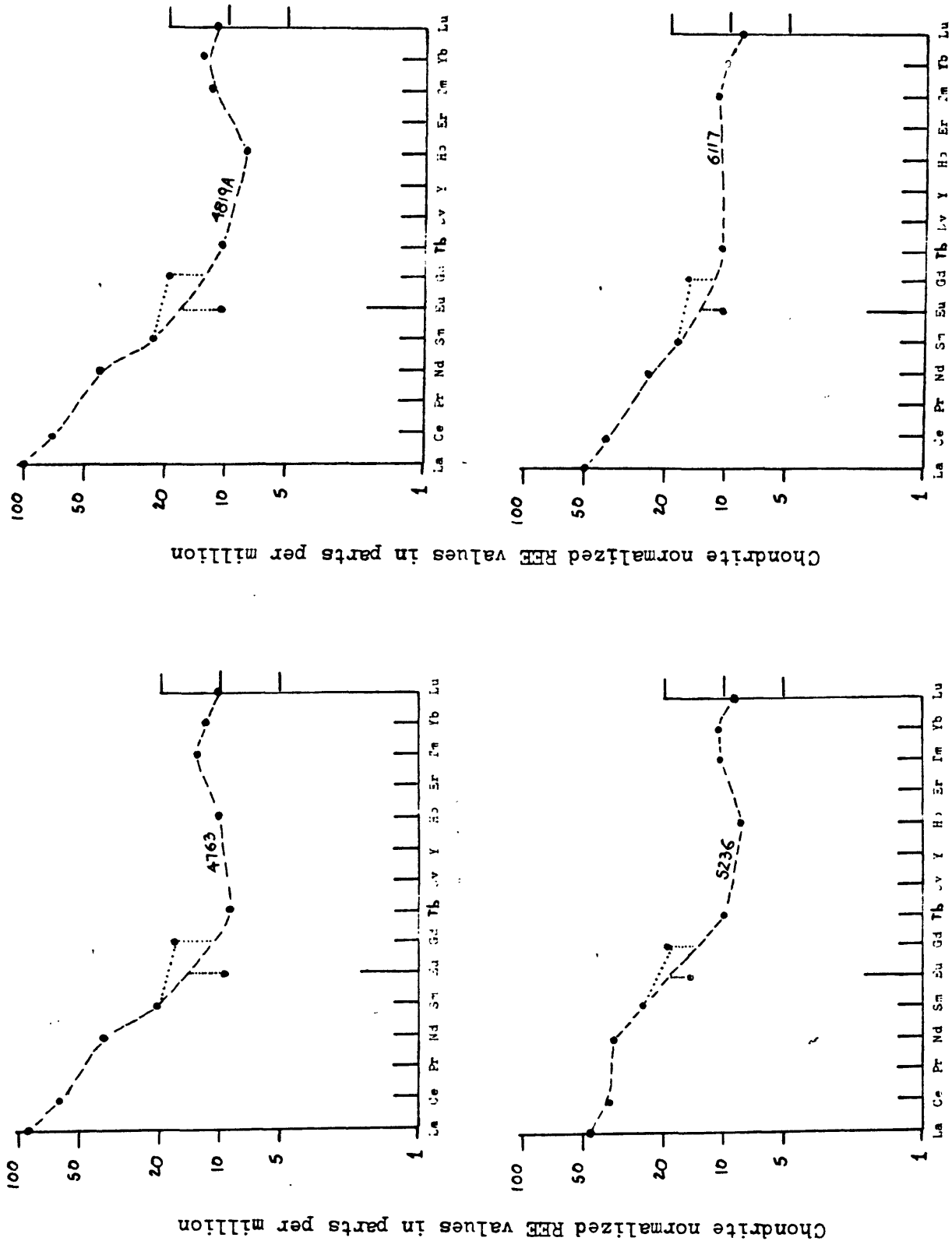


Figure 25. Examples of gadolinium (Gd) "hump" and its effect on Eu*

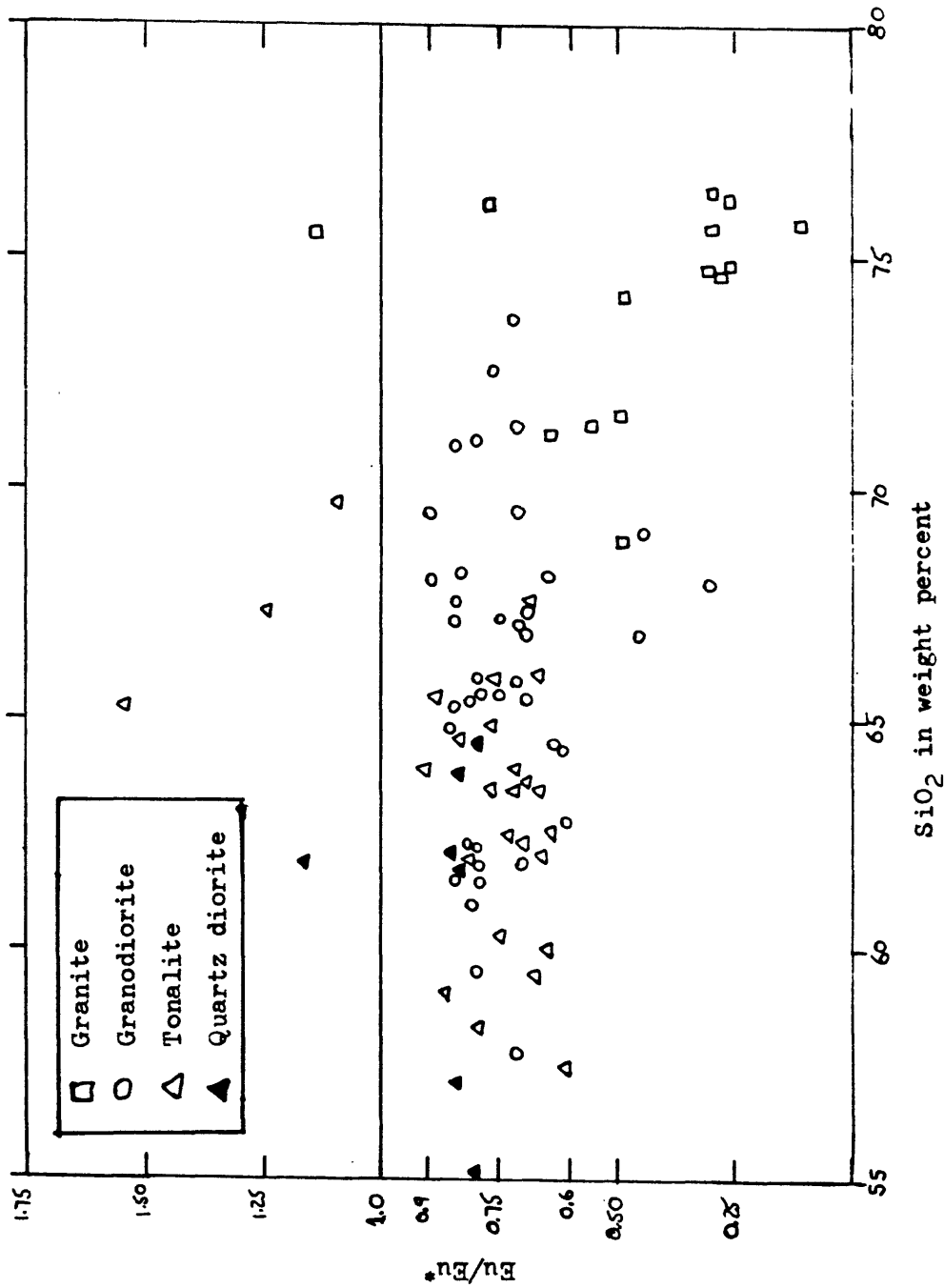


Figure 26. Europium anomalies (Eu/Eu^*) plotted against silica content content for some chemically analyzed granitic samples. Essentially no Eu anomalies for 5 granite, 15 granodiorite, 9 tonalite, and 3 quartz diorite samples.

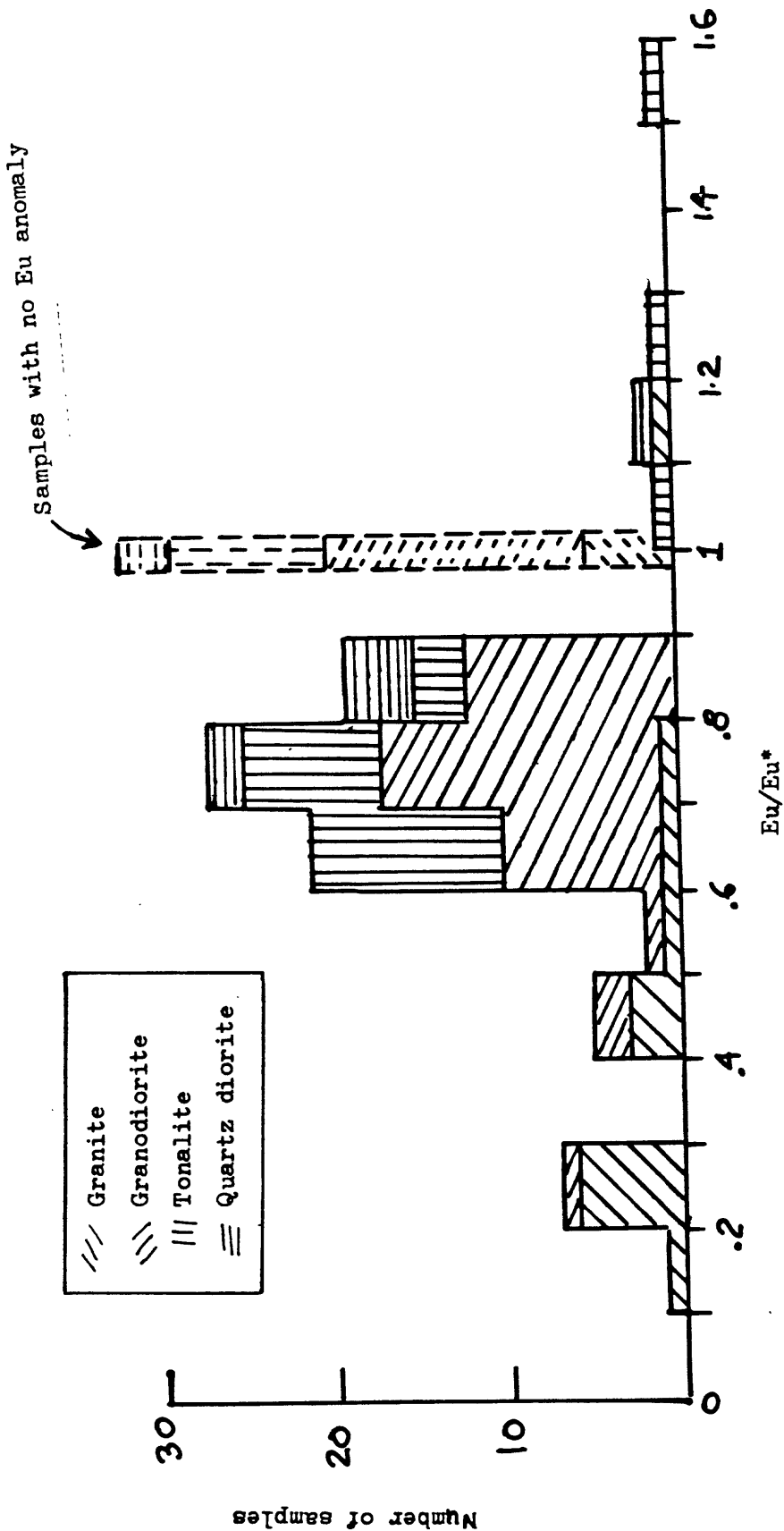


Figure 27. Histogram showing range of Eu anomalies (Eu/Eu^*) by rock type for some chemically analyzed samples.

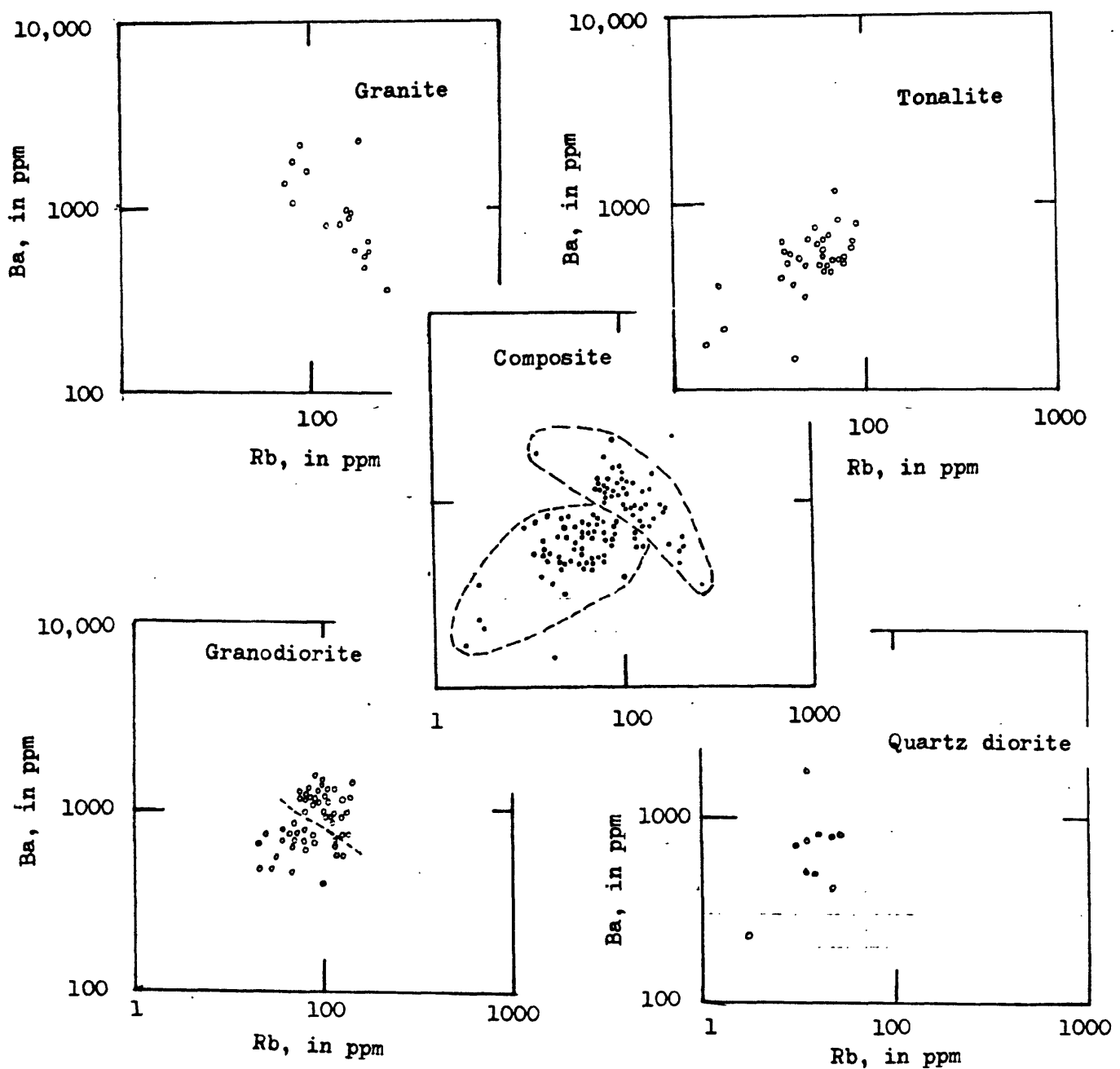


Figure 28. Barium plotted against rubidium for each rock type and a composite plot showing all granitic samples.

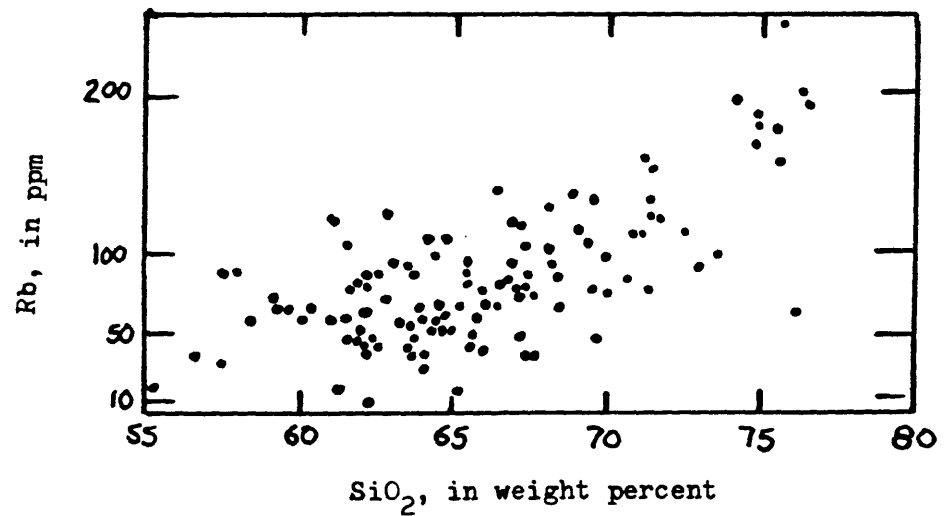
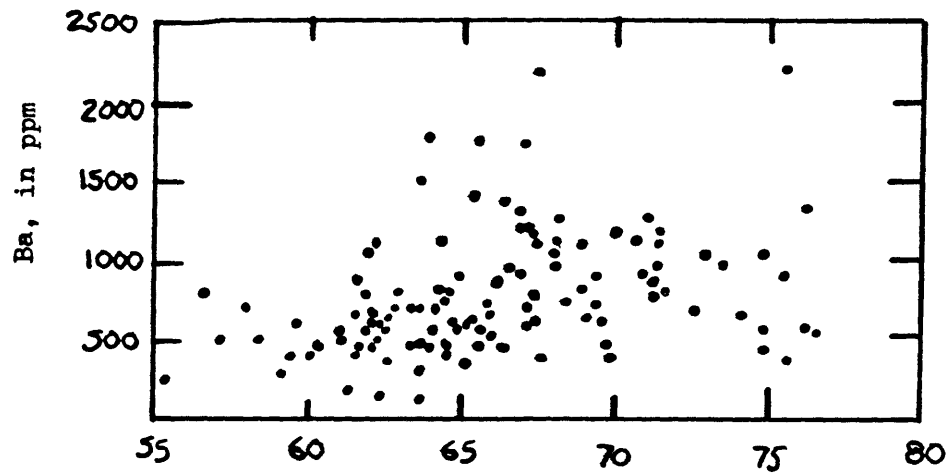


Figure 29. Barium and rubidium plotted against silica content.

Potassium content, in weight percent

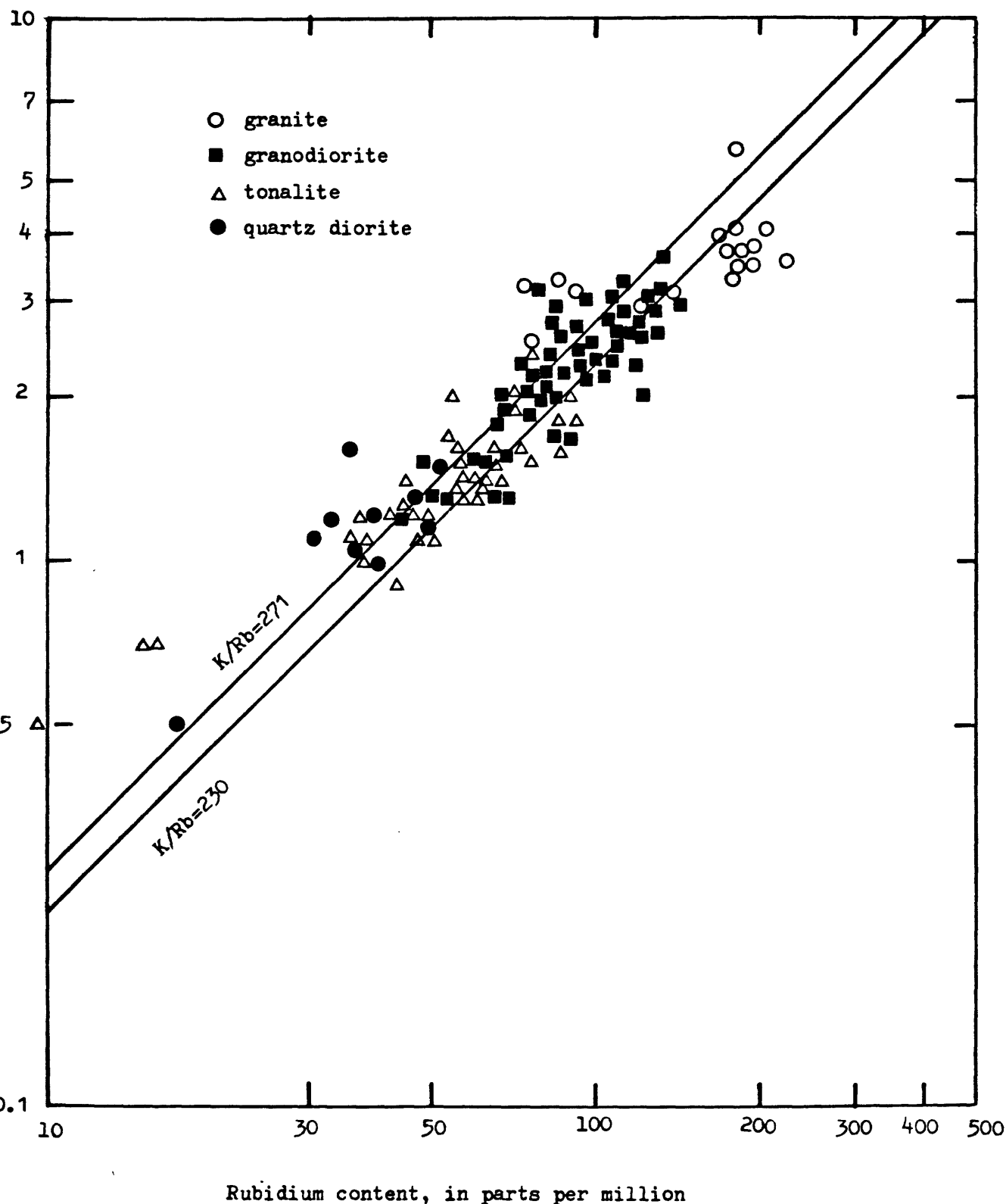


Figure 30 . Potassium plotted against rubidium for each chemically analyzed sample of granitic rock

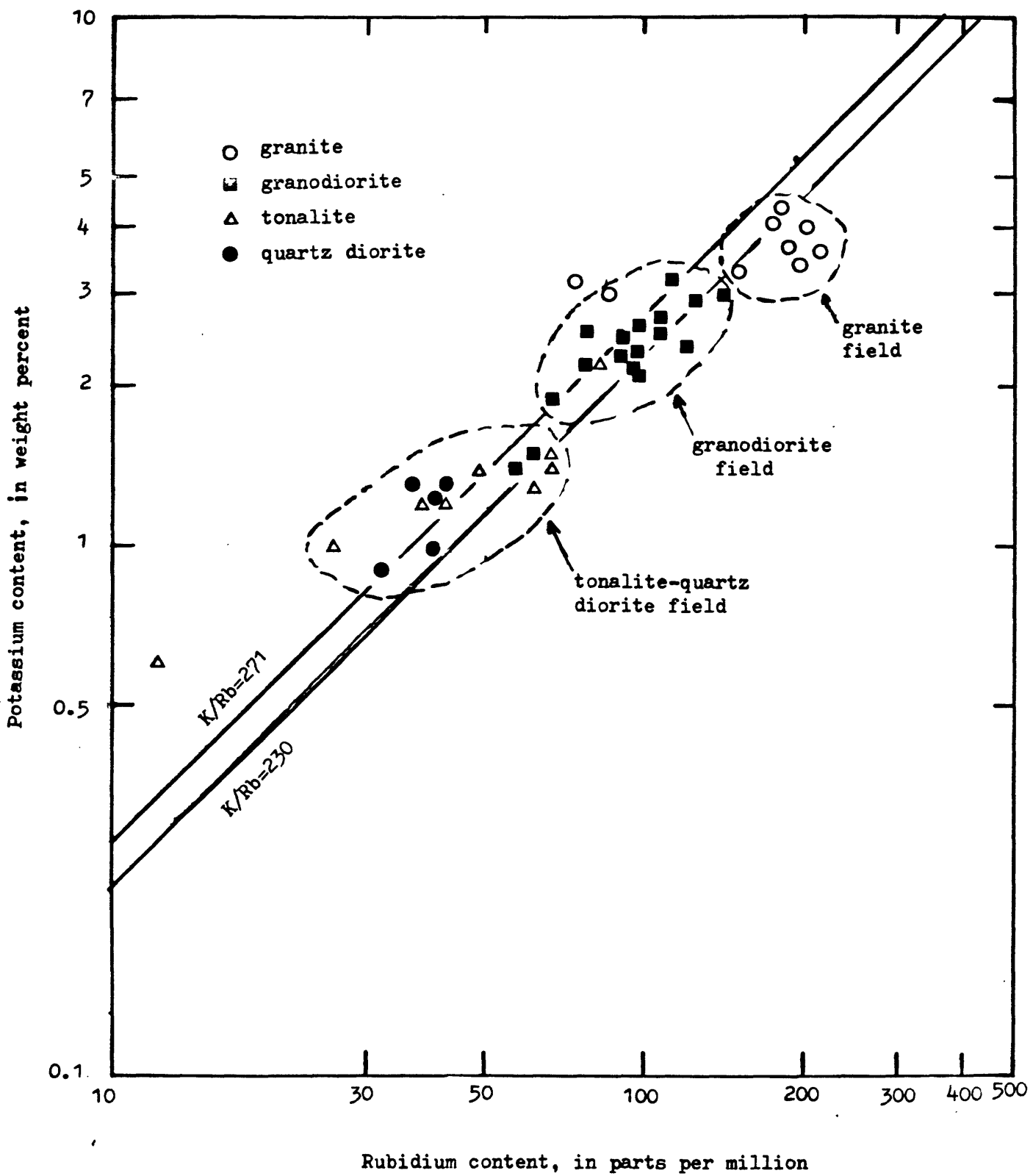


Figure 31. Potassium plotted against rubidium for average of each granitic unit - 77

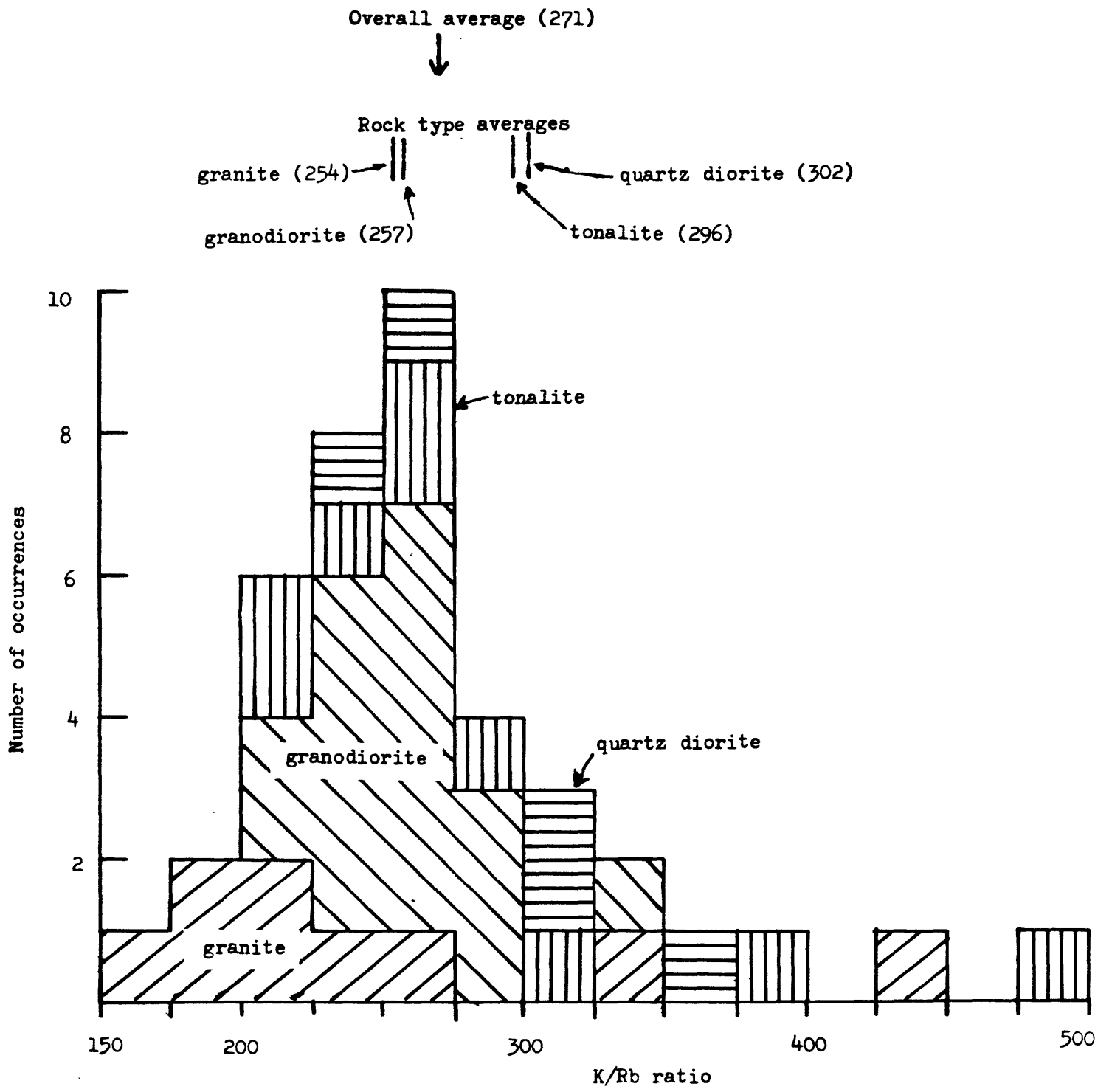


Figure 32. Histogram plotting average potassium-rubidium ratio for each granitic unit, and patterned by rock type.

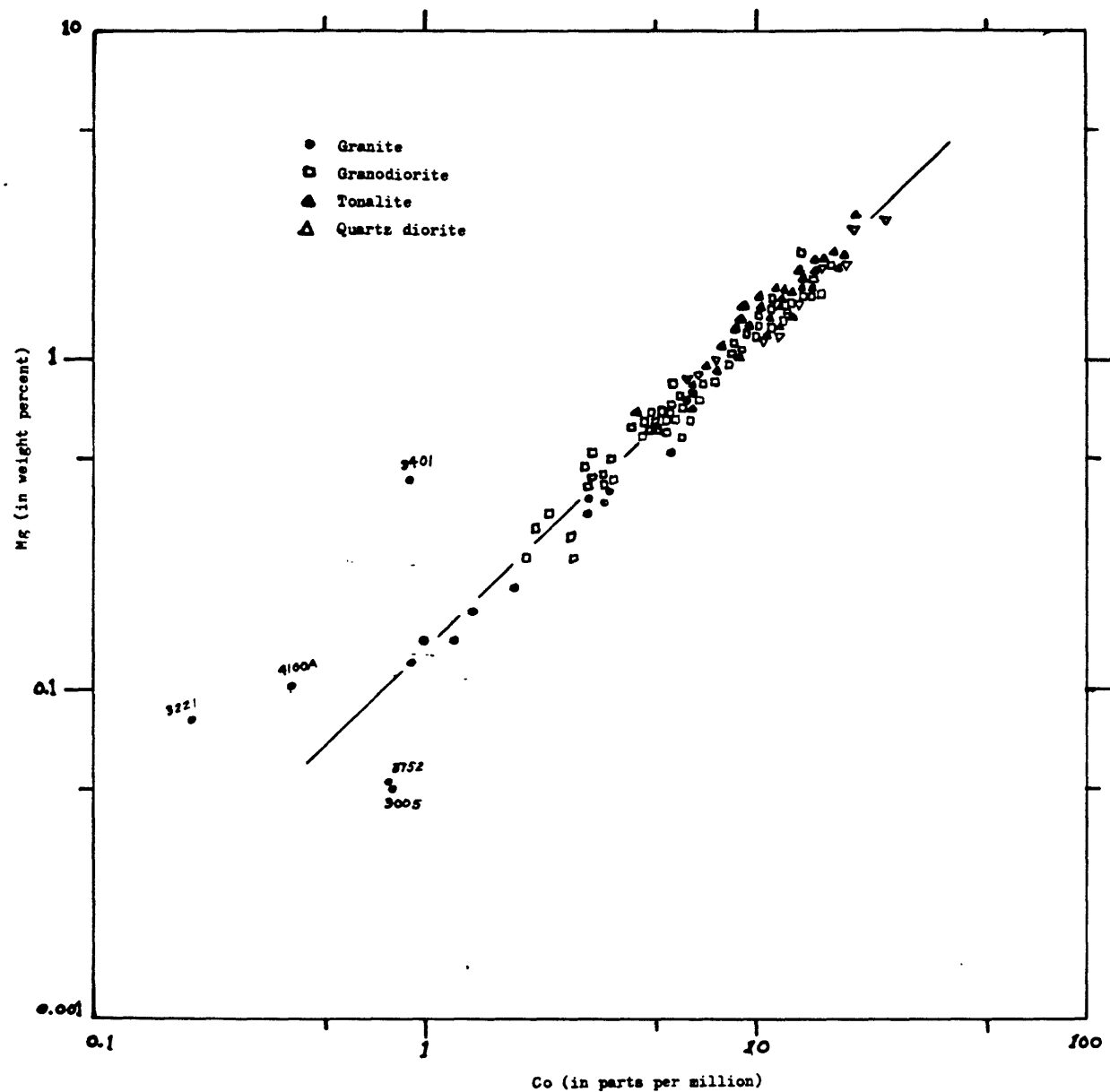


Figure 33. Cobalt plotted against magnesium.

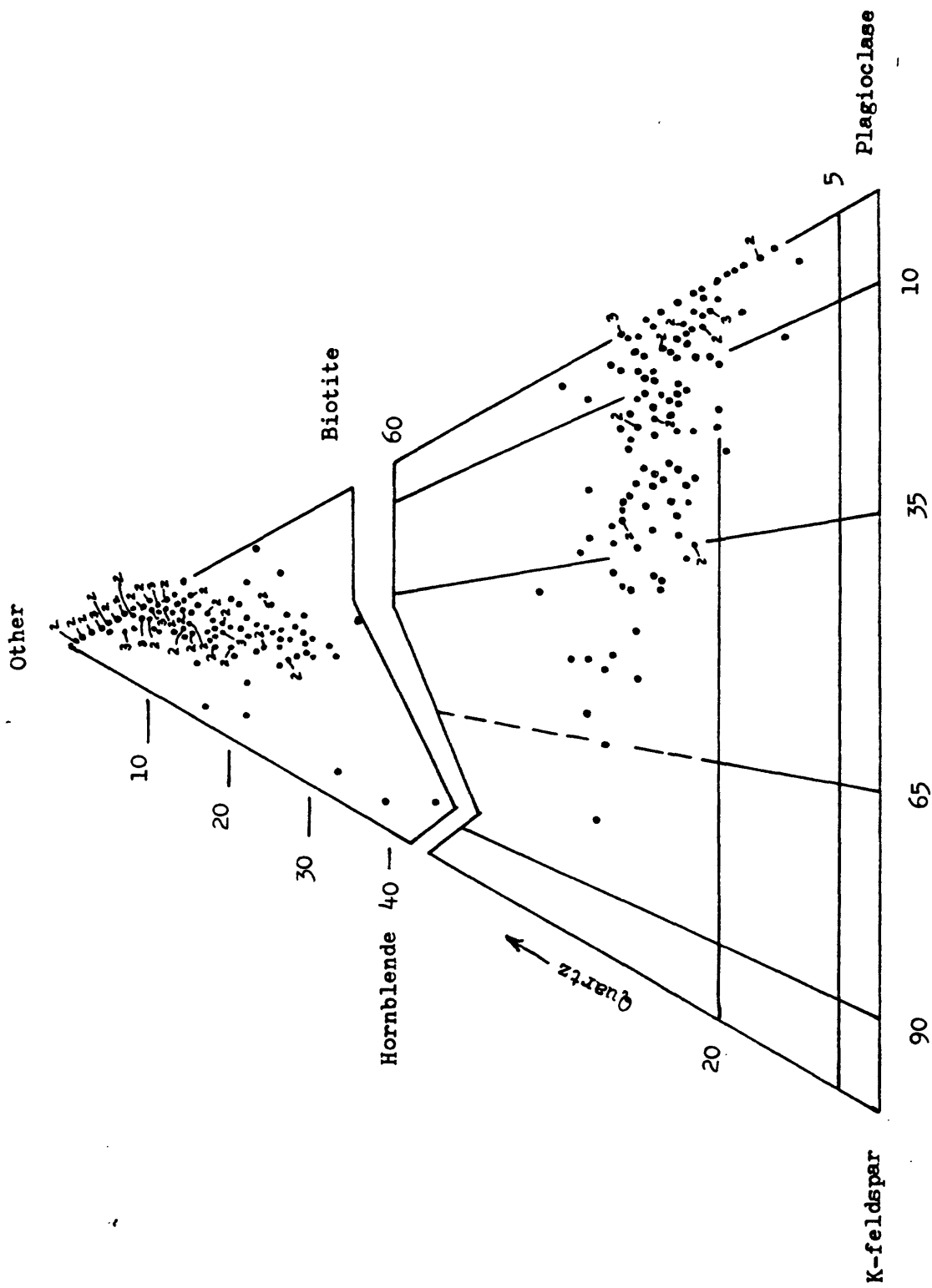


Figure 34. Modal plot of chemically analyzed samples.

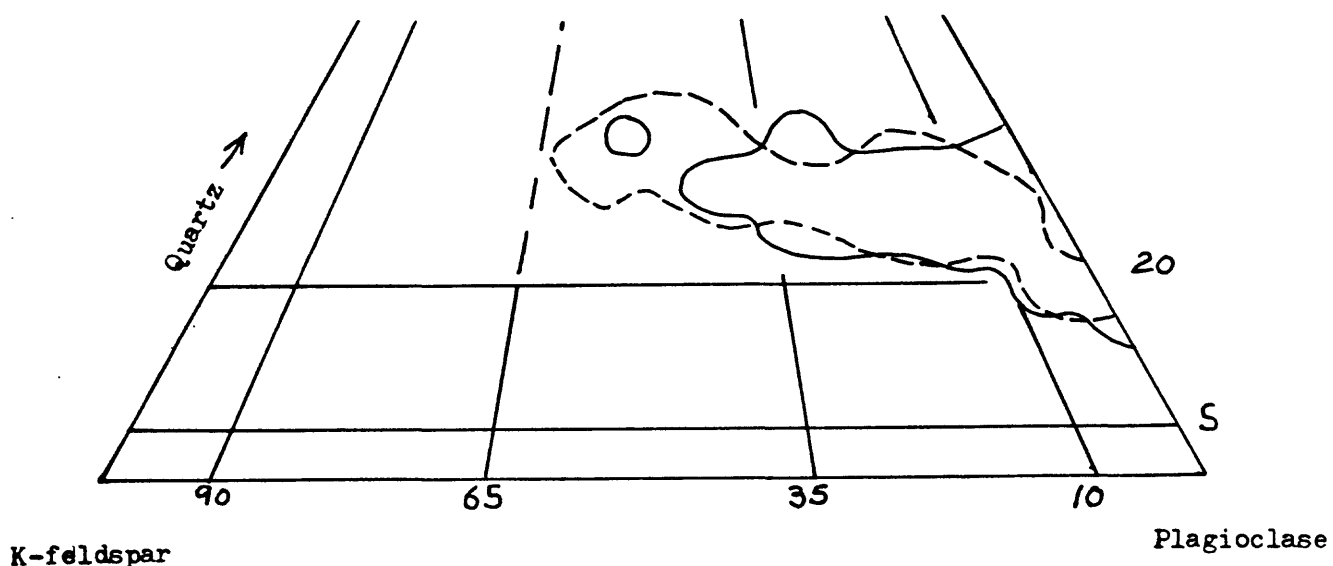
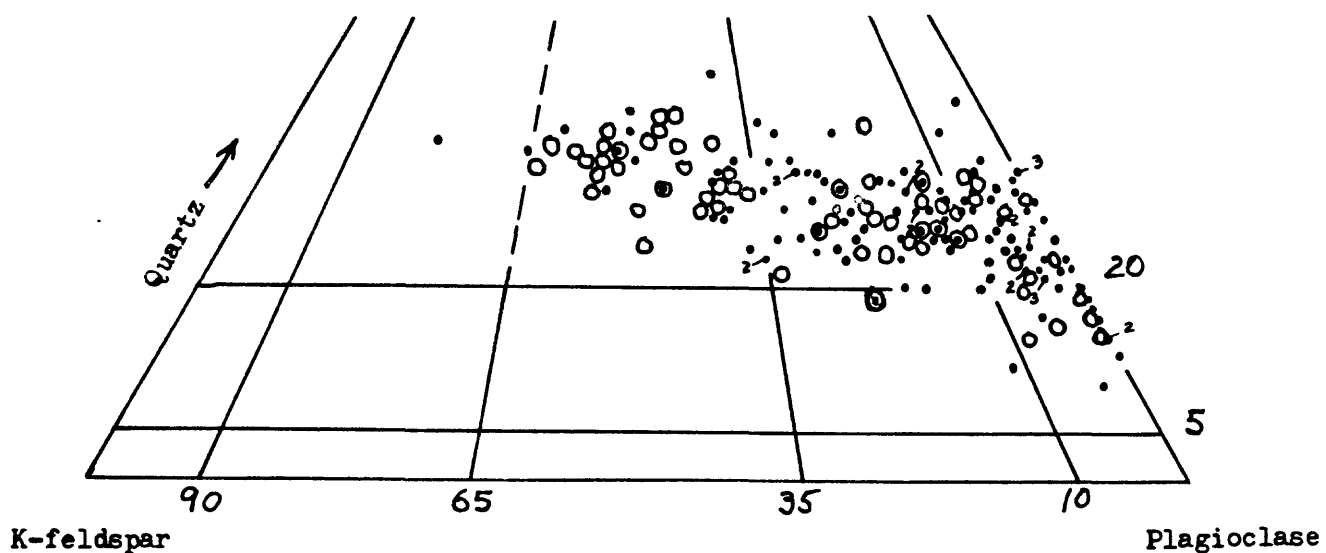


Figure 35. Modal plots showing comparison between modal distribution of chemically analyzed samples and all modal samples.

- A. Comparison of individual chemically analyzed samples (•) and average of modes for each granitic unit (○).
- B. Comparison of outlines of fields of largest concentration of modes of chemically analyzed samples and of all samples. Areas outlined contain concentrations more than 5 times greater than a random concentration of modes. Chemical sample field shown by solid lines. Total modal field shown by dashed lines.

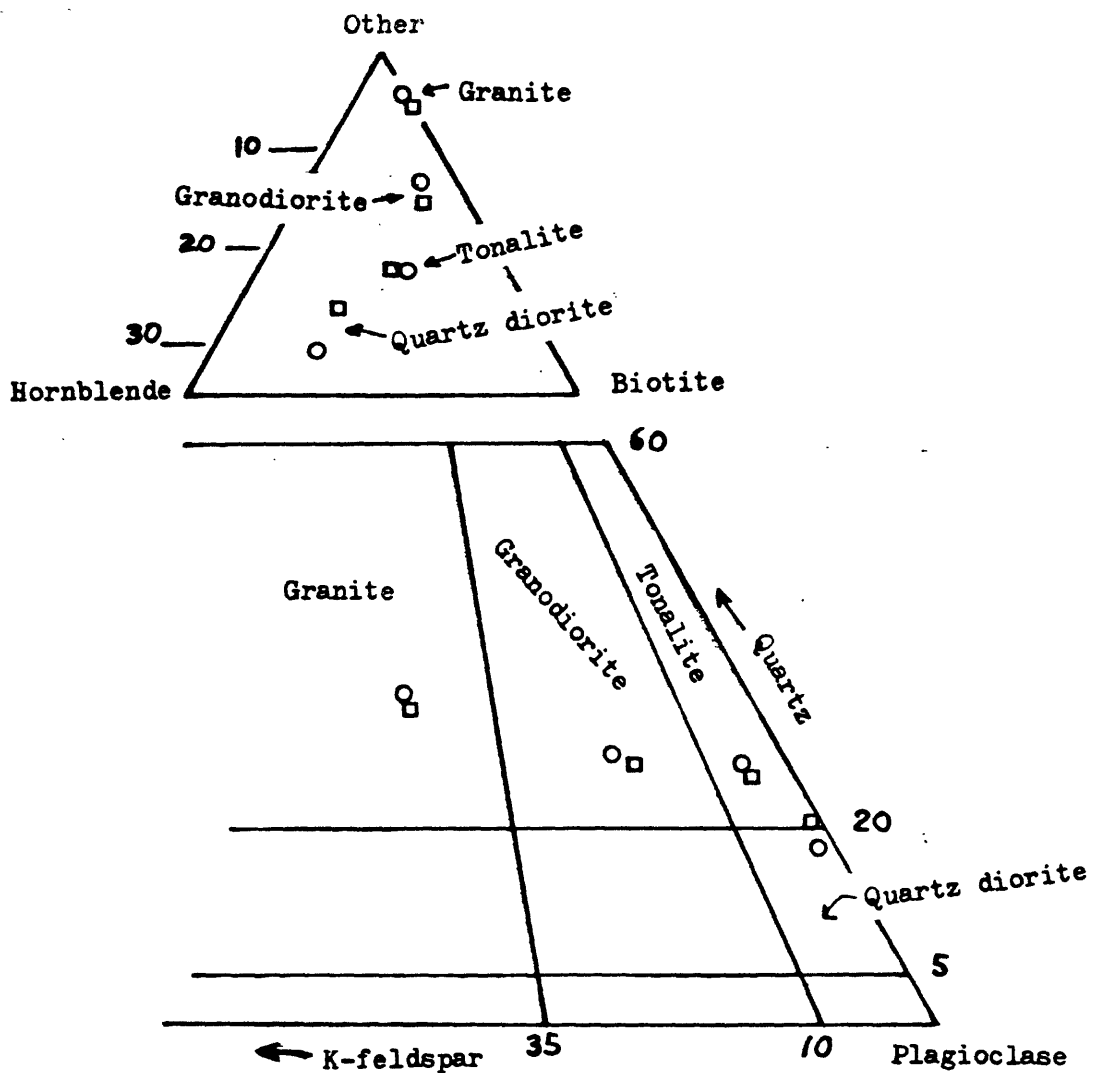


Figure 36. Modal plots of averages by rock type; chemically analyzed samples (□) compared with all modes (○).

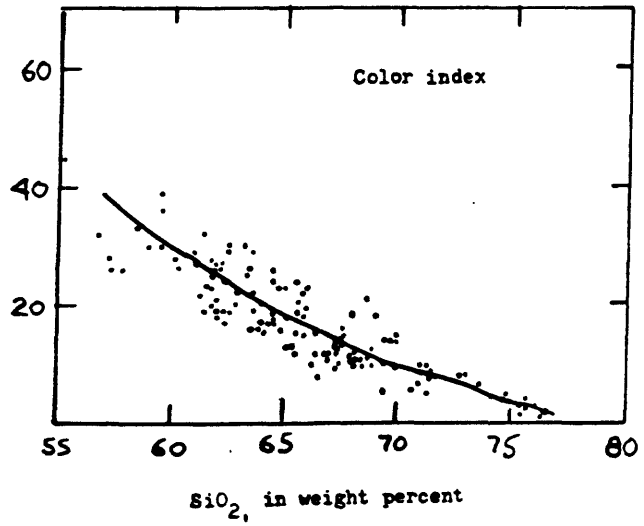
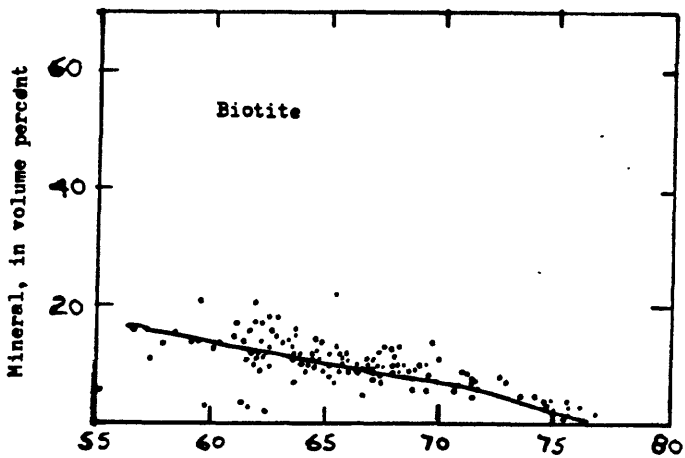
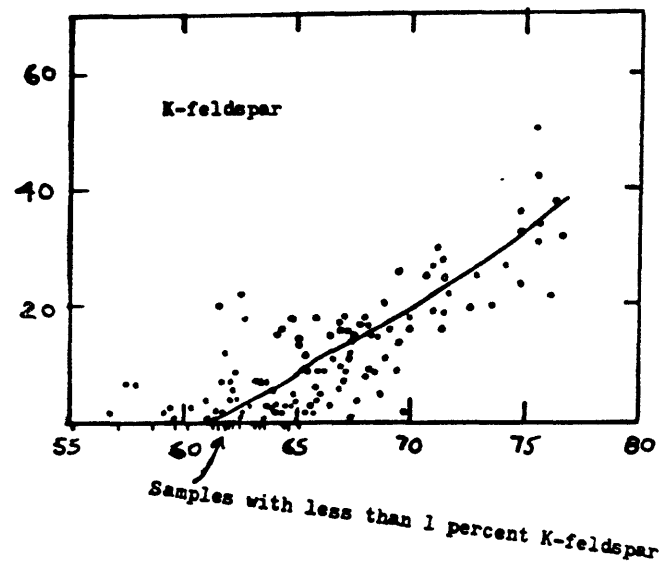
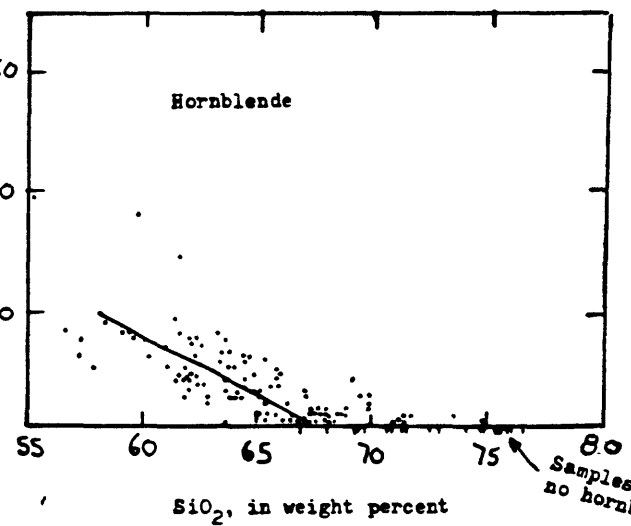
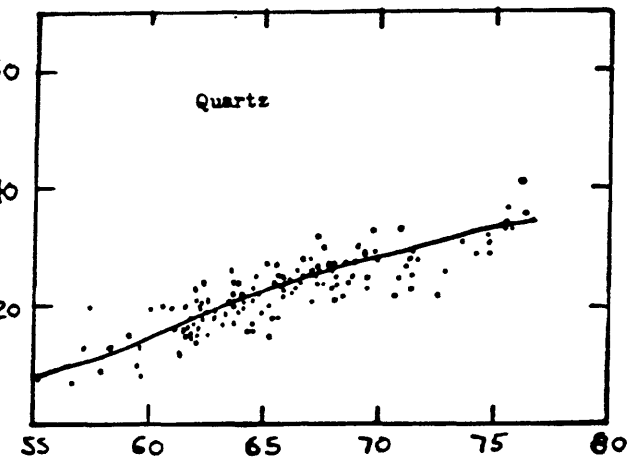
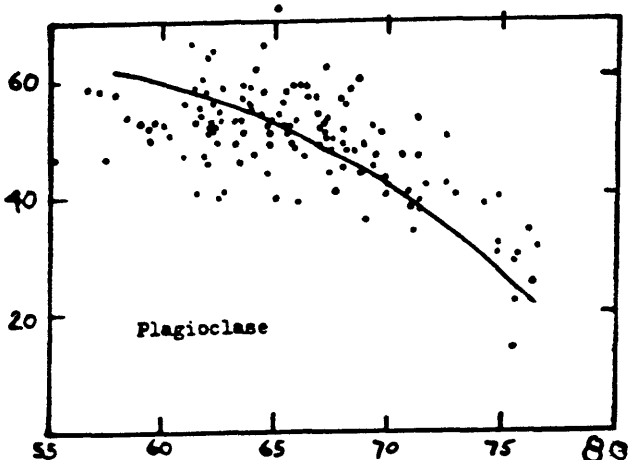


Figure 37. Modal minerals and color index plotted against silica content for chemically analyzed samples. Visually estimated trend for each mineral.

Table 1. Chemical and trace element analyses and CIPW norms for samples of granite from the southern Sierra Nevada, California

Unit	Arrastre Creek	Bodfish Canyon	Brush Mountain	Pine	Kern River	Portuguese Pass	Sherman Tehachapi Airport	Tazon Lookout										
Sample Number	6093	5071	726	3005	3221	6208	6415	6535	4763	4819A	5006	5017	5062	5139R	4100A	3401	3466	3752
Chemical analyses (weight percent)																		
SiO ₂	76.2	76.3	75.6	74.8	75.7	72.9	67.7	67.4	71.4	68.8	71.7	74.2	74.8	75.6	74.8	76.6	75.5	
Al ₂ O ₃	12.7	12.9	13.2	13.6	13.2	13.7	15.5	16.3	14.5	15.3	14.3	13.3	13.2	14.1	12.5	12.7	12.8	
Fe ₂ O ₃	.67	.63	.24	.71	.85	.98	1.71	1.26	1.	.93	1.12	.79	.85	.48	.57	1.4	1.2	1.1
FeO	.53	.32	.96	.96	.24	.89	1.74	.96	1.95	1.78	2.54	2.16	.89	1.09	.36	.5	.48	.28
MnO	.23	<.1	.17	.08	.14	.63	1.3	.67	.61	.56	.86	.33	.29	.2	.16	.71	.23	.08
CaO	1.2	.52	.87	.84	.43	2.24	3.52	3.05	1.97	1.94	3.01	1.91	1.3	.92	.67	1.4	.97	.6
MgO	3.29	3.48	3.7	3.0	3.8	3.36	3.8	4.17	3.44	3.6	3.53	4.04	3.2	3.76	3.3	4.2	3.8	2.3
K ₂ O	3.86	4.8	4.4	4.3	3.72	2.96	3.98	4.23	4.	3.76	3.47	4.57	4.41	4.9	4.8	4.2	6.9	
H ₂ O ⁺																		
H ₂ O ⁻																		
TiO ₂	.11	.04	.11	.09	.08	.33	.61	.44	.31	.28	.44	.22	.17	.13	.07	.13	.12	.08
P ₂ O ₅	<.05	.04	.04	.04	.12	.23	.19	.07	.06	.11	.07	<.05	<.05	.01	.07	.06	.05	
MnO	<.02	.07	.02	.02	.03	.05	.03	.05	.05	.06	.06	.06	.05	.03	.03	.08	.04	
CN ₂																		
Loss on ignition (900° C)	.36	.36																
Total	99.15	99.35	99.94	99.12	99.46	99.26	99.80	100.47	99.57	99.78	99.41	99.35	99.28	100.43	101.47	100.83	100.24	

		.91	2.07	3.4	8.1	2.65	1.72	3.15	3.4	2.9	4.12	4.44	4.0
		.70	1.1	3.5	7.0	4.7.0	83.4	41.2	6.2	4.9	35	70	25
		.43	1.4	3.4	7.0	2.1	2.1	2.1	2.1	2.1	2.1	2.1	2.1
		.46	3.1	3.0	2.36	4.4	4.4	4.4	4.4	4.4	4.4	4.4	4.4
		23.2	12.3	25	43	32.8	41.6	41.0	35	32	36.5	45.9	29
		46.7	16.3	57	81	58.2	92.0	79.6	63	58	70	87.1	56
		17.6	12	25	32	20.1	34.8	30.6	25	24	33	35	26
		2.74	2.62	6.5	7.5	3.2	5.58	4.68	4.2	4.0	6.46	8.11	4.0
		.579	.25	.64	.31	0.795	1.52	1.15	.68	.70	1.09	1.25	.57
		3.4	7.2	7.4	4.57	3.31	4.9	4.5	6.5	8.8	5.2	5.4	5.0
		.276	.46	1.10	1.08	0.275	0.365	0.409	.50	.44	.94	1.28	.69
		Ho							.7	.6	.6	<6	<6
		Tm							.7	.6	.6	<6	<6
		Tb							.6	.6	.6	<6	<6
		Lu											
		.104	.35	.52	.60	0.101	0.167	0.161	.38	.36	.50	.70	.43

Table 1. (cont.)

Unit	Arenite Creek	Bodfish Canyon	Brush Mountain	Pine Fingers	Kern River	Portuguese Pass	Sherman Pass	Tehachapi Airport	Tujon Lookout									
Sample Number	6093	5071	726	3005	3221	6208	6415	6535	4019A	5006	5017	5062	5133R	4100A	5201	3466	3752	
q	39.74	36.88	34.77	38.46	36.61	33.93	24.73	21.21	29.34	29.69	25.13	29.41	34.96	33.72	36.13	15	36.05 34.56	
or	23.09	28.69	26.17	26.38	25.71	22.23	17.78	23.89	25.12	23.63	22.33	20.71	27.34	26.32	29.02	21.2	24.72 40.91	
ab	28.18	29.78	31.51	25.75	32.54	28.78	32.67	35.84	29.25	30.71	30.01	34.51	27.4	32.12	27.83	35.33	32.02 19.52	
an	6.03	2.61	4.08	3.77	1.77	10.44	16.22	14.11	9.36	9.31	14.28	9.11	6.53	4.61	3.27	.07	4.34 2.66	
wo																	2.22	
sn	.58	.43	.2	.35	1.59	3.29	1.7	1.53	1.41	2.15	.83	.73	.5	.4	1.76	.57	.2	
fo	.24	1.52	1.08	.34	.88	.05	.235	2.15	3.14	3.09	.74	1.5	.13					
mt	.98	.92	.35	1.04	.61	1.44	2.52	1.86	1.46	1.36	1.63	1.16	1.25	.7	.83	1.49	1.32 .67	
il	.21	.08	.21	.17	.15	.63	1.18	.85	.59	.84	1.42	.33	.25	.13	.37	.28	.64	
ep	c	.94	1.05	.87	2.58	1.68	.36	.2	.04	.85	.87	.21	.6	.73	.57	.02	.17	.14 .12
cc					.07	.05												
Total	99.99	100.01	100.01	100.	100.01	100.03	100.02	100.01	100.02	100.01	100.01	100.01	100.01	99.99	99.97	100.03	100.01	
Normative plagioclase (An)	17.62	8.06	11.46	12.77	5.16	26.65	33.17	28.25	24.25	23.26	32.24	20.87	19.24	12.55	10.51	2.94	11.94 12.	

Table 2. Chemical and trace element analyses and CIPW norms for samples of granodiorite from the southern Sierra Nevada, California

Unit	Alder Creek					Brush Creek					Castle Rock									
	Sample Number	5236	5261	6245	6269	RHK-4	RHK-5	4796-1	5423	5031	4093	4341	4356A	4402	4472	4528	5356	5403	6539	RHK-6
Chemical analyses (weight percent)																				
SiO ₂	61.0	67.2	66.9	69.1	65.8	65.1	66.2	68.4	66.4	67.5	65.5	67.3	68.2	66.9	70.9	69.3	69.4	70.7	68.1	65.8
Al ₂ O ₃	16.5	15.6	14.8	14.4	15.1	15.2	17.2	16.9	15.6	16.3	16.5	16.1	16.0	16.2	15.4	15.6	15.4	15.9	15.9	16.2
FeO ₂	1.92	.96	3.10	1.02	0.3	1.0	1.60	.82	1.86	1.6	.93	.42	1.1	1.4	.91	1.11	1.26	1.44	1.3	1.5
FeO	4.21	2.81	1.18	2.56	3.8	3.6	1.68	1.63	2.26	2.0	3.0	3.2	1.6	2.2	1.5	1.22	1.01	.47	2.0	2.6
MnO	2.89	1.7	1.95	1.61	2.0	2.2	1.02	.73	1.43	1.2	1.0	1.0	.87	1.1	.79	.70	.68	.41	0.9	1.2
CaO	5.63	4.15	4.14	3.93	4.2	3.9	4.18	3.58	3.14	3.5	3.8	3.7	3.3	3.5	2.1	2.60	.2.69	2.28	2.4	3.5
MgO	2.97	3.14	2.67	2.80	3.1	2.9	4.07	4.29	3.32	3.6	4.0	3.8	3.7	4.1	3.6	4.06	5.88	4.13	4.1	4.0
K ₂ O	2.42	2.75	3.3	3.11	3.0	3.6	2.29	2.15	3.58	2.7	2.9	2.7	3.2	2.8	3.5	3.57	3.74	3.48	3.3	2.9
Na ₂ O ⁺						.49	.45			.61	.78		.69	.76	.73	.71		.64	.52	
H ₂ O ⁻						.29	.23			.18	.04		.14	.13	.20	.22		.27	.38	
TiO ₂	.85	.50	.54	.45	.57	.66	.51	.41	.57	.63	.70	.66	.64	.70	.37	.33	.41	.35	.52	.77
P ₂ O ₅	.15	.13	.11	.10	.12	.11	.16	.15	.15	.15	.17	.15	.17	.16	.07	.14	.13	.14	.21	.23
MnO	.09	.06	.06	.06	.06	.06	.05	.04	.06	.06	.06	.06	.06	.05	.05	.05	.04	.04	.04	.04
Co ₂																				
Loss on ignition (900° C)	.6	.84	.62	.76			.61	.77	.56								.61	.48	.84	
Total	99.23	99.84	99.37	99.90	98.85	99.26	99.57	99.87	99.33	100.07	99.6	100.13	99.87	100.21	100.22	99.09	99.32	99.44	99.7	99.67

Table 2. (cont.)

Unit Sample Number	Deer Creek		Gato-Montes			Hatchet			Keene			Lebec			
	6030	6117	3356	3534B	3733A	3756A	5865A	3695	3794A	RWK-13	686	690	698	3088	3181
Chemical analyses (weight percent)															
Si ₀₂	69.5	71.3	66.8	68.1	65.4	71.4	68.9	73.6	61.8	68.0	68.5	67.8	65.4	68.0	
Al ₂ O ₃	14.7	14.4	16.0	15.3	17.0	14.2	14.6	15.6	13.7	16.8	16.2	16.0	15.7	16.8	16.1
Fe ₂ O ₃	1.22	1.23	.64	.94	1.3	.77	.68	1.4	.72	1.2	.26	.45	.31	.90	.90
FeO	2.27	.99	2.7	2.5	2.6	1.4	1.8	2.2	1.2	4.7	2.4	2.5	2.9	2.7	2.4
MgO	1.3	.74	1.1	.97	1.3	.51	.48	.96	.42	2.2	1.	1.	1.6	1.1	1.1
CaO	3.56	2.44	3.6	3.4	4.3	1.9	2.54	3.9	2.0	4.6	3.2	3.2	3.3	4.1	3.4
Na ₂ O	3.56	3.36	4.0	4.0	4.3	3.6	3.56	3.9	3.9	4.1	3.9	3.5	3.2	3.6	3.2
K ₂ O	2.43	3.73	3.2	3.1	2.1	4.3	3.44	2.4	3.6	1.7	3.4	3.4	3.2	2.8	2.9
H ₂ O+															
H ₂ O-															
TiO ₂	.37	.27	.68	.60	.78	.35	.21	.50	.24	.91	.54	.50	.54	.76	.60
P ₂ O ₅	.11	.07	.23	.19	.27	.13	.08	.13	.07	.22	.16	.15	.15	.23	.18
MnO	.07	.04	.05	.08	.05	.03	.04	.07	.02	.09	.07	.07	.10	.03	.04
CO ₂			.02	.06											
Loss on ignition (900° C)															
Total	99.70	99.43	99.86	100.26	100.48	99.35	99.3	100.94	100.22	99.5	100.05	99.99	99.91	99.39	99.79

Table 2. (cont.)

Unit Sample Number	Peppermint Meadow			Pine Flat			Palo Plet			Rabbit Island									
	4995	5034	5852	5801R	5946	5985	6292	6247	6300	6336	6356	6373	4848	5407	5421	IS-638	IS-665	IS-727	
Chemical analyses (weight percent)																			
SiO ₂	66.6	62.2	67.2	67.3	69.9	72.6	65.9	67.2	61.9	64.5	65.6	65.8	64.2	64.8	59.6	62.19	61.74	62.55	
Al ₂ O ₃	16.5	16.7	16.3	15.7	15.4	14.6	15.5	16.1	16.5	16.1	16.4	15.8	15.6	16.1	16.3	17.0	17.21	16.19	16.29
Fe ₂ O ₃	1.75	1.91	1.37	1.39	.62	.66	2.77	1.33	1.71	1.56	1.65	1.35	1.50	2.30	1.84	2.26	1.63	1.92	1.66
FeO	1.43	3.23	1.61	2.27	1.32	1.13	1.49	2.32	3.93	3.53	2.69	3.59	3.09	2.68	2.43	4.09	2.45	2.88	2.50
MgO	1.11	2.41	1.0	1.15	.83	.56	2.06	1.28	3.05	2.49	1.99	2.37	3.22	2.09	1.78	3.22	.99	2.30	1.94
CaO	3.76	5.53	3.45	4.09	3.90	2.48	5.01	4.42	6.4	5.38	5.53	5.82	5.	4.53	4.44	6.32	>0.01	5.23	4.57
Na ₂ O	4.21	3.31	4.01	3.62	3.26	3.48	3.16	4.21	3.27	3.31	3.49	3.23	3.57	3.48	3.61	3.39	4.08	3.63	3.53
K ₂ O	2.57	2.67	2.82	2.27	2.97	3.13	2.36	1.86	1.59	1.56	1.44	1.54	1.82	2.97	3.07	1.94	2.34	2.52	3.08
N ₂ O ⁺																			
H ₂ O-																			
TiO ₂	.59	.76	.55	.53	.21	.24	.51	.44	.67	.56	.49	.58	.59	.7	.66	.88	.82	.83	.74
P ₂ O ₅	.17	.23	.16	.16	.09	.08	.11	.13	.14	.12	.14	.13	.14	.21	.20	.26	.22	.23	.19
MnO	.04	.08	.04	.05	.03	.03	.06	.06	.09	.08	.07	.07	.08	.06	.1	.08	.09	.07	
CO ₂																			
Loss on ignition (900° C)	.85	.23	.77	.65	.44	.75	.57	.45	.68	.42	.51	.46	.51	.46	.53	.54	1	1	1
Total	99.58	99.28	99.30	99.16	98.97	99.74	99.5	99.8	99.93	100.23	100.	99.55	99.71	99.8	99.72	99.6	98.02	97.56	97.12

Table 2. (cont.)

Unit	Sample Number	Sorrell Peak						Waggy Flat			Whiterock		
		6425	6472A	6483A	6523A	4366	4273	4294	4789A	5425	3737	4102	4314
Chemical analyses (weight percent)													
SiO ₂	61.6	61.9	57.9	62.8	71.	65.2	61.5	66.4	62.1	63.7	68.	64.3	
Al ₂ O ₃	16.2	15.6	17.8	16.1	15.5	16.7	17.9	16.9	17.8	16.1	16.	16.6	
Fe ₂ O ₃	2.93	3.06	3.48	2.67	.85	1.8	1.2	1.5	1.53	1.4	.97	1.3	
FeO	3.48	3.23	3.28	2.91	2.	1.9	3.9	1.84	3.14	3.	2.3	2.8	
MgO	2.54	2.53	2.66	2.2	.68	1.2	2.2	1.12	1.79	1.4	.99	1.4	
CaO	5.41	4.78	6.13	4.82	2.3	4.3	5.5	4.62	6.05	4.2	3.2	4.	
MnO	2.9	2.85	3.71	2.92	3.1	3.9	3.7	4.31	4.07	4.1	3.7	3.3	
K ₂ O	3.27	3.13	2.6	3.56	3.8	2.4	1.8	1.57	1.49	3.7	2.7	2.8	
H ₂ O ⁺				.59	.71	.85				2.1	.86	.85	
H ₂ O ⁻				.14	.29	.15				.37	.14	.15	
TiO ₂	.62	.69	.76	.58	.4	.68	.86	.66	.81	.91	.63	.75	
P ₂ O ₅	.22	.27	.29	.19	.07	.15	.18	.18	.24	.26	.11	.22	
MnO	.12	.11	.11	.10	.04	.06	.08	.05	.06	.12	.05	.07	
CO ₂					.03	.02	.03			.04	.06	.02	
Loss on ignition (900°C)	.47	1.4	.66	.54				.81	.4				
Total	99.76	99.55	99.38	99.39	100.5	99.31	99.85	99.96	99.48	101.4	99.71	98.56	

Table 2. (cont.)

Unit Sample Number	Instrumental neutron activation analyses (parts per million)										Castle Rock									
	5236	5261	6265	6269	MNK-4	MNK-5	4796-1	5423	5031	4093	4341	4354	4402	4472	4528	5336	5403	6539	MNK-6	MNK-7
Alder Creek																				
Re	586	585	916	636			883	748	1400	1130	1755	1170	1285	1240	915	1280	725	1130		
Co	15.2	8.56	10.1	8.15			4.2	3.3	7.5	5.9	5	5	3.4	4.7	3.1	3.29	3.57	2.03		
Cr	36.0	24.6	26.1	22.6			2.5	1.5	16.5	3.8	3.3	4.7	3.2	1.9	3	2.8	3.3	1.68		
Ca	7.1	7.59	6.29	6.02			2.1	2.41	6.3	1.2	2.7	2.5	1.5	1	1.7	2.41	2.96	.87		
Hf	5.4	4.71	6.42	5.77			4.	3.9	4.7	4.9	6.4	5.3	5	5.8	3.5	4.26	4.22	4.1		
Rb	122	119	120	115			68	66	140	76	84	104	92	95	112	106	135	83.9		
Ta	.72	.59	.811	.891			.56	.6	.76	.9	.75	.9	2.7	1.88	.75	.96	1.28	.432		
Tl	8.5	16.9	9.06	16.5			5.9	4.29	7.1	8.5	10.4	12	16.8	11	8.6	6.23	22.6	5.69		
U	3	3.15	2.5	5			1.3	1.02	2.7	1.8	2.5	3.3	5	3.2	2.3	3.27	3.41	1.21		
Zn	78	65	71.7	59.8			72	60	64	71	91	77	.66	74	51	40	53	50.2		
Zr	180	192	203	182			151	147	176	200	245	210	215	239	153	n.d.	n.d.	133		
Be	13.5	7.77	12.4	10.8			4.34	3.28	6.03	4.15	3.95	3.95	2	3.39	2.85	1.39	3.09	1.86		
La	16	32.8	25.8	34.7			26	15.9	21	39	50	42	40	50	29	21.4	37.1	23.5		
Ca	33	56	54	73.2			44	31.4	40	70	92	76	81	96	51	38.9	68.7	49.3		
W	22	23	25.4	31.9			21	16	21	28	35	32	29	42	20	14	25	17.9		
Sr	4.2	4.08	6.04	6.47			3.1	3.15	3.8	4.7	5.7	5.6	4	9	3.3	2.6	3.87	2.85		
Pb	.97	.85	.897	.862			.88	.86	1	1.07	1.23	1.06	.78	1.72	.71	.7	.83	.709		
Od	4.9	2.25	5.93	2.86			2	2.6	3.5	4.3	5.2	5	3.4	7.4	2.7	.8	3.1	1.69		
Tl	.47	.31	.902	.941			.27	.3	.41	.51	.55	.3	.79	.26	.27	.25	.173			
Ho	.5						.4		.5	<.7	<.9	<1.0	.3	<.9	<.7					
Ta	.3	.25	.47	.581			.16	.112	.23	.17	.22	.2	<.2	.2	.11	<.1	<.1	.058		
Tl	.21	1.37	2.86	3.16			.9	.779	1.7	.9	.8	1	1.5	.7	.65	.89	.365			
La	.29	.24	.436	.457			.13	.112	.23	.12	.13	.12	.22	.1	.13	.12	.0564			

Table 2. (cont.)

Unit Sample Number	Deer Creek		Gato-Montes		Hatchet Peak		Keene		Lebec					
	6030	6117	3356	3534B	3733A	3756	5863A	3695	3794A	686	690	698	3088	3181
Instrumental neutron activation analyses (parts per million)														
La	604	781	1320	970	650	1180	1120	1103	959				1435	1090
Co	6.21	3.6	5.3	4.5	6.5	2.3	2.73	6	2.8				5.7	6.4
Cr	10	7.21	4.7	<8.8	3.1	2.3	1.32	4.7	2.3				5.6	9.8
Ca	4.68	2.2	2.5	3.8	2.9	1.5	6.88	2.4	.7				2.8	2.7
Hf	4.2	3.46	4.8	5.9	6.3	5.1	5.11	4.3	3.8				5.9	4.2
Rb	79	76.9	83	129	88	135	124	86	99				96	95
Ta	.57	.637	.88	2.74	1.2	1.1	.868	.51	.37				1.9	.76
Th	11.5	11.2	8.4	18.	13.9	10.1	17.6	7.4	3				9.7	9.9
U	3.54	2.24	2	4.3	2.1	1.4	4.97	1.6	1.7				4.2	
Zn	41.8	23.5	84	100	100	64	38.3	62	41				98	74
Zr	121	140	222	269	305	227	159	94	138				212	188
Sc	8.81	5.1	3.4	4.06	4.68	3.3	4.49	7.6	4.95				4.53	4.43
La	19.3	16.7	40	45	45	33	30.3	16	13				36	
Ca	39.1	33.5	74	82	88	62	64.4	40	29				70	63
Md	17	14.7	27	35	34	27	23.6	14	16				35	26
Sm	3.64	3.18	4.1	6	5.1	4.7	4.56	3.4	3.3				6.9	
Tu	.816	.7	1.2	1.16	1.23	.91	.816	1.03	.71				1.28	1.02
Gd	3.88	3.3	5.3	4.1	3.8	4.79	3.3	2.8					5.5	3.9
Tb	.601	.505	.47	.8	.59	.5	.658	.68	.46				.64	.34
Ho		<.6	<.8	<.7	<.6			.5	<.8					
Tm		.343	.21	.46	.24	.21	.457	.34	.27				.22	.26
Yb		2.72	2.04	.7	2.2	.9	1	2.94	1.9	1.6			1.5	.7
Lu		.421	.294	.11	.33	.14	.15	.449	.3	.25			.2	.12

- 92 -

Table 2. (cont.)

Unit Sample Number	Peppermint Meadow			Pine Flat			Instrumental neutron activation analyses (parts per million)						Rabbit Island				
	4995	5034	5852	5801R	5946	5965	6292	6297	6300	6336	6356	6373	4848	5407	5421	18-638	18-655
Instrumental neutron activation analyses (parts per million)																	
Re	917	1130	1220	713	397	693	681	714	554	438	554	484	773	449	922	625	
Co	5.	11.6	5.25	5.78	3.73	2.35	10.1	6.69	13.7	12.8	9.56	12.2	11.1	10.1	9.16	16.9	
Cr	1.5	23.5	5.47	4.84	5.96	1.49	26.4	11.2	48.3	29.8	23.3	28.9	21.2	13.7	11.7	45.4	
Ca	4.3	2.99	3.06	5.42	6	4.48	4.06	2.28	2.68	3.67	2.77	6.01	2.54	5.1	4.02	3.49	
Mg	4.	4.79	3.9	4.32	3.47	3.98	3.97	6.1	3.74	4.31	3.94	4.35	3.93	4.6	4.38	4.31	
Nb	80.	79.	79.5	75.4	98.1	114.	77.1	48.7	53.4	52.6	44.7	68	59.2	111	110	66	
Ta	.7	.96	.634	.791	.679	1.33	.397	.354	.346	.334	.322	.492	.295	1.2	1.51	1	
Th	7.3	10.6	5.54	10.1	18.9	17.8	20.9	8.19	3.43	4.94	5.88	5.57	8.31	12.4	14.8	8.6	
U	1.7	2.88	1.46	2.77	5.19	5.32	3.79	1.75	1.09	2.7	1.47	2.29	.847	3.7	3.78	2.39	
Zn	72.	73.	59.1	54.9	25.7	49.5	63.1	68.8	97	69.3	79.7	74.3	75.9	75	71	87	
Zr	164	134	141	87.2	114	123	200	128	126	116	139	141	203				
Sc	3.28	9.78	3.69	4.8	5.31	2.19	12.6	10.7	18.8	15.1	12.3	15.1	12.9	6.79	5.75	14.3	
La	26.	27.2	22.7	22.7	7.68	20.1	11.8	18.4	13.6	12.6	11.9	9.35	20.4	34	37.2	24.1	
Co	48.	50.8	47.9	50.6	16.0	49.2	26.3	38.6	31.8	27.9	27.4	24.1	42.1	53	63.7	46.1	
Mn	22	26	19.3	20.6	7.36	16.4	11.7	19.	17.5	14.8	16.2	12.9	17.4	24	24	22	
Sr	3.2	4.95	3.53	3.74	1.9	3.4	3.18	4.36	4.53	2.9	3.79	3.06	3.92	3.3	4.37	4.78	
Ru	.9	1.12	.96	.99	.673	.759	.766	.964	.94	.818	.937	.852	.911	.86	1	1.15	
Cd	3.	3.6	2.43	2.87				4	3.92	2.71	3.54	3	3.83	3.7	3.2	4.7	
Tb	.22	.56	.317	.359	.278	.378	.492	.677	.633	.493	.534	.492	.593	.27	.38	.61	
No	.2													.4			
Ta	.13	.2	.122	.141	.178												
Tb	.6	1.3	.618	.778	1.14	.976	1.97	2.52	2.09	1.95	1.7	2.05	2.01	1.1	.92	1.8	
La	.09	.21	.0931	.113	.18	.139	.29	.359	.303	.319	.251	.304	.305	.14	.17	.28	

Table 2. (cont.)

Unit Sample Number	Sorell Park						Waggy Flat			Whiterock		
	6425	6472A	6483A	6523A	4366	4273	4294	4789A	5425	3737	4102	4314
Instrumental neutron activation analyses (parts per million)												
Rs	910	1090	737	715	1265	619	687	460	647	1519	1100	1150
Co	15.1	14.5	15.6	12.1	3.5	5.6	10.2	5.2	8.84	5.7	5.1	7.1
Cr	4.34	11.4	14.5	5.55	3.7	2.4	9.8	3.1	7.9	4.3	3.7	12.2
Cs	4.62	1.68	2.1	4.24	3.8	3.1	2.6	4.9	2.	2.1	3.1	3.3
Hf	4.91	5.04	6.64	5.03	4.5	3.8	3.2	3.8	4.01	5.8	4.1	5.1
Rb	105.	83.9	88.1	126.	112.	69	60	68	44	89	104	100
Ta	1.05	.938	.558	.928	.73	.63	.71	.92	.57	1.13	.87	1.68
Th	13.6	16.8	7.78	18.9	13.6	10.1	7.	12.2	5.1	3.4	6.3	11.5
U	2.48	2.93	2.38	3.07	3.2	3	1.4	3.7	1.26	1.9	2.7	3.4
Zn	76.1	84.8	95.7	76.6	64	75	86	67	93	93	78	80
Zr	<170.	177.	233.	210.	182	138	120	156	168	215	162	200
Sc	15.5	14.2	14.1	13.8	3.03	3.73	6.7	4.26	8.07	4.71	2.96	5.78
La	35.	42.1	30.8	40.1	37	18	27	20	24.9	21	25	37
Ce	67.2	75.6	65.	74.7	68	35	53	47	47.1	52	49	75
Nd	31.7	29.3	30.1	30.2	25	17	26	27	26	27	20	37
Sm	6.08	5.48	6.17	5.92	4.5	3.3	4.6	4.1	4.99	5.1	3.9	7.8
Ba	1.33	1.27	1.31	1.12	.94	.87	1.1	1.08	1.2	1.47	.94	1.31
Cd	5.43	4.95	5.17	5.56	4.	2.8	4.1	3.6	4	3.7	3.7	7.1
Tb	.832	.748	.808	.817	.45	.45	.55	.3	.53	.39	.41	.81
Ho					<.7	<.7	.5	.35		<.8	<.9	1
Tm	.485	.4	.404	.456	.17	<.1	.23	.13	.18	<.14	.14	.35
Tb	3.14	2.52	2.52	2.92	.9	.7	1.1	1	.99	.9	.8	2.2
Lu	.456	.364	.359	.418	.12	.1	.16	.13	.15	.13	.11	.27

Table 2. (cont.)

Unit Sample Number	5236	5261	Alder Creek	6245	6269	RMK-4	RMK-5	4796-1	5423	5031	4093	4341	4354	4402	4472	4528	5356	5403	6539	RMK-6	RMK-7	CIPW norme (weight percent)	
Q	17.03	25.94	27.87	29.43	22.36	21.46	23.51	26.33	23.57	27.11	21.66	24.55	27.1	23.66	31.14	25.74	26.31	28.65	25.74	22.09			
or	14.5	16.42	19.75	18.54	18.35	21.68	13.68	12.82	21.42	16.07	17.35	16.08	19.11	16.67	20.83	21.38	22.36	20.86	19.46	17.35			
ab	25.48	26.84	22.88	23.9	27.25	24.63	34.8	36.63	28.44	30.39	32.62	31.59	30.51	33.9	29.94	34.81	33.22	35.44	35.63	34.27			
an	24.88	19.94	18.89	17.69	16.35	18.07	19.9	16.93	16.79	16.5	17.96	17.52	15.42	16.44	10.03	12.15	12.64	10.55	11.12	15.87			
vo	1.02	.5	.55	.93	.35																		
en	7.3	4.28	4.92	4.05	5.	5.5	2.57	1.84	3.61	3.01	2.52	2.51	2.19	2.76	1.98	1.77	1.71	1.04	3.04	3.03			
fe	4.98	3.69	3.26	5.94	5.28	1.03	1.73	1.81	1.43	3.74	4.59	1.08	1.89	1.5	.88	.21					2.37		
wt	2.82	1.41	2.47	1.49	.46	1.39	2.34	1.2	2.73	2.34	1.37	.61	1.61	2.05	1.33	1.63	1.85	.51	1.86	2.2			
hm			1.44																				
il	1.64	.96	1.04	.86	1.22	1.37	.98	.79	1.1	1.21	1.35	1.26	1.23	1.34	.71	.64	.79	.67	.91	1.48			
ep	.36	.31	.26	.24	.34	.34	.38	.36	.36	.36	.36	.41	.36	.41	.38	.17	.34	.31	.37	.34	.55		
c	.23																						
cc																							
Total	100.01	100.02	100.02	100.01	100.22	100.09	100.01	100.01	100.02	99.94	99.6	99.79	99.74	99.76	99.83	100.01	100.	100.01	99.63	100.03			
Normative Plagioclase (An)	49.41	42.63	45.22	42.54	40.24	42.32	36.38	31.61	37.12	35.19	35.51	35.68	33.58	32.66	25.09	25.86	27.57	22.93	23.79	31.65			

Table 2. (cont.)

Unit Sample Number	Deer Creek			Gato-Montes			Hatchet Peak			Keene			Lebec		
	6030	6117	3356	3534B	3733A	3756	5865A	3695	3794A	RHK-13	686	690	698	3088	3181
CIPW norms (weight percent)															
q	29.28	31.6	21.3	23.9	24.64	29.31	30.82	26.74	32.07	16.54	23.52	26.06	27	23.19	29.09
or	14.49	22.37	19.1	18.5	7.2	25.77	20.57	14.19	21.39	10.21	20.23	20.22	19.06	16.8	17.33
ab	30.4	28.84	34.18	34.11	36.94	30.9	30.48	33.01	33.18	35.26	33.23	29.8	27.32	30.92	27.39
an	17.1	11.82	16.39	14.75	19.9	8.7	12.22	17.98	9.29	21.22	13.72	14.3	13.6	18.55	15.51
wo				.26				.22		.09					
en	3.27	1.87	2.77	2.43	3.29	1.29	1.21	2.39	1.05	5.57	2.51	2.51	4.02	2.78	2.77
fs	2.7	.44	3.43	3	2.54	1.43	2.5	2.19	1.26	6.41	3.5	3.55	4.4	3.06	2.78
wt	1.79	1.81	.94	1.37	1.91	1.13	1.	2.03	1.05	1.77	.4	.66	.5	1.33	1.32
re															
11	.71	.52	1.3	1.15	1.5	.67	.4	.95	.46	1.76	1.03	.96	1.04	1.47	1.15
ap	.26	.17	.55	.45	.65	.31	.19	.31	.17	.53	.4	.36	.36	.55	.43
c	.57	.01			1.48	.49	.6			.57	1.12	1.37	2.05	1.17	2.09
cc		.05	.14							.19	.44	.25	.69	.21	.12
Total	100.	100.	100.02	100.06	100.05	100.	99.99	100.01	100.01	100.03	100.1	100.04	100.08	100.03	99.98
Normative Plagioclase (An)	36	29.06	32.41	30.13	35.01	21.97	28.62	35.26	21.87	37.57	29.22	32.43	33.27	37.5	36.15

Table 2. (cont.)

Unit Sample Number	Peppermint Meadow			Pine Flat			Pine Flat			Pine Flat			Rabbit Island					
	4993	5034	5032	5001R	5046	5053	6292	6297	6300	6336	6337	6339	6373	6403	5421	19-65%	19-65%	18-72%
	Climb scores (weight percent)																	
a	23.21	17.3	26.36	26.9	29.96	34.35	25.91	23.9	17.96	22.00	24.53	23.22	23.08	19.91	20.86	13.89	16.6	17.79
or	15.39	15.93	17.27	13.62	17.82	18.69	14.1	11.07	9.47	9.26	8.56	9.19	10.84	17.67	18.29	11.58	14.42	15.6
o	36.08	20.28	34.42	31.09	28.	29.75	27.03	35.06	27.88	20.06	29.68	27.56	26.45	20.8	28.96	35.07	31.5	30.86
m	17.77	23.04	16.17	19.53	18.89	11.9	21.37	19.67	23.84	24.51	24.94	24.29	21.34	19.67	19.36	23.48	22.19	20.89
s	1.91					.06		1.27	.65	2.18	1.65	.71	1.57	1.15	.64	1.76	.93	2.09
m	2.8	6.06	2.93	2.91	2.1	1.41	5.2	3.21	7.46	6.22	4.96	5.16	5.07	5.24	4.47	8.1	5.99	6.91
r	.20	3.23	1.01	2.27	1.65	1.2		2.57	4.9	4.41	2.91	4.71	3.62	2.03	1.90	4.42	1.85	2.11
st	2.17	2.8	2.02	2.05	.91	.97	3.26	1.94	2.5	2.3	2.41	1.99	2.19	2.36	2.69	2.31	2.59	2.94
j							.59											
l	1.14	1.5	1.06	1.02	.41	.46	.66	.26	1.26	1.07	.94	1.11	1.13	1.36	1.26	1.59	1.52	1.52
ap	.41	.56	.43	.39	.22	.19	.26	.31	.33	.29	.33	.31	.33	.5	.46	.62	.36	.36
c	.37		.75	.24		1.19												
cc																		
Total	100.02	100.03	100.02	100.02	100.	100.03	100.02	100.	100.03	100.01	100.02	100.	100.02	100.01	100.03	100.	100.	100.
Nonnative plastocleses (An)	44.9	31.9%	36.3%	40.2%	39.5%	44.1%	35.4%	40.1	46.6%	45.6%	46.82	41.2	39.0%	30.4	47.	36.7%	39.87	39.32

Table 2. (cont.)

<u>Unit</u>	<u>Sacatar</u>					<u>Sorrell</u>			<u>Wagy Flat</u>			<u>Whiterock</u>		
<u>Sample Number</u>	6425	6472A	6483A	6523A	4366	4273	4294	4789A	5425	3737	4102	4314		
Q	16.97	19.63	10.18	18.76	31.82	22.79	16.65	23.94	16.98	15.14	27.66	23.68		
or	19.47	18.85	15.57	21.29	22.51	14.43	10.76	9.4	8.89	22.1	.5.16	16.96		
ab	24.71	24.57	31.8	25.	26.07	33.42	31.45	36.78	34.76	35.07	31.27	28.47		
an	21.68	20.91	24.55	20.54	10.98	20.7	26.41	21.93	26.14	14.76	15.36	18.87		
wo	1.63	.61	1.81	1.						1.07	1.81			
en	6.37	6.42	6.71	5.54	1.7	3.04	5.54	2.81	4.5	3.52	2.5	3.57		
fs	3.19	2.52	2.13	2.39	2.39	1.01	4.96	1.15	3.31	3.11	2.51	3.03		
nt	4.28	4.52	5.11	3.92	1.24	2.66	1.76	2.19	2.24	2.05	1.43	1.93		
hm														
il	1.19	1.34	1.46	1.11	.76	1.31	1.65	1.26	1.55	1.75	.1.21	1.46		
ap	.53	.65	.7	.46	.17	.36	.43	.43	.57	.62	.26	.53		
c													1.54	1.46
cc											.09			
Total	100.02	100.02	100.02	100.	99.96	99.98	99.95	100.03	100.01	100.02	99.9	99.96		
Normative plagioclase (An)	46.73	45.98	43.57	45.11	29.64	38.25	45.64	37.35	42.92	29.62	32.94	39.86		

Table 3. Chemical and trace element analyses and CIPW norms for samples
of tonalite from the Southern Sierra Nevada, California

Unit Sample Number	Antimony Peak			Bear Valley Springs						Carver-Bowen						
	784B	3023	3158	3427B	3575	3670	3791	3837	3858	4181	4184	4281	6369	5980	6079A	RWK-3
	Chemical analyses (weight percent)															
S10 ₂	62.3	61.3	62.3	63.6	62.5	62.1	62.3	57.4	60.3	64.7	60.1	63.5	63.6	63.7	61.7	65.8
Al ₂ O ₃	20.8	20.2	16.2	16.2	16.3	16.1	16.2	16.1	16.7	16.8	17.9	17.1	16.	15.7	16.3	15.9
Fe ₂ O ₃	1.3	1.3	1.5	1.6	1.7	1.6	1.6	2.3	1.7	1.5	1.7	1.3	1.5	.02	1.5	1.6
FeO	2.2	2.2	2.4	3.8	4.0	4.2	4.2	5.8	4.6	3.2	4.4	3.5	3.77	.4	4.07	2.6
MgO	2.4	2.6	2.4	2.2	3.1	3.0	2.7	4.5	3.2	2.2	3.3	2.	2.66	.56	2.85	2.1
CaO	6.3	6.7	3.8	5.4	6.1	6.2	6.	6.9	6.5	4.8 ¹	6.2	4.8	6.78	.06	5.73	5.
Na ₂ O	3.9	3.6	2.3	3.8	3.3	3.3	3.8	3.0	3.2	3.7	3.2	3.4	3.29	3.27	3.08	3.8
K ₂ O	.56	.63	3.4	1.9	1.9	1.8	1.5	2.4	1.9	1.7	1.5	2.2	1.05	1.29	1.82	1.8
H ₂ O ⁺	.44	.63	2.2	.97	.87	.81	.98	1.	.53	.67	.68					.52
H ₂ O ⁻	.4	.36	.22	.15	.15	.11	.1	.21	.16	.12	.17	.11				.28
TiO ₂	.33	.36	.86	.72	.79	.74	.74	.77	.6	.69	.54	.62	.6	.65	.52	
P ₂ O ₅	.16	.18	.21	.16	.17	.16	.16	.15	.16	.1	.11	.77	.14	.15	.14	.16
MnO	.08	.07	.07	.08	.09	.08	.08	.15	.1	.08	.11	.09	.09	.09	.09	.08
CO ₂	.02		.19		.01			.01		.03	.03	.02				.04
Loss on ignition (900° C)													.52	.68	.85	
Total	101.19	100.13	100.05	100.58	100.96	100.38	100.21	100.64	99.79	100.06	100.01	100.02	98.96	98.78	100.2	

Table 3. (cont.)

Unit Sample Number	5008	5285	5871	5887	5922	5974	6004	Dunlap Meadows		Fountain Springs	
								Chemical analyses (weight percent)			
S10 ₂	59.1	59.4	58.4	63.9	63.3	62.1	61.1	.64.	.66.		
Al ₂ O ₃	16.9	16.6	17.0	16.2	16.8	16.4	17.2	16.2	15.5		
Fe ₂ O ₃	2.59	1.73	1.83	1.64	1.46	1.43	1.57	1.74	1.28		
FeO	4.54	5.08	5.1	3.4	2.82	3.6	4.14	2.87	2.68		
MgO	3.45	3.29	3.37	2.31	2.2	2.5	2.63	2.21	1.76		
CaO	6.68	6.92	6.91	5.6	6.	5.61	6.38	5.52	5.19		
Na ₂ O	2.88	3.07	3.01	3.2	3.28	3.01	3.22	3.58	3.31		
K ₂ O	1.97	1.74.	1.56	1.65	1.52	2.07	1.58	1.29	1.43		
H ₂ O ⁺											
H ₂ O ⁻											
T10 ₂	.79	.69	.73	.65	.54	.61	.75	.53	.37		
P ₂ O ₅	.13	.15	.15	.15	.17	.15	.19	.15	.12		
MnO	.12	.11	.12	.07	.07	.08	.09	.07	.08		
CO ₂											
Loss on ignition (900° C)	.45	.59	.88	.96	1.17	1.5	.58	.51	1.11		
Total	99.6	99.37	99.06	99.73	99.33	99.06	99.43	98.67	98.83		

Table 3. (cont.)

Unit Sample Number	Hoffman Canyon			Mt. Adelaide			Walt Klein			Zumwalt			
	3842A	RWK-9	3631	4189	6061	6088	6096?	6281A	6314-1	RWK-1	RWK-2	6123	
	Chemical analyses (weight percent)												
S10 ₂	62.8	63.8	65.2	67.3	67.6	69.7	64.8	63.7	69.9	65.6	63.2	68.7	
Al ₂ O ₃	16.8	16.3	17.8	16.8	16.	16.1	15.7	16.8	15.	15.9	16.5	15.7	
Fe ₂ O ₃	1.8	1.7	1.3	.77	1.13	.65	1.21	1.62	.94	1.74	.7	1.1	
FeO	3.0	3.4	2.2	2.4	2.38	1.83	3.45	3.12	1.87	2.66	4.3	2.2	
MgO	1.8	2.1	1.6	2.4	1.55	1.1	2.46	2.2	1.22	2.1	2.8	1.2	
CaO	4.8	4.5	5.2	4.1	4.38	4.44	5.65	5.68	3.76	5.53	5.8	6.	
Na ₂ O	4.	3.7	4.6	3.9	3.54	3.59	3.05	3.56	3.13	3.46	3.3	4.2	
K ₂ O	2.3	2.8	.84	1.4	1.33	1.33	1.7	1.19	2.84	1.44	1.8	1.47	
H ₂ O ⁺	1.	.45	1.1	.74						.53	.54		
H ₂ O ⁻	.16	.28	.36	.18						.25	.26		
TiO ₂	.92	.87	.55	.47	.34	.28	.52	.58	.34	.48	.62	.44	
P ₂ O ₅	.29	.23	.19	.11	.13	.12	.13	.17	.1	.15	.15	.15	
MnO	.07	.06	.05	.06	.06	.04	.07	.08	.04	.08	.07	.04	
CO ₂	.26	.04	.01	.03						.03	.05		
Loss on ignition (900° C)					.76	.43	.5	.37	.51	.6		.4	
Total	100.	100.23	101.	99.66	99.7	99.61	99.24	99.07	99.65	99.74	100.05	100.17	99.53

Table 3. (cont.)

Unit Sample Number	Antimony Peak		Near Valley Springs									
	784B	3023	3158	3427B	3575	3670	3791	3837	3858	4181	4184	4281
Instrumental neutron activation analyses (parts per million)												
Na	174	212	742	581	667	636	645	480	640	434	770	148
Co	9.2	10.3	12.6	13.9	15.4	14.3	20.3	15.3	11.	16.6	11.	12.4
Cr	23.4	32.3	15.3	45.	30.9	28.4	71.2	36.8	34.	42.6	21.5	35.
Cs	.8	.5	1.4	4.5	1.9	1.3	4.	4.3	2.5	3.5	4.3	4.12
Hf	2.7	2.9	5.	3.3	3.2	3.4	2.2	3.2	3.5	3.9	3.97	
Rb	9.	16.	56	87	65	49	87	67	60	60	92	43.2
Ta	.14	.11		.62	.93	.38	.45	.43	.59	.26	.34	.53
Th	.3	.4		5.4	8.4	13.	.8	4.	6.	8.	8.4	5.7
U	<2.0	<2.0	<1.1	1.5	<1.	<.9	2.1	1.5	1.5	1.7	1.6	2.18
Zn	54	47	91	88	92	105	134	98	64	74	53	72
Zr	120	140	198	<310	<319	<314	<422	<377	135	150	150	126.
Sc	11.2	10.8	14.59	15.96	16.42	16.43	26.29	18.51	9.	18	1.	7
La	7	7	28	25	32	12	12	13	10	11	10	12
Ca	14	14	56	52	59	29	27	29	21	24	30	24
Md	13	<20	26	16	24	19	18	16	10	14	14	13.7
Sm	2.3	2.1	4.7	5.5	4.3	4.3	4.6	3.8	2.5	3.4	3.3	3.14
Eu	.78	.7	1.03	1.1	.93	1.04	.92	.88	.66	.76	.75	.797
Gd	2.	2.4	4.8	5.5	4.3	4.5	4.9	3.5	2.7	3.9	3.8	3.3
Tb	.34	.29	.77	.95	.67	.81	<1.38	<1.23	.44	.58	.45	.546
Ho												
Tm	.19	.12										
Tb	1.3	1.1										
Lu	.21	.18										

- 102 -

Table 3. (cont.)

Unit Sample Number	Carver-Brown			RWK-3			5008			5285			5871			5887			5922			5974			6004			6024			6106			Instrumental neutron activation analyses (parts per million)			Dunlap Meadow			Fountain Springs		
	5980	6079A																																								
Ba	312	679		497	422		526	467		469		500		536		562		519																								
Co	12.2	14.7		17.5	18.4		11.7	10.5		12.4		10.7		10.7		9.04																										
Cr	42.9	45.9		34.3	37.3		33.	31.3		30.		26.8		20		37.6		12.6																								
Cs	3.77	4.53		3.9	4.57		3.12	4.13		4.17		4.73		3.33		1.59		2.34																								
Hf	6.99	6.15		3.9	2.76		5.29	3.81		4.05		4.33		3.88		5.98		4.34																								
Rb	47.5	76.6		74	67		57.8	65.5		56.7		86.7		60.2		37.9		39.5																								
Ta	.393	.369		.69	.63		.653	.76		.524		.665		.541		.372		.347																								
Th	8.84	7.97		7.1	8.8		6.97	11.1		8.14		14.1		6.19		5.82		6.69																								
U	1.76	1.95		2.1	1.9		2.29	2.97		2.67		3.72		1.74		1.36		.889																								
Zn	52			76	79		67.5	56.7		49.		56.1		68.2		48.7		47.9																								
Zr	280	210		150			190	120		127		127		139		200		140																								
Sc	20.5	19.7		18.4	20.9		21.7	11.3		13.		14.3		12.9		17.1		16.																								
La	14.	14.2		19	24.2		19.6	20.8		12.5		25.2		16.6		17.7		17.3																								
Ce	32.3	32.5		41	46.2		48.8	45.1		33.4		55.1		40.6		39.6		39.2																								
Nd	18.1	18.7		23	26		22.3	16.1		16.4		20.7		18.4		20.5		18.8																								
Sr	4.52	4.29		4.	4.96		4.78	3.37		3.63		4.01		3.83		5.		4.4																								
Ru	1.03	1.03		1.03	1.08		1.16	.955		1.04		.96		1.06		1.14		.944																								
Gd				6.4	5.4		4.48	3.34		3.63		4.16		3.64		5.69																										
Tb	.821	.741		.52	.78		.715	.439		.461		.548		.472		.82		.718																								
Ho				.6																																						
Tm	-489	.435		.39	.46			.232		.238				.318		.248		.493		.525																						
Tb	2.72	2.46		2.6	2.93		2.68	1.21		1.51		1.97		1.44		2.8		2.8																								
Lu	.407	.375		.39	.43		.423	.207		.24		.304		.215		.408		.436																								

Table 3. (cont.)

Unit	Hoffman Canyon	Mt. Adelaide									Zumwalt	
Sample Number	3642A	RWK-9	3631	4189	6061	6088	6096?	6281A	6314-1	RWK-1	RWK-2	6123
Instrumental neutron activation analyses (parts per million)												
Ba	81.6		363	603	393	468	583	479	1180	474		362
Co	8.5		7.2	6.8	7.79	4.92	11.4	9.83	6.04	9.32		14.5
Cr	7.5		11.2	13.5	12.3	9.33	36.9	23.2	13.6	24.2		44.4
Ca	1.3		<1	1.6	2.21	3.41	2.54	3.58	4.	3.69		2.45
Hf	5.6		2.9	2.2	3.11	3.6	4.37	2.91	3.56	4.38		6.37
Rb	71		15	37	36.4	49.2	53.4	37.6	76.1	46.3		42.9
Ta	1.06		<.57	.26	.412	.382	.385	.375	.417	.383		.545
Th	8.2		3.3	1.4	7.52	2.76	5.67	3.81	2.8	10.6		7.2
U	1.4		<.8	.5	1.75	1.06	1.53	.966	1.35	1.79		2.05
Zn	96		71	60	39.2	39.5	49.	91.1	54.8	80.9		53.
Zr	333		<227	88	93.8	107	147	96.	107.	170.		221.
Sc	7.25		6.28	5.85	9.73	5.64	16.7	10.4	6.75	15.8		18.8
La	32		16	8	17.6	9.82	10.5	15	6.19	24.8		16.2
Ce	64		32	15	36.5	20.6	26.9	28.1	15.	50.1		38.1
Nd	31		12	8	15.8	9.92	14.5	13.6	8.07	22.5		20.9
Sm	4.9		1.7	1.8	2.88	2.81	4	3.25	2.37	5.06		5.19
Ba	1.38		.8	.63	.787	.915	.925	.927	.706	1.		1.24
Gd	4.1		1.5	2.			4.3	2.72	2.15	4.72		6.88
Tb	.66		<.7	.23	.415	.359	.686	.413	.327	.679		.91
Ho	<.9		<.6	.2								
Tm	.21		<.11	.12	.256							.491
Yb	1.2		.3	.7	1.63	1.14	2.4	1.25	1.17	2.23		3.21
Lu	.18		.06	.09	.242	.164	.357	.187	.184	.337		.466

Table 3. (cont.)

Unit Sample Number	Antimony Peak			Bear Valley Springs									
	7848	3023	3158	34278	3575	3670	3791	3837	3858	4181	4281	6369	
	CIPW norms (weight percent)												
q	19.66	19.25	23.33	18.74	17.76	17.7	17.05	8.33	17.73	21.94	15.51	22.38	21.75
or	3.3	3.76	20.58	11.29	11.23	10.71	8.93	14.26	11.74	10.11	8.93	15.1	6.24
ab	32.89	30.76	19.93	32.33	27.94	28.12	32.38	25.53	28.32	31.27	27.06	28.85	27.98
an	29.98	32.34	16.67	21.65	24.07	23.97	22.88	23.51	16.78	23.3	30.27	18.93	25.92
wo			1.77	2.13	2.46	2.47	4.12 ¹		6.34				2.91
en	5.96	6.53	6.12	5.51	7.73	7.52	6.77	11.27	8.33	5.51	8.28	5.02	6.66
fs	2.56	2.52	5.69	4.64	4.79	5.37	5.36	7.85	6.04	3.82	5.78	4.67	4.85
mt	1.88	1.9	2.23	2.33	2.47	2.34	2.34	3.35	2.58	2.19	2.48	1.9	2.19
hm													
il	.63	.69	1.67	1.38	1.5	1.42	1.42	1.41	1.53	1.15	1.32	1.03	1.18
ap	.38	.43	.51	.38	.4	.36	.43	.36	.4	.24	.26	1.84	.33
c	2.74	1.86	2.84							.43	.05	2.29	
cc	.05	.44			.02		.02	.24					
Total	100.03	100.01	100.02	100.02	100.01	100.03	100.01	100.03	100.03	99.96	99.94	100.01	100.01
Normative Plagioclase (An)	47.69	51.25	45.55	40.11	46.28	46.02	41.4	47.94	37.21	42.7	52.8	39.62	48.09

Table 3. (cont)

Unit Sample Number	Carver-Bowen			Dunlap Meadow			Mountain Springs			
	5980	6079A	RWK-3	5008	5285	5887	5922	5974	6004	6024
	CIPW norms (weight percent)									
Q	22.31	19.14	23.46	14.57	14.08	13.72	22.83	22.13	20.12	17.64
or	7.76	10.98	10.56	11.74	10.41	9.39	9.87	9.15	12.54	9.45
ab	28.15	26.61	31.96	24.58	26.3	25.94	27.41	28.27	26.11	27.56
an	24.78	25.81	21.41	27.6	26.7	28.79	25.28	27.13	25.75	28.13
wo	2.01	.95	1.04	2.07	2.95	2.14	.78	.86	.74	1.1
en	6.49	7.25	5.3	8.67	8.3	8.55	5.83	5.58	6.38	6.63
fs	5.48	5.44	2.64	5.46	7.05	7.	3.99	3.27	4.69	5.3
mt	1.51	2.22	2.55	3.79	2.54	2.7	2.41	2.16	2.13	2.3
il	1.16	1.26	.91	1.51	1.33	1.41	1.25	1.05	1.19	1.44
ap	.36	.34	.34	.31	.36	.36	.41	.36	.46	.36
C										.3
cc										
Total	100.01	100.	100.17	100.	100.02	100.	100.01	100.01	100.01	100.02
Normative Plagioclase (An)	46.81	49.23	40.12	52.9	50.38	52.6	47.97	48.96	49.66	50.51

Table 3. (cont.)

Unit Sample Number	Hoffman Canyon				Mt. Adelaide				Walt Klein				Zumwalt
	3842A	RWK-9	3631	4189	6061	6088	6096?	6281A	6314-1	6321	RWK-1	RWK-2	6123
CIPW Norms (weight percent)													
Q	18.31	18.25	21.38	27.78	28.45	32.06	24.01	22.28	30.5	24.96	19.08	27.24	18.72
or	13.75	16.63	4.99	8.38	7.95	7.93	10.18	7.13	16.93	8.59	10.56	10.56	8.77
ab	34.24	31.47	39.1	33.2	30.28	30.63	26.14	30.52	26.71	29.53	27.77	35.63	31.24
an	20.51	19.7	24.6	19.87	23.61	21.42	24.43	26.69	18.16	23.8	25.3	18.07	23.91
wo	.41						1.29	.31		1.2	1.28		2.14
en	4.54	5.26	4.	3.53	3.9	2.76	6.21	5.56	3.07	5.28	7.	3.	7.06
fs	2.66	3.53	2.16	3.15	3.02	2.46	4.67	3.63	2.19	2.83	6.47	2.51	3.54
mt	2.64	2.48	1.89	1.13	1.66	.95	1.78	2.38	1.38	2.56	.93	1.62	2.98
hm													
il	1.77	1.66	1.05	.9	.65	.54	1.	1.12	.65	.92	1.22	.76	1.28
ap	.7	.55	.45	.26	.31	.29	.31	.48	.24	.36	.34	.34	.36
c	.3		.35	1.74	.18	.98			.18				.31
cc	.6	.09	.02										
Total	100.02	100.03	99.99	99.94	100.01	100.02	100.1	100.01	100.03	99.95	100.04	100.	
Normative Plagioclase (An)	37.46	38.5	38.62	37.44	43.82	41.15	48.32	46.66	40.46	44.63	47.67	33.65	43.36

Table 4. Chemical and trace element analyses and CIPW norms for samples
of quartz diorite from the southern Sierra Nevada, California

Unit Sample Number	Calliente	Freeman Junction			Long Valley			Tehachapi Mountains			Walker Pass		
		3635R	6438A	6439	6509A	3097	3098A	3442	6179	6220	6226	6391	
Chemical analyses (weight percent)													
SiO ₂	62.2	57.2	64.5	56.7	59.7	55.2	61.6	64.1	61.8	63.9	64.5		
Al ₂ O ₃	17.4	17.7	16.2	18.	17.2	15.5	17.2	17.2	16.8	16.8	17.4		
Fe ₂ O ₃	1.78	3.48	2.43	3.3	.89	1.2	1.7	2.44	2.93	2.51	2.23		
FeO	3.25	4.44	2.67	3.99	5.8	7.1	4.7	1.95	2.96	1.87	1.93		
MgO	2.55	3.28	2.06	3.17	3.4	4.4	4.1	1.44	2.13	1.55	1.44		
CaO	6.	6.95	5.19	7.27	7.	8.2	6.9	5.86	6.3	5.7	5.2		
Na ₂ O	3.45	3.5	3.49	3.85	3.2	2.8	2.8	4.06	3.49	3.75	4.27		
K ₂ O	1.23	1.27	1.81	1.49	.26	.59	1.4	1.33	1.62	1.94	1.41		
H ₂ O ⁺					.58	1.	1.1						
H ₂ O ⁻					.16	.27	.19						
TiO ₂	.64	.72	.47	.75	.82	1.1	.67	.47	.49	.46	.44		
P ₂ O ₅	.16	.24	.17	.37	.18	.21	.14	.17	.23	.18	.16		
MnO	.07	.15	.1	.14	.11	.01	.08	.14	.15	.16	.09		
CO ₂					.05	.04	.01						
Loss on ignition (900° C)	.85	.9	.65	.69				.21	.52	.51	.47		
Total	99.58	99.83	99.74	99.72	99.35	99.42	100.89	99.37	99.82	99.33	99.54		

-100 -

Table 4. (cont.)

Unit Sample Number	Calliente	Freeman Junction	Long Valley	Tehachapi Mountains	Walker Pass									
					3635R	6438A	6439	6509A	3097	3098A	3442	6179	6220	6226
Instrumental neutron activation analyses (parts per million)														
Ba	512	522	821	826	264	439	730	803	1800	1800	762			
Co	12.3	18.6	10.7	16.4	25.1	20.1	6.8	11.5	7.37	7.37	6.44			
Cr	39.2	6.95	16.6	21.7	69.2	104.7	3.18	1.09	.837	.837	1.29			
Ca	1.39	2.64	2.14	1.02	1.1	1.2	1.98	3.21	1.53	1.53	1.87			
Hf	3.51	4.31	4.02	4.93	4.0	2.6	2.38	3.84	3.49	3.49	2.97			
Rb	40	36.1	50.4	38.7	17.	48.	30.3	45.9	35.4	35.4	33.			
Ta	.24	.473	.495	.333	.46	.33	.406	.435	.511	.511	.753			
Th	.47	7.12	4.87	4.51	2.5	.4	3.06	5.96	2.84	2.84	2.26			
U	.35	1.7	1.25	1.2	1.6	<.9	1.16	1.4	1.15	1.15	.98			
Zn	71.	97.	68.7	93.6	101.	94.	80.2	80.6	80.8	80.8	66.4			
Zr	139.	149.	134.	190.	150.	<353	84.9	135.	113.	113.	105.			
Sc	12.7	17.7	11.9	16.8	34.5	20.89	6.55	10.3	8.65	8.65	6.32			
La	7.	15.4	16.1	27.9	11.	10.	13.4	16.2	14.	14.	12.1			
Ce	15.7	33.7	32.4	58.6	27.	25.	28.	31.8	29.8	29.8	28.1			
Nd	14.	18.7	17.	30.5	<40.	18.	14.8	17.1	16.	16.	15.1			
Sm	3.15	4.66	3.68	6.69	5.	3.5	2.71	3.42	3.1	3.1	2.81			
Eu	.84	1.25	.955	1.87	1.18	.84	.869	.983	.871	.871	.898			
Gd	3.2	4.81	3.64	5.88	5.1	2.8	2.44	3.07	2.49	2.49	2.74			
Tb	.48	.779	.563	.841	.87	.68	.387	.511	.426	.426	.394			
Ho							.5							
Tm	.21	.446	.374	.398	.53	.32	.246	.346	.289	.289	.27			
Yb	F.47	2.84	2.25	2.36	3.4	2.1	1.61	2.23	1.9	1.9	1.76			
Lu	.215	.423	.338	.337	.51	.32	.256	.306	.31	.31	.269			

Unit	Calliente	Freeman	Junction	Long	Tehachapi Mountains			Walker Pass				
					Sample	Number	6438A	6439	6509A	3097	3098A	3442
					CIPW norms (weight percent)							
q	19.92	11.89	23.03	9.12	17.23	10.05	18.36	21.56	18.98	21.31	21.23	
or	7.36	7.59	10.8	8.89	1.56	3.55	8.31	7.93	9.64	11.6	8.41	
ab	29.57	29.94	29.8	32.9	27.46	24.14	23.79	34.65	29.74	32.11	36.47	
an	28.72	29.15	23.4	27.7	32.25	33.23	25.69	24.99	26.67	23.56	24.37	
wo	.15	1.72	.61	2.62	.61	2.74	3.21	1.34	1.38	1.62	.26	
en	6.43	8.26	5.18	7.97	8.59	11.17	10.25	4	3.62	5.35	3.91	3.62
fa	3.62	4.42	2.33	3.66	8.89	10.63	6.29	1.06	2.5	.91	1.16	
mt	2.61	5.1	3.56	4.83	1.31	1.77	2.48	3.57	4.28	3.68	3.26	
il	1.23	1.38	.9	1.44	1.58	2.13	1.28	.9	.94	.88	.84	
ap	.38	.58	.41	.86	.43	.51	.33	.41	.55	.43	.38	
c												
cc							.11	.09	.02			
Total	99.99	100.03	100.02	99.99	100.02	100.01	100.01	100.03	100.01	100.01	100.	
Normative Plagioclase (An)	49.28	49.33	43.99	45.71	54.01	57.92	51.92	41.9	47.28	42.32	40.06	

Table 5. Chemical analysis and CIPW norm for sample of quartz monzonodiorite from the southern Sierra Nevada, California

Chem. anal.	Norm RMK-11	Norm RMK-11
	q	6.91
SiO ₂	59.	or
Al ₂ O ₃	16.8	ab
Fe ₂ O ₃	1.4	an
FeO	4.5	wo
MgO	2.6	en
CaO	5.2	fs
Na ₂ O	4.7	wt
K ₂ O	2.6	11
H ₂ O ⁺	.75	ap
H ₂ O ⁻	.35	-
TiO ₂	1.2	C
P ₂ O ₅	.38	cc
MnO	.1	
CO ₂	.08	
Total	100.02	
Loss on ignition		30.02
(900° C)		Plagioclase. (An)
Total	99.66	

- 111 -

Table 6. Analysts (all U.S.G.S.) for chemical data on tables 1, 2, 3, 4, and 5.

Chemical analyses

1. Hezekiah Smith, samples 784B, 3005, 3023, 3088, 3097, 3098A, 3158, 3181, 3221.
2. N. Skinner, samples 3356, 3401, 3427B, 3442, 3466, 3534B, 3575, 3631, 3670, 3695, 3733A, 3737, 3752, 3756A, 3791, 3794A, 3837, 3842A, 3858.
3. J. Reid, P. Hearn, H. Rose, and J. Lindsay, samples 4093, 4100A, 4102A, 4181, 4184, 4189, 4273, 4281, 4294, 4314, 4341, 4354, 4366, 4402, 4472, 4528.
4. J. S. Wahlberg, J. E. Taggart, Jr., and J. W. Baker, samples 4763, 4789A, 4796-1, 4819A, 4848, 4995, 5008, 5031, 5062, 5236.
and
5. A. J. Bartel, K. Stewart, J. E. Taggart, samples 3635R, 5006, 5017, 5034, 5071, 5133R, 5261, 5285, 5356, 5403, 5407, 5421, 5423, 5425, 5801R, 5852, 5865A, 5871, 5887, 5922, 5946, 5965, 5974, 5980, 6004, 6024, 6030, 6061, 6079, 6088, 6093, 6096, 6106, 6117, 6123.
6. R. V. Mendes, A. J. Bartel, K. Stewart, J. E. Taggart, Jr., and L. Espo, samples 6179, 6208, 6220, 6226, 6245, 6269, 6281A, 6292, 6297, 6300, 6314-1, 6321, 6336, 6356, 6359, 6369, 6373, 6391, 6415, 6425, 6438A, 6439, 6472A, 6483A, 6509A, 6523A, 6535, 6539.

Instrumental neutron activation analyses

- L. J. Schwarz, samples 3356 to 5236 (lists 2, 3, and 4 above)
- J. S. Mee, samples 5006 to 5425 (first part of list 5 above)
- J. Budahn and R. Knight, samples 5801R to 6123 (last part of list 5 above)
- D. M. McKown, R. Budahn, and R. Knight, samples 6197 to 6539 (list 6 above)

Previously published chemical analyses

Fox (1981), samples IS-638, 665, and 727.

Kistler and Peterman (1978, p. 2), samples RWK-1, 2, 3, 4, 5, 6, 7, 9, 11, and 13.
Ross (1972, p. 71), samples 686, 690, 698, and 726.

Table 7. CaO, Na₂O, and K₂O values for trondhjemite samples plotted on figure 10.

Locality	Sample no.	CaO	Na ₂ O	K ₂ O
Sierra Nevada				
Ward Mountain	ML-12	2.5	4.4	2.2
	ML-43	3.0	4.5	1.7
	SJ-1	2.3	4.3	2.2
Rocklin	-	2.6	4.8	1.4
Bald Rock				
(Turner)	95	3.18	4.91	1.71
(Hietanen)	19(204)	2.65	5.12	2.04
(Larsen and Poldervaart)	H	2.65	5.11	2.04
	MH	2.2	5.7	2.6
	F	2.5	5.5	1.5
	BR5	2.9	4.5	2.1
	BR15	2.9	4.6	2.2
	BR13	3.1	5.1	1.8
	T	3.18	4.91	1.71
	FS/26	3.1	4.8	1.7
	BR4	3.0	4.7	1.9
	F3/16	3.3	5.1	1.8
	RRC	3.1	4.7	1.6
	BR2	3.2	5.2	1.6

Table 7 .(cont.)

Locality	Sample no.	CaO	Na ₂ O	K ₂ O
Klamath Mountains				
Gibson Peak	5	4.1	5.2	1.3
Caribou Mountain	14-33	4.40	4.69	.96
	Ave.-3 cores	3.2	5.3	1.3
Craggy Peak	24	3.4	4.7	.95
White Rock	54	3.6	4.8	.84
	55	3.4	4.7	.95
Idaho				
Riggins	-	5.0	4.6	0.7
(values estimated from variation diagrams)	-	4.2	4.6	1.0
	-	5.0	4.6	0.3
	-	2.0	5.5	0.7
	-	1.2	5.1	1.3
Norway				
Guldalen	-	3.34	6.00	1.39
Skavlien	-	1.98	5.43	2.04
Kvikne	-	1.65	6.63	2.22
West Norway	I	2.94	6.30	1.69
	II	3.03	4.84	1.87
	III	3.52	4.30	1.45
	IV	1.71	5.75	2.61
	V	1.97	5.99	2.50
	VI	2.50	4.85	0.57
	VIII	3.50	4.23	0.25
	Aplite	1.87	6.00	1.28
Average		3.0	5.0	1.5
s.d.		0.8	0.6	0.7

Table 8. CaO, Na₂O, and K₂O estimated from modes and modes for selected samples of tonalite of Cedar Creek.

Sample number	6349	6349R	6360	6659	6687	6690	6703
CaO	4.2	4.5	4.7	4.3	3.3	4.4	3.7
Na ₂ O	4.4	5.2	4.2	3.8	4.3	3.6	4.4
K ₂ O	1.1	1.6	1.1	1.3	1.0	1.1	1.8
Normalized to 100 for triangular plot							
CaO	43	40	47	46	38	48	37.5
Na ₂ O	46	46	42	40	50	40	44.5
K ₂ O	11	14	11	14	12	12	18
Modes							
Plagioclase	58	63	58	54	50	54	55
K-feldspar	2	2	-	3	-	2	-
Quartz	29	20	29	34	38	37	34
Biotite	9	15	13	9	10.5	7	10
Hornblende	2	<1	<1	<1	1.5	-	-
Opacques	-	<1	-	-	-	-	1
Total	100	100	100	100	100	100	100
An of plagioclase	36 ^{2/}	35 ^{1/}	40 ^{1/}	40 ^{2/}	30 ^{1/}	44 ^{2/}	33 ^{1/}

1/ measured on albite twinning in thin section

2/ measured in index oils on fragments from stained slab

(An determinations by both methods are approximate average values)

Table 9. Averages of chemical analyses of units "A" and "B"
of Kernville pluton of Fox (1981)

	Average of 7 samples of unit "A"		Average of 14 samples of unit "B"	
	Average	Standard deviation	Average	Standard deviation
SiO ₂	45.50	1.97	57.23	2.76
Al ₂ O ₃	19.74	2.03	16.85	0.97
Total Fe	9.08	2.44	6.75	0.91
MgO	6.03	1.88	3.90	2.37
CaO	13.35	1.40	6.58	1.16
Na ₂ O	1.77	0.43	3.32	0.54
K ₂ O	0.45	0.48	1.94	0.51
TiO ₂	1.28	0.62	1.02	0.22
P ₂ O ₅	0.15	0.09	0.24	0.07
MnO	0.15	0.04	0.13	0.02
Total	97.50	-	97.96	-

Table 10. Comparison of crustal abundance estimates for the Lanthanide series between Turekian and Wedepohl (1961) and Taylor (1965).

(in parts per million)

	Granite		Granodiorite	
	T & W	Taylor	T & W	Taylor
Sc	7	5	14	10
La	55	25	45	--
Ce	92	46	81	--
Nd	37	18	33	--
Sm	10	3	8.8	--
Eu	1.6	--	1.4	--
Gd	10	2	8.8	--
Tb	1.6	0.05	1.4	--
Tm	0.3	--	0.3	--
Yb	4	0.06	3.5	--
Lu	1.2	0.01	1.1	--

Table 11 . Averages of potassium and rubidium values and K/Rb ratios of chemically analyzed samples for each plutonic unit in the southern Sierra Nevada, California.

Number of samples	Unit	K(%)	Rb(ppm)	K/Rb	Number of samples	Unit	K(%)	Rb(ppm)	K/Rb
<u>Granite</u>									
1	Arrastre	3.2	74	432	2	Antimony Peak	0.6	12	497
1	Bodfish	4.0	202	198	10	Bear Valley Spr.	1.5	66.6	227
2	Brush Mtn	3.6	214	175	2	Carver-Bowen	1.3	62	214
3	Five Fingers	3.0	85.8	345	7	Dunlap Meadow	1.4	66.8	215
3	Kern River	3.3	150.3	220	2	Fountain Spr.	1.2	38.2	302
2	Portuguese Pass	3.4	159.5	216	1	Hoffman Cany.	2.2	81	266
1	Sherman Pass	3.7	189	196	2	Mt. Adelaide	1.0	26	396
1	Tehachapi Air.	4.1	158	259	6	Walt Klein	1.4	49.8	271
3	Tejon Lookout	4.4	181	244	1	Zumwalt Ranch	1.2	42.9	280
		Average	254					Average	295
								(Average without Antimony Peak)	271
<u>Granodiorite</u>									
4	Alder Creek	2.4	119	202	1	Caliente	1.0	40	250
2	Alta Sierra	1.9	67	276	2	Freeman Jct.	1.3	42.3	311
1	Brush Creek	3.0	140	214	1	Long Valley	1.2	38.7	310
9	Castle Rock	2.6	98.4	272	2	Tehachapt Mtns.	0.9	32	272
2	Deer Creek	2.6	78	328	4	Walker Pass	1.3	36.2	365
4	Gato-Montes	2.7	109	247				Average	302
1	Hatchet Peak	2.9	124	234					
2	Keene	2.5	91	275					
2	Lebec	2.3	95	242					
3	Peppermint Meadow	2.2	77.7	285					
3	Pine Flat	2.3	95.8	245					
7	Poso Flat	1.4	57.7	253					
3	Rabbit Island	2.2	95.7	234					
4	Sacatar	2.6	100.8	264					
1	Sorrell Peak	3.2	112	286					
4	Wagy Flat	1.5	60.3	251					
3	Whiterock	2.1	97.3	263					
		Average	257						
								Grand average (without Antimony Peak)	271

Table 12. Average modes by rock type for chemically analyzed samples and for all modes

	<u>Chemically analyzed samples</u>				
	Plagioclase	K-feldspar	Quartz	Biotite	Hornblende
Granite	34	29	31	5	1
Granodiorite	50	12	23	11	4
* Tonalite	54	3	20	12	10
* Quartz diorite	57	1	15	9	17
	<u>All modes</u>				
* Granite	33	30	32	4	-
Granodiorite	50	13	24	10	3
Tonalite	54	3	21	13	9
Quartz diorite	55	1.5	12	9	21 (Pyroxene, 1.5)

* Only total 99 percent because of rounding